

BETACOOOL Physics Guide

for simulation of long term beam dynamics in ion storage rings

(since 1995)

I.Meshkov, A.Sidorin, A.Smirnov, G.Trubnikov, R.Pivin

**Joint Institute for Nuclear Research
Joliot Curie, 6, Dubna, 141980 Russian Federation**

<http://lepta.jinr.ru/betacool>

Dubna, 2007

Introduction

General goal of the BETACOOOL program is to simulate long term processes (in comparison with the ion revolution period) leading to variation of the ion distribution function in 6 dimensional phase space. The ion beam motion inside a storage ring is supposed to be stable and it is treated in linear approximation.

BETACOOOL code was developed in the frame of collaboration with different scientific centers:

- BNL, Upton, USA
- Fermilab, Batavia, USA
- RIKEN, Wako, Japan
- NIRS, Chiba, Japan
- Kyoto Univ., Japan
- CERN, Geneva, Switzerland
- GSI, Darmstadt, Germany
- FZJ, Juelich, Germany
- Erlangen Univ., Germany
- ITEP, Moscow, Russia
- BINP, Novosibirsk, Russia
- Uppsala Univ., Sweden

BETACOOOL package is distributed as different folders:

BETACOOOL – executable and interface files for Windows, input files, MAD8 program.

PDF – Physical guide and User Manual for BETACOOOL, documentation for MAD8, GEANT.

SRC – project and source files for C++ Compilers.

Contents

I. Numerical Algorithms	6
Introduction.....	6
1. RMS Dynamics.....	7
1.1. Physical model.....	7
1.2. Phase space diagrams of growth rates.....	9
1.3. Additional Heating effect.....	11
2. Model Beam.....	12
2.1. Physical model.....	12
2.2. The beam rotation with the matrix.....	14
2.3. Kick procedure at IBS.....	14
2.4. Kick procedure at ECOOL.....	15
2.5. Kick procedure at Additional Heating.....	15
3. Multi Particle Tracking.....	17
3.1. Algorithm of the calculations.....	17
3.2. Models of optic elements.....	19
3.3. Molecular Dynamics.....	21
3.4. Crystalline beams.....	22
References.....	23
II. Electron Cooling	24
1. Introduction.....	24
2. Structure of the algorithm.....	25
3. Friction force in the particle rest frame.....	28
3.1. Non-magnetized electron beam	28
3.1.1. Binary collision model.....	28
3.1.2. Numerical integration	29
3.1.3. Asymptotic representations at flattened velocity distribution.....	33
3.2. Magnetized electron beam. Derbenev-Skrinsky-Meshkov formulae	35
3.2.1. Magnetized collisions	35
3.2.2. Friction force at small impact parameters.....	37
3.2.3. Asymptotic representation by I.Meshkov	38
3.3. Magnetized electron beam. Semi-empirical formula by Parkhomchuk.....	39
3.4. Model of electron cooling friction force developed by Erlangen University	40
3.4. Probability of the particle loss	43
3.4.1. Simulation of ion-electron recombination in presence of undulator field	43
4. Map of the cooling section.....	45
4.1. Models of electron beam.....	48
4.1.1. Uniform cylinder.....	48
4.1.2. Gaussian bunch	48
4.1.3. Uniform bunch	49
4.1.4. Gaussian cylinder.....	49
4.1.5. Hollow beam.....	50
4.1.6. Parabolic beam.....	51
4.1.7. Distribution of electron density from file	52
4.2. Space charge effects of the electron beam.....	53
4.2.1. Space charge effect in the hollow electron beam.....	55
4.3. Model of the cooler.....	57
5. Kick of the ion momentum components in the electron cooling section.....	58
6. Algorithm of the electron cooling time calculation	58
6.1. Calculation of the characteristic times of the ion motion invariant changing	59

6.2. Calculation of the characteristic times of emittance variation using Monte Carlo method	61
References.....	62
III. Intrabeam scattering.....	63
1. Introduction.....	63
2. Structure of the effect.....	63
3. Models of IBS.....	64
3.1. Analytical model of the multiple particle collisions.....	65
3.2. Molecular Dynamics techniques.....	70
4. Analytical models of IBS.....	72
4.1. Piwinski model.....	72
4.2. Martini model.....	73
4.3. Jie Wei model.....	75
4.4. Bjorken – Mtingwa model.....	77
4.5.1. High energy approach.....	78
4.5.2. Kinetic model of IBS on the basis of Bjorken-Mtingwa theory.....	79
4.5. Gas Relaxation model.....	85
4.5.1. High energy approach.....	87
4.7. Calculations of IBS in the case of transverse coupling.....	87
5. Kick of the ion momentum components due to IBS.....	88
5.1. Mean growth rates.....	88
5.2. Detailed calculation of the momentum kick.....	89
5.2.1. Burov's model.....	89
5.2.2. Bi-Gaussian model.....	90
5.2.3. Parzen's model for bi-Gaussian distribution.....	91
References.....	93
IV. Stochastic cooling.....	94
1. Introduction.....	94
2. Characteristic time calculation.....	94
2.1. Transverse degrees of freedom.....	94
2.1.1. Cooling rate calculation.....	94
2.1.2. Power consumption.....	96
2.2. Longitudinal degree of freedom.....	97
2.2.1. Cooling rate calculation.....	97
2.2.2. Power consumption.....	99
3. Kick of the ion momentum components due to action of stochastic cooling.....	99
3.1. Transverse degrees of freedom.....	101
3.2. Longitudinal degree of freedom.....	102
References.....	103
V. Internal Target.....	104
1. Introduction.....	104
2. Map of the internal target.....	104
2.1. Detailed simulation of the interaction with a target.....	105
2.1.1. Longitudinal degree of freedom. Urban model.....	105
2.1.2. Transverse degree of freedom. Plural scattering.....	108
2.2. Scattering in accordance with Gaussian law.....	109
2.3. Calculation of the particle loss probability.....	111
3. Variation of the ion momentum in Model Beam algorithm.....	113
3.1. Number of the crossings in the case of pellet target.....	114
3.2. The pellet target as a fiber at mean density.....	117
4. Different types of target.....	120
4.1. Gas storage cell and solid targets.....	121
4.2. Gas jet, cluster beam and pellet targets.....	121

4.2.1. Calculation of the target effective density from geometry parameters	122
4.2.2. Monte Carlo method of the effective density calculation	122
References	124
VI. Colliding Mode	125
1. Luminosity of colliding beams	125
1.2. Luminosity calculation in RMS dynamics	125
1.2. Luminosity calculation in Model Beam	125
2. Beam-beam effect	127
2.1. Analytical formulae for beam-beam parameter	127
2.2. Numerical algorithms for beam-beam parameter calculation	130
2.3. Results of benchmarking	132
VII. Barrier RF Bucket simulation	134
1. Synchrotron motion in a square wave barrier bucket	134
2. Modifications of RMS dynamics algorithm	139
2.1. Internal target and IBS	139
2.2. Electron cooling time calculation	139
3. Model beam algorithm	141
3.1. Generation of the ion initial distribution in the given ring position	141
3.2. The betatron and synchrotron motion simulation	143
4. Numerical model of barrier bucket	144

I. Numerical Algorithms

Introduction

Initially BETACOOOL [1] code was developed as a program for simulation of particle dynamics in ion storage rings under the action of electron cooling force. Further development leads to the including into the program other different effects and a few numerical algorithms. First of them is RMS Dynamics which calculates evolution in time of the r.m.s. (root mean square) parameters of the ion beam distribution function and particle number. RMS Dynamics algorithm is based on solution of equation for the second order momentum of the distribution function. Characteristic times of the beam parameter evolution for a few general effects are calculated under assumption of Gaussian shape of the distribution function. No any particles are in the ion beam.

Model Beam algorithm was developed on the base of SIMCOOL code which was developed by Novosibirsk group. This algorithm uses a few thousands of test particles with arbitrary distribution. The action from IBS on the each test particle is calculated from the current distribution of test particles. This algorithm can reach a good accuracy when the distribution of test particle is closed to Gaussian. Some modification of this method was made for simulation of IBS in the case of non Gaussian distribution.

Evolution of the ion distribution function is described by the Fokker-Plank equation. Friction and diffusion terms in the general case depend on the distribution function. However in some cases, when the effects acting on the distribution function do not lead to change of its shape, the Fokker-Plank equation can be reduced to equation for the second order moments of the distribution function.

In general case the Fokker-Plank equation can be reduced to Langevin equation in invariant or momentum space. The Model Beam algorithm realizes solution of Langevin equation in momentum space using Monte Carlo method. In the frame of this algorithm the ion beam is presented as a particle array. Each particle is presented as a 6 co-ordinate vector:

$\vec{X} = \left(x, \frac{p_x}{p}, y, \frac{p_y}{p}, s - s_0, \frac{\Delta p}{p} \right)$, where x and y are the horizontal and vertical co-ordinates, p_x and p_y

are corresponding momentum components, $s - s_0$ is the distance from the bunch center (in the case of coasting beam – distance from a reference particle), Δp is the particle momentum deviation from momentum of reference particle p . Action of each effect is simulated as the particle momentum variation in accordance with the following equation:

$$(p_{x,y,s} / p)_{fin} = (p_{x,y,s} / p)_{in} + \Lambda_{x,y,s} \Delta T + \sqrt{D_{x,y,s} \Delta T} \xi_{x,y,s}, \quad (1.1)$$

where p_s is the particle longitudinal momentum deviation, subscript *in* correspond to initial momentum value, subscript *fin* relates to final particle momentum after action of the effect, Λ and D are the drift and diffusion terms for corresponding degree of freedom, ΔT is step of the integration over time, ξ is Gaussian random number at unit dispersion.

Tracking algorithm uses real particles with arbitrary distribution. The special method named Molecular Dynamics (MD) [2] is used for simulation of Intrabeam Scattering (IBS) in the ion beam. This algorithm assumes that particles have the periodical distribution in longitudinal direction. Usual number of particles per cell is about 10-100. It can simulate the crystalline state of ion beam

for very low temperature in the beam rest frame. MD simulation can be used for testing of analytical formulas for IBS effect also.

Three different numerical methods permit to verify each other and the validity of action from different physical effects. If initially the Gaussian distribution is chosen then the evolution of r.m.s. parameters should be the same while the shape of the distribution doesn't change. It is a good way to keep the development time for new program objects.

1. RMS Dynamics

1.1. Physical model

The physical model to be investigated with BETACOOOL program is based on the following general assumptions:

- 1) the ion beam has Gaussian distribution over all degrees of freedom, and is not changed during the process.
- 2) algorithm for analysis of the problem is considered as a solution of the equations for r.m.s. values of the beam phase space volumes of three degrees of freedom.
- 3) maxima of all the distribution functions coincide with equilibrium orbit.

The evolution of the ion beam parameters during its motion inside the storage ring is described by the following system of four differential equations:

$$\begin{cases} \frac{\varepsilon_{hor}}{dt} = \varepsilon_{hor} \sum_j \frac{1}{\tau_{hor}}, \\ \frac{\varepsilon_{ver}}{dt} = \varepsilon_{ver} \sum_j \frac{1}{\tau_{ver}}, \\ \frac{\varepsilon_{lon}}{dt} = \varepsilon_{lon} \sum_j \frac{1}{\tau_{lon}}, \\ \frac{dN}{dt} = N \sum_j \frac{1}{\tau_{life}}, \end{cases} \quad (1.2)$$

where N is the particle number. For transverse degrees of freedom parameters ε_{hor} and ε_{ver} corresponds to the horizontal and vertical emittances, for longitudinal degree of freedom it is given by the following expression:

$$\varepsilon_{lon} = \begin{cases} \left(\frac{\Delta p}{p} \right)^2, & \text{coasting beam;} \\ \left(\frac{\Delta p}{p} \right)^2 + \frac{1}{\Omega_s^2} \left[\frac{d}{dt} \left(\frac{\Delta p}{p} \right) \right]^2, & \text{bunched beam.} \end{cases} \quad (1.3)$$

In Eq. (1.3) the upper line corresponds to a coasting beam, lower line to a bunched beam with constant parameters (for variable synchrotron frequency it is necessary to use adiabatic invariant instead of energy; presently a depression of the synchrotron tune due to the action of the beam space charge is not taken into account during dynamics simulation). Ω_s – is the synchrotron

frequency. Therefore the second expression in Eq. (1.3) corresponds to the square of momentum oscillation amplitude.

Characteristic times (τ_{hor} , τ_{ver} , τ_{lon}) are functions of all three emittances and particle number and have positive sign for a heating process and negative for cooling one. The negative sign of the lifetime (τ_{life}) corresponds to the particle loss and the sign of the lifetime can be positive in the presence of particle injection, when particle number increases.

Index j in Eq.(1.2) is the number of process involved into calculations. The program structure is designed in such a way that allows including any process into calculation, which can be described by cooling or heating rates.

During numerical solution of the system (1.2) the parameters, which characterise beam stability are also calculated. They are incoherent betatron tune shift value, depression of the synchrotron tune, dimensionless parameters describing the beam from the side of longitudinal and transverse coherent instabilities.

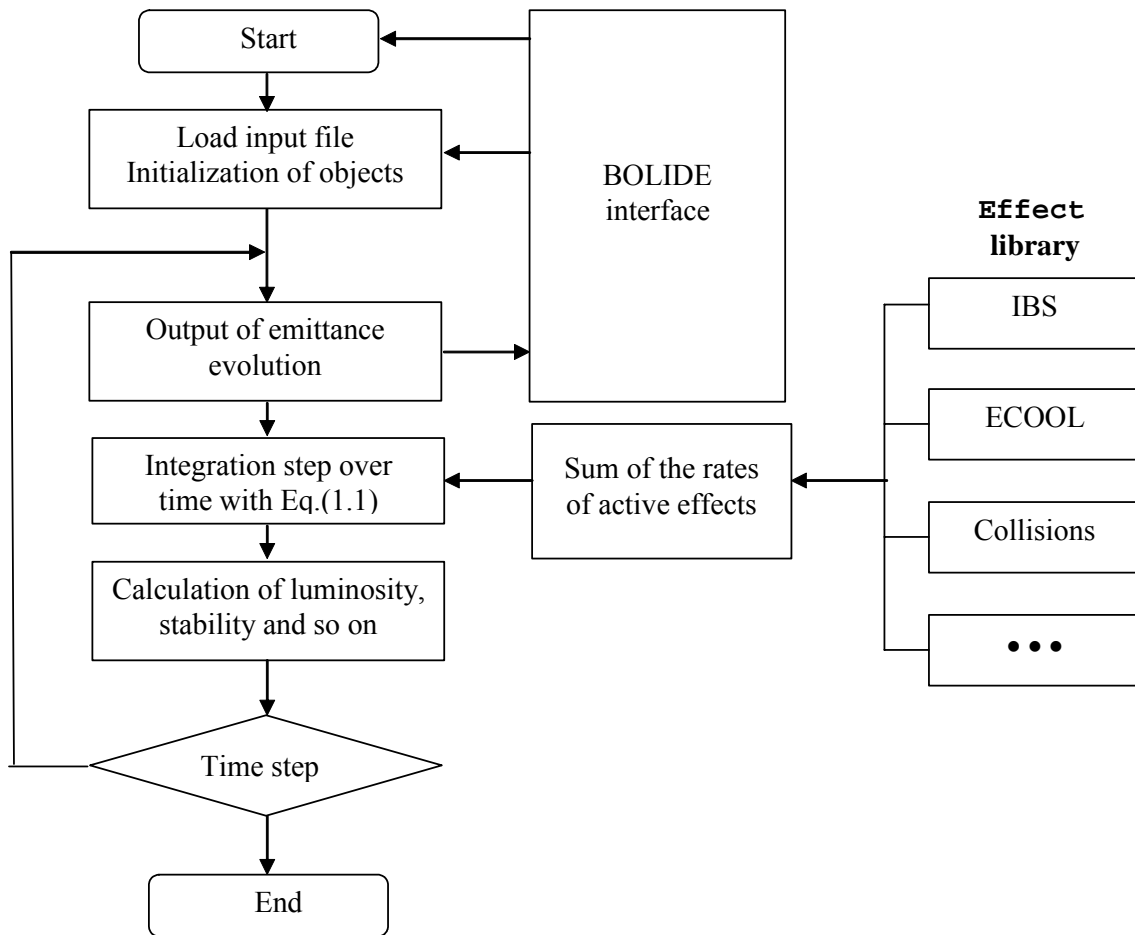


Fig. 1.1 Block-scheme of the r.m.s. beam parameter evolution simulation

Numerical solution of the system (1.2) is performed using Euler method with automatic step variation. In principle, the system can be solved using arbitrary method - for instance, one of the Runge-Kutta methods. Choice of the procedure for integration is determined by optimisation of the calculation speed.

Algorithm of the numerical integration of the system (1.2) realised in the program is illustrated in the Fig. 1.2. This document is dedicated mainly to description of the physical and mathematical models using for calculations of characteristic times for different effect from the **Effect** library.

Further improvement of the program is related to modification of the basic physical model. This improvement is necessary due to serious disadvantage of the model namely assumption of Gaussian shape of the ion distribution function. This assumption is more or less realistic in an equilibrium state of the ion beam when the equilibrium is determined by many processes of stochastic nature. If the equilibrium does not exist due to fast particle loss or at initial stage of the beam cooling the ion distribution function can be far from Gaussian. The same situation takes place in an experiment with internal targets which dimensions are not coinciding to the ion beam dimensions. The ionisation energy losses of the ion beam in the target can not be correctly calculated in the frame of existing model also.

Investigation of the ion beam dynamics at arbitrary shape of the distribution function can be performed using multi particle simulation. The structure of basic objects of the new code namely - the models of the ion ring and the ion beam, are developed in such a way, that allows realising multi particle simulation using Monte Carlo method without any change of the program structure.

1.2. Phase space diagrams of growth rates

The example of r.m.s. evolution during cooling process for HESR is presented on Fig.1.2. After cooling process all parameters achieved constant value and does not change for a long time. Particle loss rates are in a few orders less in comparison with cooling time and don't take into account during these simulations.

An unexpected behaviour of emittance can be explained with 3D diagram of space phase (Fig.1.3). These diagrams presented dependence of growth rates on the momentum spread and horizontal emittance. The vertical emittance is assumed to be equal to the horizontal one.

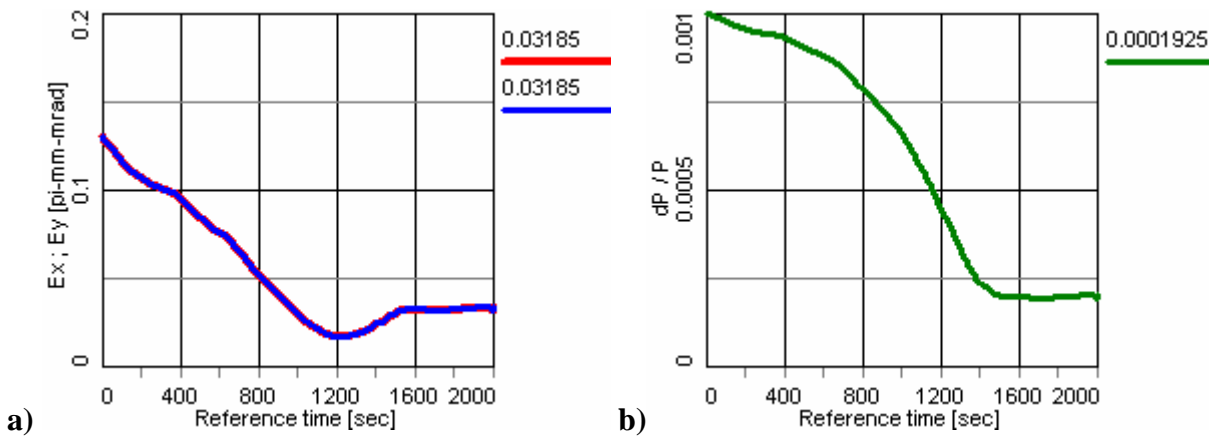


Fig.1.2. r.m.s. beam dynamics for HESR under action from IBS and ECOOL effects.

a) transverse emittances, b) momentum spread

IBS growth rates (Fig.1.3a,b) are calculated in accordance with Martini model [3]. Colour areas indicate different values of growth rates. White area for longitudinal component means that in this region of beam parameters the momentum spread is decreased and emittances is increased. The temperature relaxation exists for large momentum spread and small emittance. Beam parameters due to IBS come to the equilibrium temperature between all degree of freedom. Cooling rates for

EC (Fig.1.3c,d) are calculated in accordance with Parkhomchuk formula of cooling force [4]. Transverse and longitudinal components of cooling rates have approximately the same behaviour.

Summary of cooling and heating rates are presented on Fig.1.3e,f. Boundaries between colour and white areas shows the equilibrium between IBS and EC for transverse and longitudinal components. Equilibrium point can be found if one overlaps these pictures each other (Fig.1.3g). Position of this point does not depend on initial coordinate. For very complicate pictures more then one equilibrium points can be found. In this case the equilibrium parameters can be depend on initial values.

Fig.1.3g shows the dependence of the transverse emittance on the momentum spread during cooling process for r.m.s. dynamics on Fig.1.2. Initially the electron cooling force achieves the equilibrium with transverse component of IBS. During this process the emittance and momentum spread are decreased (evolution from start point on Fig.1.3). Then cooling process continues and beam parameters change in accordance with the equilibrium boundary of transverse component. Momentum spread continues to decrease but transverse emittance begins to increase.

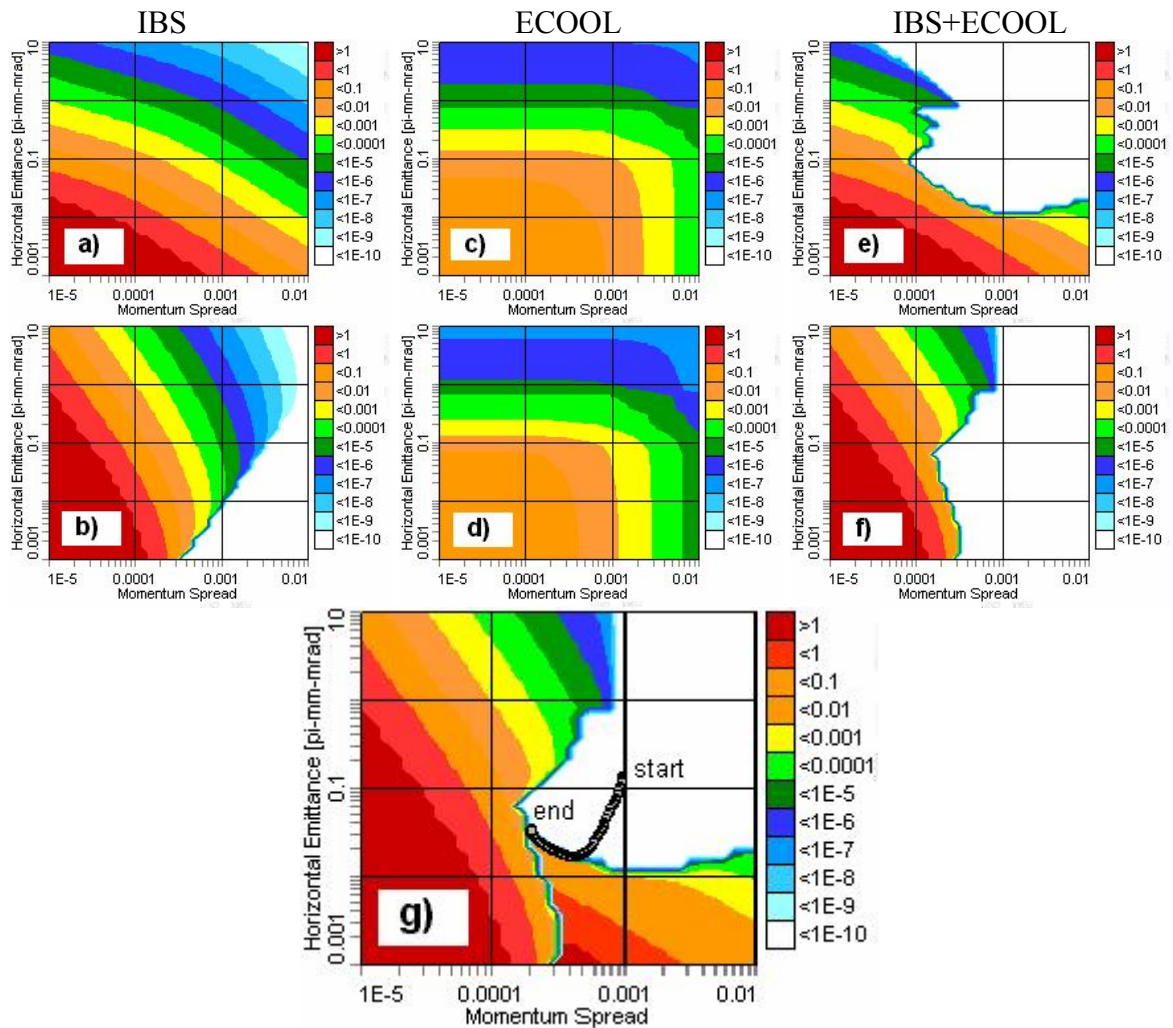


Fig.1.3. Phase space diagram of growth rates [sec^{-1}] for HESR.

a, b – transverse and longitudinal components of IBS growth rates, **c, d** – transverse and longitudinal cooling rates of EC, **e, f** – summary of cooling and heating rates, **g**– overlapping picture **f** over **e** and r.m.s dynamics in accordance to Fig.1.2.

When the cooling force also reach the equilibrium with longitudinal component of IBS then beam parameters achieve the equilibrium point, which does not depend on initial parameters (end point on Fig1.3). r.m.s. dynamics is rather difference and the cooling time can be change very large. It means

that initial parameters of ion beam don't influence on the equilibrium point but its have a large influence on the cooling time.

1.3. Additional Heating effect

The simplest physical effect in BETACOOOL program is Additional Heating. This effect can be used for modelling of additional heating or cooling effects which are not included in the standard set of physical effects. Here presented the example of program code for Additional Heating object:

```
class xHeat
{
public:
    bool rate;                // flag of constant growth rate
    doubleU Rate[3];          // array of constant growth rates
    bool linear;              // flag of linear growth rates
    doubleU Linear[3];        // array of linear growth rates
    bool power;               // flag of power growth rates
    doubleU Power[3];         // array of power growth rates
    bool diffusion;           // flag of diffusion growth rates
    doubleU Diffusion[3];     // array of diffusion growth rates

    xHeat();                  // constructor
    int OnGet();              // reading parameters from input file
    int OnRun();              // reading parameters during simulation

    vectorU Rates(xTime&, xBeam&, xRing&);    // calculates growth rates
    void Kick (xTime&, xBeam&, xRing&);       // calculates kicks
};
```

Additional Heating effect includes four different types:

- 1) constant rates which don't depend on current emittances;
- 2) linear rates which have linear dependence on current emittances;
- 3) diffusion rates which don't depend on current emittances;
- 4) diffusion rates which have dependence on current emittance.

RMS Dynamics algorithm calculates the summary of growth rates in accordance with Eq.(1.1). Rates procedure of Additional Heating is

```
vectorU xHeat::Rates(xTime&t, xBeam& beam, xRing& ring)
{
    vectorU rates(s_^-1);
    for (int i = 0; i < 3; i++)
    {
        if (rate)
            rates[i] += Rate[i];
        if (linear)
            rates[i] += Linear[i] / beam.Emit[i];
        if (power)
            rates[i] += Power[i] * 2;
        if (diffusion)
            rates[i] += Diffusion[i] / (beam.Emit[i]^2) * 2;
    }
    return rates;
}
```

2. Model Beam

Initial plans did not presume the development of the **Model Beam** algorithm in the frame of the BETACOOOL program and main attention was attracted to development of **Monte-Carlo** algorithm which is not included in current version of BETACOOOL. However, the **Model Beam** algorithm has a few obvious advantages in comparison with the **Monte-Carlo** one. Main of them is simplicity and as a result - high calculation speed. Therefore, the results of simulations using **Model Beam** algorithm can be effectively used for benchmarking of **Monte-Carlo**.

From the other hand, the **Model Beam** algorithm is under independent development in the frame of the SIMCOOL program. The possibility to compare results of the same numerical model realized in independent programs is very fruitful for benchmarking each of them. For this aim in the frame of BETACOOOL program one can realize data output in the SIMCOOL program format. In the frame of BETACOOOL the **Model Beam** algorithm can be used with all developed models of general effects. In principle one can repeat accurately the models of the processes using in SIMCOOL program (it is mainly related to IBS and electron cooling processes) and after benchmarking the code using results of SIMCOOL program to compare different models in the BETACOOOL program.

2.1. Physical model

Investigation of the ion beam dynamics at arbitrary shape of the distribution function is performed using multi particle simulation in the frame of **Model Beam** algorithm. In this algorithm the ion beam is presented by array of modeling particles. The heating and cooling processes involved into simulations lead to change of the particle momentum components and particle number, what is calculated in accordance with step of dynamics simulation over time.

Each effect is located in some position of the ring characterizing by the ring lattice functions. Transformation of the beam inside the ring is provided using linear matrix at random phase advance between the effect locations.

The numerical realization of the algorithm described by the formula (2.1) has the following peculiarity. The regular variation of the particle momentum due to action of drift term can be rewritten as

$$(p_{x,y,s} / p)_{fin} = (p_{x,y,s} / p)_{in} \left(1 + \frac{\Lambda_{x,y,s}}{(p_{x,y,s} / p)_{in}} \Delta T \right). \quad (2.1)$$

At large value of ΔT the absolute value of the term $\frac{\Lambda_{x,y,s}}{(p_{x,y,s} / p)_{in}} \Delta T$ can be larger than unity (in the case of cooling this term has a negative sign). In this case direct application of the formula (2.1) will lead to change a sign of corresponding momentum component and can lead also to increase of its absolute value. This situation corresponds to artificial diffusion heating of the beam on numerical algorithm. To avoid this “numerical” diffusion at $\left| \frac{\Lambda_{x,y,s}}{(p_{x,y,s} / p)_{in}} \Delta T \right| > 1$ the formula (2.1) is transformed to the following form

$$(p_{x,y,s} / p)_{fin} = (p_{x,y,s} / p)_{in} \times \exp \left\{ \frac{\Lambda_{x,y,s}}{(p_{x,y,s} / p)_{in}} \Delta T \right\}, \quad (2.2)$$

which includes the (2.3) as a limit case at small ΔT .

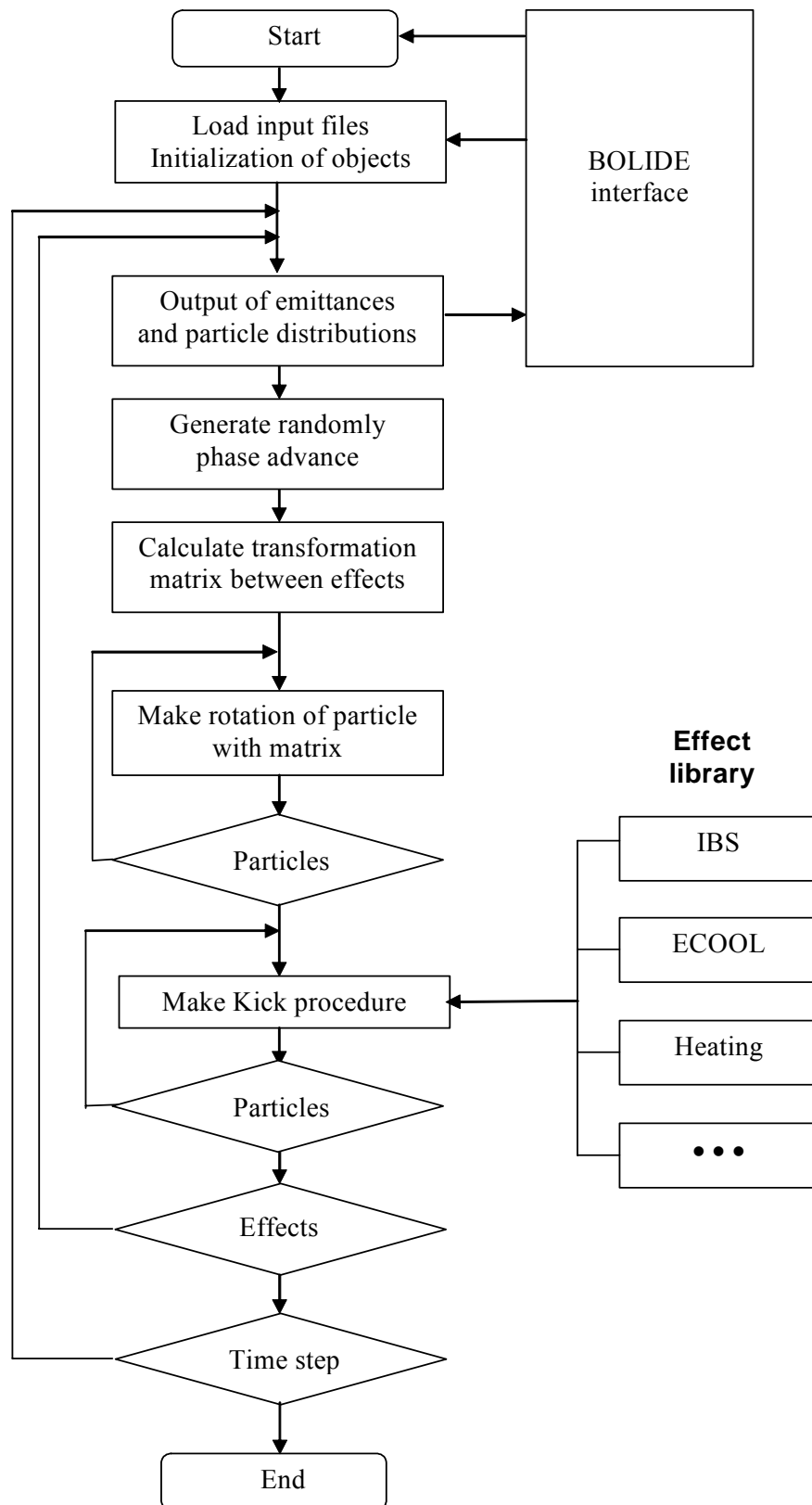


Fig. 2.1. Block scheme of the Model Beam algorithm.

The **Model Beam** algorithm can be illustrated by the scheme presented in the Fig. 2.1 and includes the following steps:

- initially the storage ring optic structure is loaded from external file (MAD output file), mean ring parameters and RF system parameters are loaded from input BETACOOOL file,
- in the initial position of the ring an array of particles is generated using random number generator and matched with the ring lattice functions and synchrotron function,
- on each cycle over effects the transformation matrix between two effects is calculated from its lattice functions, phase advance is generated with random low,
- each particle is rotated in accordance with transformation matrix,
- kick procedure from the current effect is applied to each particle.

2.2. The beam rotation with the matrix

To avoid the problems related to the beam mismatching and coupling between longitudinal and transverse coordinates the beam rotation in the ring is provided in the following steps.

The betatron coordinates are transformed in accordance with the coefficients of the ring matrix in the point of the array generation:

$$\begin{pmatrix} x \\ x' \end{pmatrix}_{i+1} = \begin{pmatrix} R_{11} & R_{12} \\ R_{21} & R_{22} \end{pmatrix} \begin{pmatrix} x \\ x' \end{pmatrix}_i, \quad \begin{pmatrix} y \\ y' \end{pmatrix}_{i+1} = \begin{pmatrix} R_{33} & R_{34} \\ R_{43} & R_{44} \end{pmatrix} \begin{pmatrix} y \\ y' \end{pmatrix}_i, \quad (2.3)$$

where notation of the matrix coefficients is explained in the following table:

$$M_{RING} = \begin{pmatrix} R_{11} & R_{12} & R_{13} & R_{14} & R_{15} & R_{16} \\ R_{21} & R_{22} & R_{23} & R_{24} & R_{25} & R_{26} \\ R_{31} & R_{32} & R_{33} & R_{34} & R_{35} & R_{36} \\ R_{41} & R_{42} & R_{43} & R_{44} & R_{45} & R_{46} \\ R_{51} & R_{52} & R_{53} & R_{54} & R_{55} & R_{56} \\ R_{61} & R_{62} & R_{63} & R_{64} & R_{65} & R_{66} \end{pmatrix}. \quad (2.4)$$

The beam rotation in the longitudinal plane is provided with the usual rotation matrix:

$$\begin{pmatrix} s - s_0 \\ \frac{\Delta p}{p} \end{pmatrix}_{i+1} = \begin{pmatrix} \cos \mu & B_s \sin \mu \\ -\frac{1}{B_s} \sin \mu & \cos \mu \end{pmatrix} \begin{pmatrix} s - s_0 \\ \frac{\Delta p}{p} \end{pmatrix}_i, \quad (2.5)$$

where μ value can be arbitrary non-zero.

After the beam rotation in the longitudinal plane new values of the particles transverse co-ordinates are calculated from the betatron ones and new value of the longitudinal momentum deviation.

2.3. Kick procedure at IBS

In the case of IBS calculation using mean growth rates, the mean growth rates are calculated in accordance with one of the analytical model developed in BETACOOOL and the ring structure loaded from output MAD file. When the growth rates are known one can calculate mean square of

the scattering angle taking into account multiplication factor. The mean square angle after one revolution in the ring is equal:

$$\langle \theta^2 \rangle = \frac{\varepsilon}{\beta} \frac{T_{rev}}{\tau}, \quad (2.6)$$

where β is the beta function in the point of the particle array generation, τ is characteristic growth time in corresponding degree of freedom. Here the angular deviation of the particle trajectory means relative momentum components: $\theta_{x,y} = \frac{p_{x,y}}{p}$, $\theta_s = \frac{\Delta p}{p}$. After N_{turn} revolutions in the ring the square of the scattering angle is equal to the sum of the square angles at each revolution:

$$\langle \theta^2 \rangle = \frac{\varepsilon}{\beta} \frac{T_{rev}}{\tau} N_{turn}. \quad (2.7)$$

The variation of the particle trajectory angular deviation is calculated in accordance with

$$\Delta\theta = \sqrt{\langle \theta^2 \rangle} \cdot \xi \quad (2.8)$$

where ξ is the random value with Gaussian distribution at unit dispersion.

2.4. Kick procedure at ECOOL

In the frame of Model Beam algorithm the action of the electron cooling on the ion momentum components is calculated in accordance of the cooler representation as a thin lens. In this case the ion angle variation is calculated in accordance with

$$\Delta\theta = \frac{F}{Mc^2\beta^2\gamma} l_{cool} N_{turn}, \quad (2.9)$$

where F is the friction force in LRF, M is the ion mass, l_{cool} is the cooling section length, N_{turn} is the revolutions number using as a multiplication factor. The ion co-ordinates are not changed inside cooler. The friction force components can be calculated using all the friction force formulae and all the models of electron beam developed in the BETACOOOL.

2.5. Kick procedure at Additional Heating

Additional Heating effect can apply four different kinds of kicks. An angle variation in the case of constant and linear heating (or cooling) is calculated with formula:

$$\Delta\theta_i = \theta_i \times \begin{cases} \frac{b}{\varepsilon_i} \cdot \frac{T_{rev}}{\tau_i} N_{turn}, & \frac{b}{\varepsilon_i} \cdot \frac{T_{rev}}{\tau_i} N_{turn} > -1 \\ \exp\left(\frac{b}{\varepsilon_i} \cdot \frac{T_{rev}}{\tau_i} N_{turn}\right) - 1, & \frac{b}{\varepsilon_i} \cdot \frac{T_{rev}}{\tau_i} N_{turn} \leq -1 \end{cases}, \quad (2.10)$$

where θ_i – angles, $i=0\div 2$ – index of degree of freedoms: $i = 0$ – horizontal, $i = 1$ – vertical, $i = 2$ – longitudinal, T_{rev} – revolution frequency, τ_i – heating growth rates, N_{turn} – number of turns, $b = 1$ for any case and $b = 2$ for longitudinal direction in the case of bunch beam. In the case of constant rates $\varepsilon_i = 1$. In the case of linear rates ε_0 corresponds to horizontal emittance, ε_1 corresponds to vertical emittance, ε_2 corresponds to momentum spread in accordance with Eq.(1.3).

The diffusion heating applies random kicks to momentums of ions. In the case of diffusion heating with constant power the kick doesn't depend on the current values of emittances. In other case the diffusion heating kick depends on current emittances:

$$\begin{aligned}\Delta\theta_{hor} &= \theta_{hor} \sqrt{\frac{4}{\beta_x} \cdot \frac{T_{rev}}{\tau_{hor}} N_{turn} \cdot \varepsilon_{hor}^a} \cdot \xi \\ \Delta\theta_{ver} &= \theta_{ver} \sqrt{\frac{4}{\beta_y} \cdot \frac{T_{rev}}{\tau_{ver}} N_{turn} \cdot \varepsilon_{ver}^a} \cdot \xi \\ \Delta\theta_{lon} &= \theta_{lon} \sqrt{2b \cdot \frac{T_{rev}}{\tau_{lon}} N_{turn} \cdot \varepsilon_{lon}^a} \cdot \xi\end{aligned}\tag{2.11}$$

where β_x, β_y are horizontal and vertical beta functions, $a = 1$ for diffusion heating with constant power and $a = -1$ for diffusion heating which depends on current emittances, ξ is the random value with Gaussian distribution at unit dispersion.

Here presented the program code of Kick procedure for Additional Heating effect:

```
void xHeat::Kick (xTime&time, xBeam&beam, xRing&ring)
{
    beam.Emit = beam.Get_Emit(Lattice);
    double r[3], k = 1;
    if (beam.bunched) k = 2;
    if (rate)
    {
        for (int i = 0; i < 3; i++)
        {
            r[i] = (Rate[i]*time.dt)(U1_);
            if(i == 2)
                r[i] *= k / 2.;
            if(r[i] > -1.)
                r[i] += 1.;
            else
                r[i] = exp(r[i]);
        }
        for (int j = 0; j < beam.Number(); j++)
            for (int i = 0; i < 3; i++)
                beam(j, i*2+1, beam(j, i*2+1) * r[i]);
    }
    if (linear)
    {
        for (int i = 0; i < 3; i++)
        {
            r[i] = (Linear[i]*time.dt/beam.Emit[i])(U1_);
            if(i == 2)
                r[i] *= k / 2.;
            if(r[i] > -1.)
                r[i] += 1.;
            else
                r[i] = exp(r[i]);
        }
        for (int j = 0; j < beam.Number(); j++)
            for (int i = 0; i < 3; i++)
```



```

        beam(j, i*2+1, beam(j, i*2+1) * r[i]);
    }
    if (power)
    {
        r[0] = ((2*Power[0]*time.dt*2*beam.Emit[0]/Lattice.betax)^0.5)(U1_);
        r[1] = ((2*Power[1]*time.dt*2*beam.Emit[1]/Lattice.betay)^0.5)(U1_);
        r[2] = ((k*Power[2]*time.dt*2*beam.Emit[2]
                )^0.5)(U1_);
        for (int j = 0; j < beam.Number(); j++)
            for (int i = 0; i < 3; i++)
                beam.Add(j, i*2+1, r[i] * xDistributor::Gaussian());
    }
    if (diffusion)
    {
        r[0] = ((2*Diffusion[0]*time.dt*2/beam.Emit[0]/Lattice.betax)^0.5)(U1_);
        r[1] = ((2*Diffusion[1]*time.dt*2/beam.Emit[1]/Lattice.betay)^0.5)(U1_);
        r[2] = ((k*Diffusion[2]*time.dt*2/beam.Emit[2]
                )^0.5)(U1_);
        for (int j = 0; j < beam.Number(); j++)
            for (int i = 0; i < 3; i++)
                beam.Add(j, i*2+1, r[i] * xDistributor::Gaussian());
    }
}

```

3. Multi Particle Tracking

3.1. Algorithm of the calculations

To provide simulation of the ion distribution function evolution in time one needs to develop algorithm resolving the following problems: to simulate dynamics of a large number of particles from one hand and to simulate a large number of the revolution in the ring from the other hand.

There are two possibilities to reduce number of particles involved into calculations. For a coasting ion beam one can use Molecular Dynamics technique. In this case the motion equations are solved for small number of particles located inside a short cell. Influence of all other particles is tacking into account through periodic boundary conditions for the particle distribution function and usage of Evald's sum for calculation of Coulomb forces.

For bunched beam one can simulate the beam dynamics using so called "macro" particles, each of them has charge to mass ratio the same as a real particle, but the mass of the macro particle is larger than the mass of real particle by the factor of the particle increase. Macro particle dynamics simulation is necessary to calculate the processes related with the ion beam space charge – first of all for Intrabeam Scattering. Correspondingly number of macro particles required for calculations is determined by the accuracy of the beam space charge calculation. Usually to perform particle distribution function accurately one needs about 10-30 thousand of particles for each degree of freedom or for three dimensional problem of about 100 thousands of particles. Electron cooling and interaction with an internal target are not depending on the ion beam intensity and number of particles required for simulations is determined by the required accuracy of characteristic time calculation and can be of about 10 -20 thousand depending on geometry of the task.

Required period of the beam dynamics calculation follows to characteristic times of investigated processes. Revolution period of a beam inside a storage ring usually is of the order of $10^{-5} - 10^{-6}$ sec. Characteristic times of the general processes, which lead to variation of the beam distribution function, depend on the beam energy, number of particles, target density, luminosity and so on and can be of the order of $10^2 - 10^3$ sec. In more important cases the time of experiment is about one order of magnitude longer. Correspondingly one needs to calculate the particle dynamics during $10^8 - 10^9$ revolutions in the ring.

The problems of the calculation speed and numerical algorithm stability can be solved using Monte Carlo method for the beam dynamics simulation. The algorithm of the Monte Carlo simulations can be realised, for instance, in the following steps:

1. Initially the program generates the beam as a particle array in accordance with initial distribution. Each particle is presented by six-component vector including three co-ordinates and three components of momentum. The array has to be matched with the ring lattice.
2. The invariants of the motion for each particle in the beam are calculated using particle co-ordinates and ring lattice parameters in the particle position.
3. The beam is propagated through the ring by solution of the motion equation in each optic element of the ring.
3. After given number of revolution the new values of the invariants for each particle are calculated.
4. From initial and new values of invariants the rates of invariant variation for each particle are calculated.
5. One makes a step over long period of time - for each particle new values of invariants expected after given long period of time are calculated.
6. New particle co-ordinates are calculated in accordance with ring lattice parameters by random generation of phases of the betatron and synchrotron oscillations.

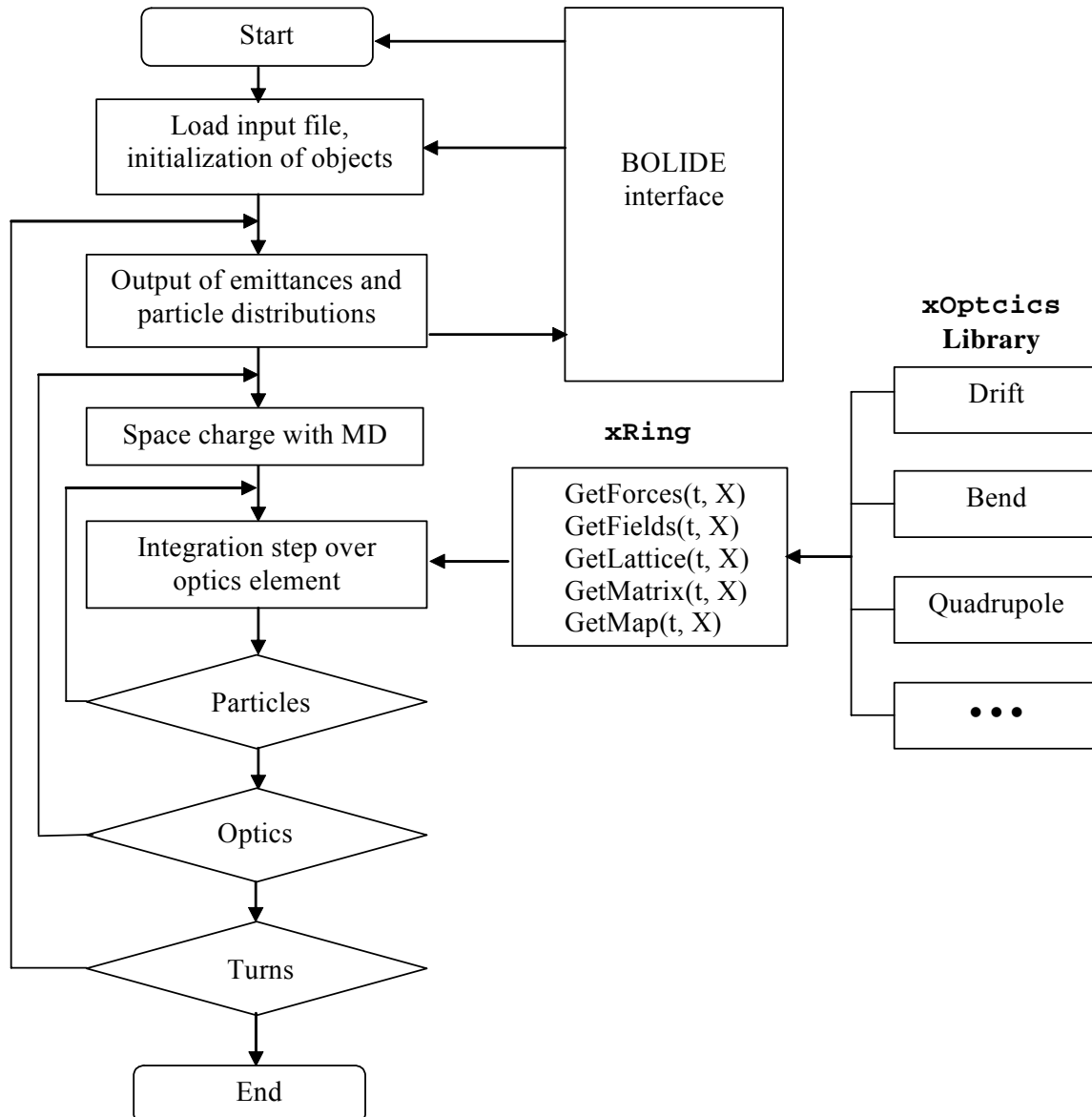


Fig. 3.1 Block-scheme of the Tracking algorithm.

Both the algorithms – Molecular Dynamics and Macro Particle simulations are based on the solution of the particle motion equation in the external electric and magnetic fields taking into account interaction between particles. External fields are calculated for different optic elements of the ring in accordance with the model of the element. The models of the optic elements are collected in the Library of elements – **xOptics**. The ion ring structure is described in an input file. The program is oriented to the input file format using in MAD program and procedures for reading the MAD input file are under development now. The models of general elements of the ring are described in the chapter 3.2.

As a first step for Intrabeam process simulation using multi particle tracking the Molecular Dynamics calculation of the ion beam space charge is realized in the program now. The algorithm of MD simulation is described in the chapter 3.3.

3.2. Models of optic elements

The equations of the particle motion in external fields are solving in the following canonical conjugated variables. Transverse motion is described in the traditional variables: co-ordinate and transverse momentum normalised on the longitudinal momentum. Longitudinal motion is defined by the “scaled arrival time” and the longitudinal momentum spread. The vector of canonical variables is

$$X = \left(x, p_x = \frac{P_x}{P_s}, y, p_y = \frac{P_y}{P_s}, z = -(t - t_0)\beta_0 c, p_z = \frac{E - E_0}{P_s \beta_0 c} \right), \quad (3.1)$$

where x, y are the horizontal and vertical positions, p_x, p_y are the corresponding normalised momenta, z is the “arrival time” of the particle multiplied by $-c\beta_0$, p_z is the normalised momentum deviation $p_z = \Delta P / P_s$.

A Hamiltonian for studying similar problem - an ordered state of the beam - was derived by J. Wei [5], who used the theory of general relativity. Here, we start from the Hamiltonian with the independent variable s , which gives a slight difference e.g. of the coherent tunes from his Hamiltonian with independent variable t . However this difference is small and the two Hamiltonians should give essentially the same results. The merits of using s as independent variable are:

- a) We found it easier to develop the code this way.
- b) With t as independent variable, and if some particle is longitudinally far away from others, there is large transverse phase difference. So, it is difficult to adapt the MD technique to this system.

Including space charge Hamiltonian in our case can be expressed as:

$$H = -\frac{xp_z}{\rho} + \frac{p_z^2}{2\gamma_0^2} + \frac{p_x^2 + p_y^2}{2} + \frac{x^2}{2\rho^2} + \frac{K_1}{2}(x^2 - y^2) + \frac{K_2}{6}(x^3 - 3xy^2) + \frac{r_{ion}}{\gamma_0^2 \beta_0^2} \sum_i \frac{1}{\sqrt{(x - x_i)^2 + (y - y_i)^2 + \gamma_0^2(z - z_i)^2}}, \quad (3.2)$$

where ρ is the curvature radius of the reference orbit. The effect of multipole components of the magnets is included with the parameters K_1 and K_2 , which are defined as

$$K_1 \equiv \frac{1}{B\rho} \frac{\partial B_y}{\partial x}, \quad K_2 \equiv \frac{1}{B\rho} \frac{\partial^2 B_y}{\partial x^2}, \quad (3.3)$$

where $B\rho = p_0/q$ is the magnetic rigidity. The last term of Eq. (6.2) corresponds to the space charge effect. The Hamiltonian equations of motion is

$$F = \frac{d}{ds} \left(x, p_x, y, p_y, z, p_z \right) = \left(\frac{\partial H}{\partial p_x}, -\frac{\partial H}{\partial x}, \frac{\partial H}{\partial p_y}, -\frac{\partial H}{\partial y}, \frac{\partial H}{\partial p_z}, -\frac{\partial H}{\partial z} \right). \quad (3.4)$$

Each optic element of the ring can be presented as a combination of the forces corresponded to different components of the external fields. Below we present examples of the force components for general types of the fields:

$$\begin{aligned} \text{drift} \quad F_{\text{drift}} &= \left(p_x, 0, p_y, 0, \frac{p_z}{\gamma_0^2}, 0 \right) \\ \text{bend} \quad F_{\text{bend}} &= \left(0, \frac{p_z}{\rho} - \frac{x}{\rho^2}, 0, 0, -\frac{x}{\rho}, 0 \right) \\ \text{quadrupole} \quad F_{\text{quad}} &= (0, -K_1 x, 0, K_1 y, 0, 0) \\ \text{sextupole} \quad F_{\text{sext}} &= \left(0, -\frac{K_2}{2} (x^2 - y^2), 0, K_2 xy, 0, 0 \right). \end{aligned} \quad (3.5)$$

The force acting on the particle inside an optic element is calculated as a sum of the forces corresponded to different types of the fields included in this element. The drift components are included into each element of non zero length. Besides the components of the field, each optic element includes also procedures describing action of the fringe fields at the entrance and at the exit of element. Different types of the optic elements are collected in the optic library. The ring structure in the input file includes an array of the pointer to the optic element type and values of all the field components for each concrete element.

For solution of the motion equations two integration methods can be used: Runge-Kutta and symplectic integrator of the 1st order. Runge-Kutta method is well-known and reliable. A shortcoming is that this method does not satisfy to symplecticity condition i.e. energy conservation. So, the step value Δs should be given properly in order to do not have large energy error.

The Runge-Kutta procedure can be written in the vector form as (“Euler method”)

$$\bar{X} = X + \Delta s \times \sum_j F_j(X). \quad (3.6)$$

Here the bar means new value of the variable, i.e. X and \bar{X} - are the co-ordinate vectors before and after of the integration step, $F_j(X)$ - any force from (3.5), which are derived from differentiation of Hamiltonian (3.2).

The symplectic integrator of 1st order in the vector form is

$$\begin{aligned}
\bar{X} &= X + \Delta s \times \sum_j F_j(X) \\
\bar{F} &= \sum_j F_j(\bar{X}) \\
\bar{\bar{X}}[x, y, z] &= \bar{X}[x, y, z] + \Delta s \times \bar{F}[x, y, z]
\end{aligned} \tag{3.7}$$

First step (3.7) looks like simple Euler method. On the next step we calculate the force with the new vector of coordinates. And on last step, we recalculate the coordinates using the new vector of forces keeping new normalised momenta, as calculated on first step.

3.3. Molecular Dynamics

Since the calculation of the space-charge effect is time consuming, we approximate the situation using a periodic boundary condition, or Molecular Dynamics (MD) technique [2, 5]. When ions of charge $q=Ze$ are set at position $(s, r)=(0,0),(\pm L,0),(\pm 2L,0),\dots$ the electrostatic potential in the region $|s| < L/2$ is [2]

$$U_{sc}(s, r) = \frac{1}{4\pi\epsilon_0} \left(\frac{q}{a} + \frac{2q}{L} \int_0^\infty \frac{J_0(kr/L) \cosh(ks/L) - 1}{\exp(k) - 1} dk \right), \tag{3.8}$$

where q - particle charge, $a = \sqrt{s^2 + r^2}$ - distance between particles, $s = z - z_i$, $r = \sqrt{(x - x_i)^2 + (y - y_i)^2}$, L - MD cell size, J_0 is the Bessel function of 0th order. The space charge force vector from the i -th particle for optics library (6.5) can be derived from Eq.(6.8):

$$F_{MD} = (0, F_{px}, 0, F_{py}, 0, F_{pz}). \tag{3.9}$$

Here

$$\begin{aligned}
F_{px} &= \frac{1}{4\pi\epsilon_0} \frac{q^2(x - x_i)}{m_0 c^2 \gamma_0^2 \beta_0^2} \left(\frac{1}{a^3} - \frac{2I_1}{rL^2} \right), \\
F_{py} &= \frac{1}{4\pi\epsilon_0} \frac{q^2(y - y_i)}{m_0 c^2 \gamma_0^2 \beta_0^2} \left(\frac{1}{a^3} - \frac{2I_1}{rL^2} \right), \\
F_{pz} &= \frac{1}{4\pi\epsilon_0} \frac{q^2(z - z_i)}{m_0 c^2 \gamma_0^2 \beta_0^2} \left(\frac{1}{a^3} - \frac{2I_0}{sL^2} \right),
\end{aligned} \tag{3.10}$$

where

$$I_1 = -\int_0^\infty \frac{k J_1(kr/L) \sinh(ks/L) - 1}{\exp(k) - 1} dk, \quad I_0 = -\int_0^\infty \frac{k J_0(kr/L) \cosh(ks/L) - 1}{\exp(k) - 1} dk, \tag{3.11}$$

J_1 is the Bessel function of 1st order, $m_0 c^2$ - ion rest mass. Integrals I_1 and I_0 were numerically calculated and are used in the program as table values.

To calculate IBS process using MD technique one needs to determine the particle number using in the calculations N_{cell} in accordance with the required accuracy. Then the cell length is calculated in accordance with:

$$L = \frac{N_{cell}}{N} C, \quad (3.12)$$

where C is the ring circumference, N is the ion number in the ring. The initial distribution of the particles inside the cell is generated randomly in accordance with the beam emittance and the ring lattice parameters in the initial position. Transverse particle co-ordinates and momentum components are generated in accordance with Gaussian law, longitudinal co-ordinates are distributed uniformly inside the cell. Thereafter the particles in the sell are propagated through the ring element by element in accordance with the ring structure described in the input file. The interaction between particles is calculated in accordance with the formulae (3.10).

3.4. Crystalline beams

Tracking algorithm based on Molecular Dynamics (MD) technique can be used for the simulation of crystalline ion beams. For a test of the validity of the new code an infinite constant focusing structure was used where the linear Hamiltonian is

$$H = \frac{1}{2} \left(p_x^2 + p_y^2 + \frac{p_z^2}{\gamma_0^2} \right) + \frac{k}{2} (x^2 + y^2) + \frac{r_{ion}}{\gamma_0^2 \beta_0^2} \sum_i \frac{1}{\sqrt{(x - x_i)^2 + (y - y_i)^2 + \gamma_0^2 (z - z_i)^2}}, \quad (3.13)$$

Here p_x, p_y, p_z, x, y, z are normalized momenta and corresponding coordinates, γ_0, β_0 — relativistic factors, k - gradient of the focusing structure. Fist member of Hamiltonian corresponds to the kinetic energy of particles, second one is a focusing element and third one is a space charge effect.

The shape of the crystals depends on the dimensionless linear density of particles (Fig.2.1). A linear density is defined as:

$$\lambda_{ion} \equiv \frac{N}{C} \left(\frac{3 r_{ion}}{2 k \gamma_0^5 \beta_0^2} \right)^{1/3} = \left(\frac{3 N^3 r_{ion}}{8 \pi^2 Q^2 C \gamma_0^5 \beta_0^2} \right)^{1/3}, \quad (3.14)$$

where N – particle number in the ring, C – ring circumference, $\beta_0 = v_0/c$ – relativistic factor, Q – betatron tune, r_{ion} –classical ion radius:

$$r_{ion} = \frac{1}{4\pi\epsilon_0} \frac{Z^2 e^2}{A m_p c^2}. \quad (3.15)$$

here m_p – proton mass, c – light speed.

Results of the calculation show good agreement with the theory of crystalline beams [6]: transitions between different states appear for the characteristic values of λ_{ion} , Eq.(3.14), indicated in Fig.3.2.

String ($\lambda_{ion} < 0.709$)

Zigzag ($0.709 < \lambda_{ion} < 0.964$)

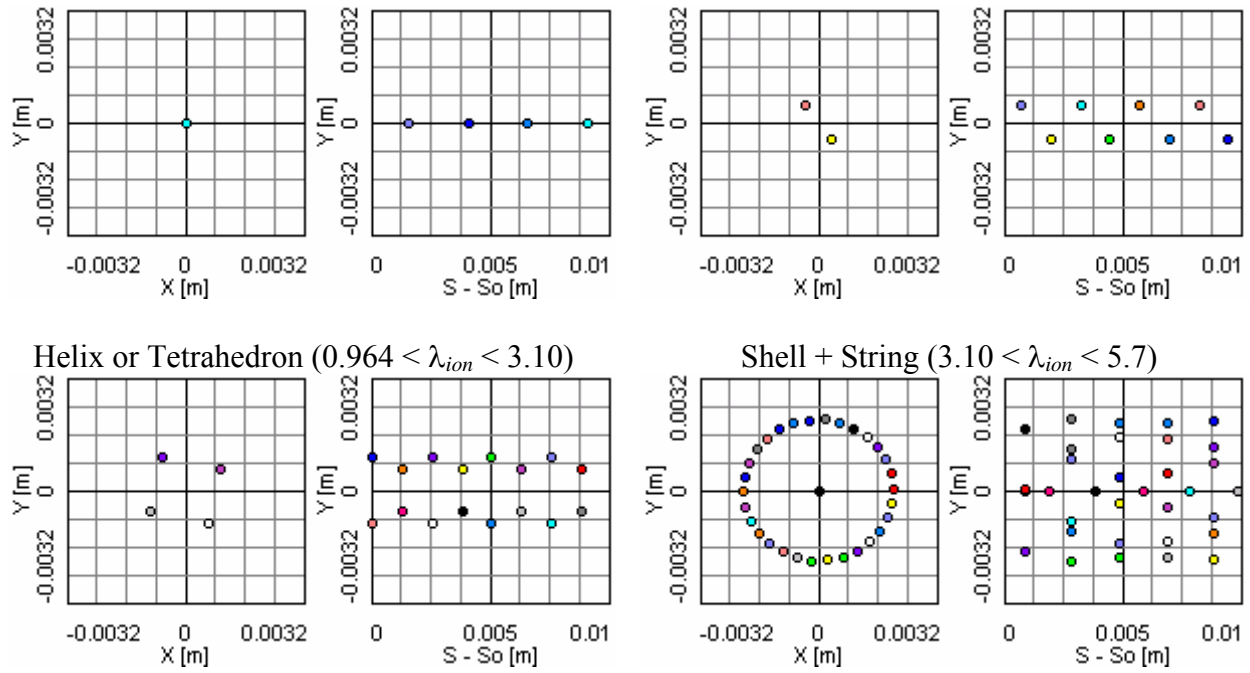


Fig.3.2. Crystalline beams in a straight (infinite) channel with constant focusing for different linear density.

References

- [1] I.N.Meshkov, A.O.Sidorin, A.V.Smirnov, E.M.Syresin, G.V.Trubnikov, P.R.Zenkevich, "Simulation of Electron Cooling Process in Storage Rings Using BETACOOOL Program" , Proceedings of Beam Cooling and Related Topics, Bad Honnef, Germany, 2001.
- [2] V.Avilov, "Calculation of Electrostatic Energy of Planar Lattices", Solid State Communications, v.44, No.4 p.555-558 (1982).
- [3] M. Martini. Intrabeam scattering in the ACOOL-AA machines. CERN PS/84-9 AA, Geneva (1984).
- [4] V.Parkhomchuk, New insights in the theory of electron cooling, NIM A 441 (2000) 9-17, p.9
- [5] J. Wei, X.P. Li, and A.M. Sessler, "Crystalline Beam Ground State", BNL-52381 (1993).
- [6] R.Hasse, J.Schiffer. "The Structure of the Cylindrical Confined Coulomb Lattice". Annals of Physics **203** (1990) p.419.

II. Electron Cooling

1. Introduction

The traditional electron cooling system [1] applied up to now is based on electron beam generated with electrostatic electron gun in DC operation mode, immersed in a longitudinal magnetic field. The magnetic field is used for electron beam transport through the cooling section from the gun to collector. The field value is determined by condition of electron “magnetization” – radius of the electron Larmor rotation in the transverse plane has to be less than mean distance between electrons. In this case intrabeam scattering in the electron beam is suppressed and electron beam keeps a non-equilibrium “flattened” velocity distribution, which appears due to the electrostatic acceleration.

Usually an action of electron cooling on the ion dynamics inside a storage ring is described using a few standard simplifications:

1. Angular deviation of the longitudinal magnetic field line is substantially less than the ion beam angular spread.
2. Ion transverse displacement inside the cooling section is substantially less than electron beam radius.
3. Ion beam temperature is substantially larger than electron one and ion diffusion in the electron beam can be neglected.
3. Electron beam has a round shape of cross-section and uniform density distribution in the radial direction.

Under these assumptions and using asymptotic of the analytical friction force presentation the formulae for characteristic times of emittance and momentum spread decrease at electron cooling were obtained [2]. Depending on the ion and electron beam parameters one can use a few analytical models of the friction force. In some cases for accurate simulation of the cooling process results of numerical calculation of the friction force is necessary.

In the last time modifications of the usual configuration of the electron cooling system were proposed. To avoid instability of the ion beam related with extremely large density of the cooled beam it was proposed to use so called “hollow” electron beam – the beam at small density in the central part. Extension of the electron cooling method in the region of electron energy of a few MeV related with an RF acceleration of the electrons. In this case one can expect Gaussian distribution of the electrons in radial plane and, if the electron bunch is shorter than the ion one, in longitudinal direction also. Calculation of the cooling times in this case requires modification both the electron beam model and the base physical model.

Other expected peculiarity of the medium energy cooling system is a big length of the cooling section – up to about 20 - 50 m. To obtain very high accuracy of the magnetic field is difficult technical task and cost of the cooling system will strongly depend on the required level of the accuracy. Therefore, before design of the cooling section solenoid, one needs to investigate influence of the magnetic field line curvature on the cooling process. All the effects can be taken into account by numerical solution of the ion motion equations in the cooling section.

To solve all the problems related with the cooling process simulation a hierarchy of objects was developed in the frame of the BETACOOOL program. Structure of the electron cooler presentation permits to extract procedures of different levels and to include them into calculation of the cooling process in other programs. The cooling simulation is based on a friction force calculation in the

particle rest frame. The next layer of the simulation is related with a cooler representation as a map, transforming particle coordinates from entrance to the exit of the cooling section. The map of the cooler can be used directly in the frame of the Molecular Dynamics algorithm, or in other tracking procedures. On the basis of the map one can calculate kick of the ion momentum after crossing the cooling section that is necessary for simulation of the ion distribution evolution in the frame of the Model Beam algorithm. The map of the cooler is used also for the cooling rate calculation that is necessary for RMS dynamics simulation.

In this chapter we describe structure of the electron cooler representation. Briefly we discuss the theory of the friction force calculation based on the binary collision model and describe analytical models for the friction force calculation using in the BETACOOOL. Calculation of the cooler map is based on a model of electron beam that provide transformation of the ion velocity to the frame related with the electron beam and takes into account real geometry of the cooler. Now in the BETACOOOL three models of electron beam are available for simulations. Algorithm for calculation of the ion momentum kick after crossing the cooler is described in the chapter 5. The cooling rate calculation can be performed using two model of the ion beam – the cooling rates for “rms particle”, or cooling rates for the ion beam with Gaussian distribution in all degrees of freedom (see chapter 6).

2. Structure of the algorithm

The uniform way of the friction force calculation is an application of the corresponding formulae given in particle reference frame (PRF), which moves with average particle velocity V_0 . For analytical expressions of the friction force the transformation of the ion velocity into PRF and the force components back to laboratory reference frame (LRF) can be provided also analytically and one can use in the calculations the formulae written in LRF. However, numerical calculation of the friction force usually is provided in PRF. To have a possibility to use the same algorithm for analytical expressions and for results of numerical calculations the transformation between the reference frames was realized as a part of cooling calculation algorithm.

In this case the calculation procedure requires transformation of certain parameters from LRF to PRF and, after the calculation of the friction force components in PRF, their transformation back to LRF. For this aim one uses relations between values of the parameters in LRF and PRF. The ion velocity components $V_{x,z}$ in PRF are equal to

$$V_{x,z} = \gamma\beta c \theta_{x,z}, \quad V_s = \beta c \theta_s, \quad (2.1)$$

To transform the friction force components from PRF to LRF the following expressions are used

$$F_{x,z} \equiv (F_{x,z})_{LRF} = \frac{1}{\gamma} (F_{x,z})_{PRF}, \quad F_s \equiv (F_s)_{LRF} = (F_s)_{PRF}. \quad (2.2)$$

Here x, z are the horizontal and vertical co-ordinates, $\theta_{x,z} = \frac{P_{x,z}}{P}$, $\theta_s = \frac{\Delta P}{P}$, $P = \beta\gamma Mc$ is the longitudinal component of the reference particle momentum, $P_{x,z}$ are the transverse components of the ion momentum, ΔP is the longitudinal momentum deviation, $s - s_0$ is the ion longitudinal distance from the bunch center (the reference particle), $\beta = V_0/c$, $\gamma = \sqrt{1 - \beta^2}$, c is the speed of light, V_0 – velocity of the reference particle.

In PRF the friction force is a function of two components of the ion velocity: across and along the magnetic field line (or electron beam axis) and the force has also only two components – transverse and longitudinal. The transverse component of the ion velocity is calculated as:

$$v_{i,\perp} = \sqrt{V_x^2 + V_z^2}. \quad (2.3)$$

The friction force x and z components are calculated from the transverse component in accordance with:

$$F_x = \frac{V_x}{v_{i,\perp}} F_{\perp}, \quad F_z = \frac{V_z}{v_{i,\perp}} F_{\perp}. \quad (2.4)$$

Such a model presumes, that a gradient of the electron beam density is negligible inside a region of effective interaction between ion and electrons.

In the present version of the program the friction force components in FRF can be calculated using one of the analytic formulae from the friction force library:

- Budker's,
- non magnetized,
- by Derbenev – Skrinsky – Meshkov,
- by Parkhomchuk,

described in the next chapter, or input from a file containing results of numerical calculations. (In the case of numerical calculation of the friction force one needs also to transform parameters of the task to the dimensionless form and back.) The library is realized as a set of independent procedures, each of them obtains at the entrance two components of the ion velocity and returns two components of the friction force. Each procedure uses for calculations the same list of input parameters. This list includes the following parameters of the ion and electron beam:

- the ion atomic and charge numbers,
- the magnetic field value,
- local electron transverse and longitudinal velocity spreads,
- local effective electron velocity spread,
- local electron density,
- the ion time of flight the cooling section,
- electron beam radius.

Each procedure of the friction force calculation does not require a total list of these parameters, but for uniform usage of the friction force all the parameters should be determined before the friction force calculation. Transformation of the ion velocity from LRF to PRF, transformation of the friction force components from PRF to LRF and calculation of the list of parameters for friction force calculation are provided by a model of the electron beam. Now in the program the following models of the electron beam are realized:

- cylinder of round cross-section at uniform density distribution,
- cylinder of elliptical cross-section and Gaussian density distribution of electrons in the transverse planes,
- ellipsoidal bunch at Gaussian density distribution in all co-ordinates.

First model of the electron beam corresponds to usual electron cooling system and this model takes into account space charge effects in electron beam. Second and third models are oriented to simulation of the electron cooling in GeV ion energy range. The elliptical cylinder can be used for modeling of coasting electron beam circulating in small ring. The Gaussian bunch corresponds to RF accelerated electron beam. In the future the model of hollow electron beam will be realized.

Usage in the program results of the electron beam dynamics simulation is also possible. Each model of the electron beam calculates the local parameters of the electron beam in the frame referenced to the electron beam orbit.

To take into account displacement and misalignment of the electron beam, an influence of the magnetic field line curvature one needs to provide transformation of the ion co-ordinates and velocity components from the frame referenced to the ion beam equilibrium orbit to the frame referenced to the electron beam orbit and back. In the case of bunched ion and electron beams one needs to transform the ion longitudinal co-ordinate measured relatively to the center of the ion bunch to the distance from the center of the electron bunch. The model of the electron beam provides all these transformations also.

All the models of the electron beam are used by uniform way: the model obtains at the entrance the ion coordinates in the form of vector:

$$\vec{X} = \{x, \theta_x, z, \theta_z, s-s_0, \theta_s\}, \quad (2.5)$$

in the laboratory frame referenced to the ion beam equilibrium orbit and returns three components of the friction force in the same frame.

The electron cooler representation in the form of map (which is necessary for tracking procedures) is based on the electron beam model. The right hand sides of the motion equation are calculated by addition to the force components the terms describing drift motion of the ion in the cooling section. Influence of the magnetic field and space charge fields of the electron beam as well as the ion motion distortion at the entrance of the cooling section can be tacking into account also. The solution of the ion motion equation is provided by one of the numerical methods developed in the program. Now the ion motion equation can be solved in the frame of thin lens approximation or by solution of the motion equation using Euler or forth order Runge-Kutta method.

The map of the cooler obtains at the entrance the initial ion co-ordinates and returns the ion co-ordinates at the exit of the cooler and probability of the ion loss due to recombination with electrons. The particle loss probability is calculated under assumption that the ion velocity is less than electron one.

The map of the cooler is used as a basis for electron cooling representation as effect acting on the ion distribution function. Electron cooling as effect includes two standard procedures. One of them provides kick of the momentum components for all ions in the model beam and calculates the particle losses due to recombination in the cooling section. Other procedure calculates characteristic times of the ion beam rms emittance variation and the beam lifetime. The characteristic times can be calculated using two model of the ion beam: single particle cooling times and cooling times for Gaussian beam obtained using Monte-Carlo method. Electron cooling as effect obtains at the entrance the ion beam in one of the form using in the program and returns the ion beam in the same form with parameters changed by action of the electron cooling.

The described structure of the electron cooling object permits to use uniformly all the models developed at the same layer of the hierarchy. Each model at some level can use all the models at the lower layers in arbitrary combination. Each layer of the hierarchy can be extracted from the BETACOOOL and used as an independent object in another program.

3. Friction force in the particle rest frame

3.1. Non-magnetized electron beam

3.1.1. Binary collision model

The friction force acting on ion is determined by Coulomb collisions with electrons (Fig. 3.1). The electron at velocity v_e in the PRF colliding with the ion which has velocity V at impact parameter ρ obtains the transverse momentum Δp_{\perp} relatively to the vector $\vec{U} = \vec{V} - \vec{v}_e$:

$$p_{\perp} \equiv \Delta p_{\perp} = \frac{2Ze^2}{|\vec{V} - \vec{v}_e| \rho}, \quad (3.1)$$

Ze , e are the charges of the ion and electron. Due to conservation of the total particle momentum $p_{\mu} = \text{const}$ the appearance of the transverse momentum p_{\perp} of electron leads to the following change of its longitudinal momentum:

$$\Delta p_{\parallel} = p_{\mu} - \sqrt{p_{\mu}^2 - \Delta p_{\perp}^2} \approx \frac{(\Delta p_{\perp})^2}{2p_{\mu}}. \quad (3.2)$$

The electron energy changes herewith by the value:

$$\Delta E_e = \frac{\Delta p_{\perp}^2}{2m}, \quad (3.3)$$

which is equal to the change of the ion energy ΔE_i . Here m is the electron mass.

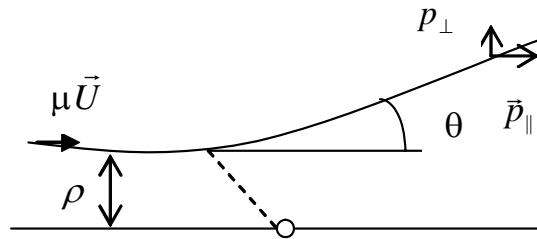


Fig. 3.1. Two-body problem

Integration over impact parameter ρ gives us the ion energy loss per unit of the length:

$$\frac{dE_i}{ds} = 2\pi \int_{\rho_{\min}}^{\rho_{\max}} n_e \Delta E_i \rho d\rho, \quad (3.4)$$

Here n_e is the electron density, ρ_{\max} , ρ_{\min} – minimum and maximum impact parameters of the collision. The minimal impact parameter ρ_{\min} approximately corresponds to electron scattering by

the angle of $\pi/2$. The maximum impact parameter corresponds to the distance between particles when the effective interaction is possible. The friction force in the extremely cold electron beam is equal to:

$$F = -\frac{dE_i}{ds} = -\frac{4\pi Z^2 n_e e^4}{mV^2} \ln \frac{\rho_{\max}}{\rho_{\min}}. \quad (3.5)$$

3.1.2. Numerical integration

When the electrons are distributed over velocities in accordance with the function $f(v_e)$ the friction force can be evaluated by numerical integration of the following formula

$$\vec{F} = -\frac{4\pi n_e e^4 Z^2}{m} \int \ln \left(\frac{\rho_{\max}}{\rho_{\min}} \right) \frac{|\vec{V} - \vec{v}_e|}{|\vec{V} - \vec{v}_e|^3} f(v_e) d^3 v_e. \quad (3.6)$$

The Coulomb logarithm $\ln \frac{\rho_{\max}}{\rho_{\min}}$ is kept under the integral because the minimal impact parameter depends on electron velocity:

$$\rho_{\min} = \frac{Ze^2}{m} \frac{1}{|\vec{V} - \vec{v}_e|^2}. \quad (3.7)$$

In the case of uniform velocity distribution of electrons, the electron beam can be described by the temperature T_e and r.m.s. electron velocity spread Δ_e , that are connected with each other in accordance with

$$T_e = m\Delta_e^2 \quad (3.8).$$

At given value of the ion velocity the maximum impact parameter is constant and it is determined by dynamic shielding radius or the ion time of flight through the electron cloud. Radius of the dynamic shielding sphere coincides with Debye radius:

$$\rho_D = \frac{\Delta_e}{\omega_p}, \quad (3.9)$$

when the ion velocity is less than the electron r.m.s velocity spread Δ_e . The plasma frequency ω_p is equal to

$$\omega_p = \sqrt{\frac{4\pi n_e e^2}{m}}. \quad (3.10)$$

When the ion velocity sufficiently larger than the electron velocity spread it determines the shielding radius

$$\rho_{sh} = \frac{V}{\omega_p}. \quad (3.11)$$

The both formulae (3.9) and (3.11) can be combined together to have a smooth dependence of the shielding radius on the ion velocity:

$$\rho_{sh} = \frac{\sqrt{V^2 + \Delta_e^2}}{\omega_p}. \quad (3.12)$$

In the case, when the shielding sphere does not contain big enough number of electrons to compensate the ion charge (such a situation takes a place in the case of magnetized electron beam at low longitudinal velocity spread) it has to be increased in accordance with the electron beam density and the ion charge. In the program this radius is estimated from the expression

$$n_e \rho^3 \sim 3Z. \quad (3.13)$$

As a result, the maximum impact parameter is calculated as a minimum from three values:

$$\rho_{\max} = \min \left\{ \max \left(\rho_{sh}, \sqrt[3]{\frac{3Z}{n_e}}, V\tau \right) \right\}. \quad (3.14)$$

The second term describes the distance, which the ion passes inside the electron beam. Here τ is the ion time of flight the cooling section in the PRF:

$$\tau = \frac{l_{cool}}{\beta\gamma c}. \quad (3.15)$$

In the case of axial symmetry the electron distribution function can be written in the following form:

$$f(v_e) = \left(\frac{1}{2\pi} \right)^{3/2} \frac{1}{\Delta_{\perp}^2 \Delta_{\parallel}} \exp \left(-\frac{v_{\perp}^2}{2\Delta_{\perp}^2} - \frac{v_{\parallel}^2}{2\Delta_{\parallel}^2} \right), \quad (3.16)$$

where Δ_{\perp} and Δ_{\parallel} are the electron rms velocity spreads in the transverse and longitudinal direction correspondingly.

Asymmetry of the electron distribution function can appear, for instance, due to electrostatic acceleration of the electron beam. In this case the temperatures of transverse and longitudinal degrees of freedom are different:

$$T_{\perp} \approx T_{cathode} + T_{optics}, \quad T_{\parallel} = \frac{T_{cathode,eff}^2}{\beta^2 \gamma^2 mc^2} + e^2 n_e^{1/3}, \quad (3.17)$$

where $T_{cathode}$ is the cathode temperature, T_{optics} describes an additional transverse velocity spread due to distortions during electron beam transportation to the cooling section (this temperature includes also the incoherent drift motion in the crossed fields (see chapter 4.2.)). The effective cathode temperature used for longitudinal temperature calculation includes a term determined by amplitude of the accelerating voltage ripple.

In the general case, for instance at RF electron beam acceleration, the temperatures of the transverse and longitudinal degrees of freedom can be calculated from electron beam parameters as follows:

$$\begin{aligned} T_{\perp} &= mc^2 \beta^2 \gamma^2 \theta^2, \\ T_{\parallel} &= mc^2 \beta^2 \left(\frac{\Delta p}{p} \right)^2, \end{aligned} \quad (3.18)$$

where θ is r.m.s. angular spread and $\Delta p/p$ – r.m.s. momentum spread of electrons in the cooling section. The angular spread can be a function of radial co-ordinates due to the drift motion of electrons or oscillations of the beam envelope. The relation between temperatures and corresponding rms velocity spread is determined similarly to formula (3.8):

$$\begin{aligned} T_{\parallel} &= m \Delta_{\parallel}^2, \\ T_{\perp} &= m \Delta_{\perp}^2. \end{aligned} \quad (3.19)$$

The shielding cloud in the case of non uniform distribution has an ellipsoidal shape which can be approximated by the sphere of radius calculated using effective electron velocity spread:

$$\Delta_e^2 = \Delta_{\perp}^2 + \Delta_{\parallel}^2. \quad (3.20)$$

The components of the friction force (1.1) can be calculated in cylindrical co-ordinate system as follows:

$$\begin{aligned} F_{\perp} &= -\sqrt{\frac{2}{\pi}} \frac{Z^2 e^4 n_e}{m \Delta_{\perp}^2 \Delta_{\parallel}} \int_0^{\infty} \int_{-\infty}^{\infty} \int_0^{2\pi} \ln \left(\frac{\rho_{\max}}{\rho_{\min}} \right) \frac{(V_{\perp} - v_{\perp} \cos \varphi) \exp \left(-\frac{v_{\perp}^2}{2\Delta_{\perp}^2} - \frac{v_{\parallel}^2}{2\Delta_{\parallel}^2} \right)}{\left((V_{\parallel} - v_{\parallel})^2 + (V_{\perp} - v_{\perp} \cos \varphi)^2 + v_{\perp}^2 \sin^2 \varphi \right)^{3/2}} v_{\perp} d\varphi dv_{\parallel} dv_{\perp}, \\ F_{\parallel} &= -\sqrt{\frac{2}{\pi}} \frac{Z^2 e^4 n_e}{m \Delta_{\perp}^2 \Delta_{\parallel}} \int_0^{\infty} \int_{-\infty}^{\infty} \int_0^{2\pi} \ln \left(\frac{\rho_{\max}}{\rho_{\min}} \right) \frac{(V_{\parallel} - v_{\parallel}) \exp \left(-\frac{v_{\perp}^2}{2\Delta_{\perp}^2} - \frac{v_{\parallel}^2}{2\Delta_{\parallel}^2} \right)}{\left((V_{\parallel} - v_{\parallel})^2 + (V_{\perp} - v_{\perp} \cos \varphi)^2 + v_{\perp}^2 \sin^2 \varphi \right)^{3/2}} v_{\perp} d\varphi dv_{\parallel} dv_{\perp}. \end{aligned} \quad (3.21)$$

In numerical calculations, within an accuracy of about 2% the upper limit of the integrals over velocity components can be replaced from infinity to three corresponding rms values and integration over φ can be performed from 0 to π due to symmetry of the formulae. In this case the friction force components can be calculated as:

$$\begin{aligned} F_{\perp} &= -\frac{4\pi Z^2 e^4 n_e}{m \cdot \text{Int}} \int_0^{3\Delta_{\perp}} \int_{-3\Delta_{\parallel}}^{3\Delta_{\parallel}} \int_0^{\pi} \ln \left(\frac{\rho_{\max}}{\rho_{\min}} \right) \frac{(V_{\perp} - v_{\perp} \cos \varphi) \exp \left(-\frac{v_{\perp}^2}{2\Delta_{\perp}^2} - \frac{v_{\parallel}^2}{2\Delta_{\parallel}^2} \right)}{\left((V_{\parallel} - v_{\parallel})^2 + (V_{\perp} - v_{\perp} \cos \varphi)^2 + v_{\perp}^2 \sin^2 \varphi \right)^{3/2}} v_{\perp} d\varphi dv_{\parallel} dv_{\perp}, \\ F_{\parallel} &= -\frac{4\pi Z^2 e^4 n_e}{m \cdot \text{Int}} \int_0^{3\Delta_{\perp}} \int_{-3\Delta_{\parallel}}^{3\Delta_{\parallel}} \int_0^{\pi} \ln \left(\frac{\rho_{\max}}{\rho_{\min}} \right) \frac{(V_{\parallel} - v_{\parallel}) \exp \left(-\frac{v_{\perp}^2}{2\Delta_{\perp}^2} - \frac{v_{\parallel}^2}{2\Delta_{\parallel}^2} \right)}{\left((V_{\parallel} - v_{\parallel})^2 + (V_{\perp} - v_{\perp} \cos \varphi)^2 + v_{\perp}^2 \sin^2 \varphi \right)^{3/2}} v_{\perp} d\varphi dv_{\parallel} dv_{\perp}, \end{aligned} \quad (3.22)$$

where the normalization factor is calculated in accordance with:

$$Int = \int_0^{3\Delta_{\perp}} \int_{-3\Delta_{\parallel}}^{3\Delta_{\parallel}} \int_0^{\pi} \exp\left(-\frac{v_{\perp}^2}{2\Delta_{\perp}^2} - \frac{v_{\parallel}^2}{2\Delta_{\parallel}^2}\right) v_{\perp} d\varphi dv_{\parallel} dv_{\perp}. \quad (3.23)$$

The minimal impact parameter is the following function of the electron velocity components:

$$\rho_{\min} = \frac{Ze^2}{m_e} \frac{1}{(V_{\parallel} - v_{\parallel})^2 + (V_{\perp} - v_{\perp} \cos \varphi)^2 + v_{\perp}^2 \sin^2 \varphi}. \quad (3.24)$$

At the ion velocity $V \gg \Delta_{\parallel}, \Delta_{\perp}$ the minimal impact parameter becomes to be constant:

$$\rho_{\min} = \frac{Ze^2}{m_e} \frac{1}{V_{\perp}^2 + V_{\parallel}^2}, \quad (3.25)$$

and Coulomb logarithm can be removed from the integral. At extremely small ion velocity the calculation of the minimal impact parameter in accordance with the formula (3.25) leads to zero friction force value, when becomes to be $\rho_{\min} > \rho_{\max}$. One can avoid this problem introducing mean minimal impact parameter in accordance with

$$\rho_{\min} = \frac{Ze^2}{m_e} \frac{1}{V_{\perp}^2 + V_{\parallel}^2 + \Delta_{\perp}^2 + \Delta_{\parallel}^2}. \quad (3.26)$$

When the Coulomb logarithm L_C is constant the two of three integrals in (3.21) can be calculated analytically and the friction force components can be written in accordance with Binney's formulae []:

$$\begin{aligned} F_{\perp} &= 2\sqrt{2\pi} \frac{n_e e^4 Z^2 L_C}{m} \frac{V_{\perp}}{\Delta_{\perp}^3} B_{\perp} \\ F_{\parallel} &= 2\sqrt{2\pi} \frac{n_e e^4 Z^2 L_C}{m} \frac{V_{\parallel}}{\Delta_{\perp}^3} B_{\parallel}, \end{aligned} \quad (3.27)$$

where B_{\perp} and B_{\parallel} are the following integrals:

$$\begin{aligned} B_{\perp} &= \int_0^{\infty} \frac{\exp\left(-\frac{V_{\perp}^2}{2\Delta_{\perp}^2} \frac{1}{1+q} - \frac{V_{\parallel}^2}{2\Delta_{\perp}^2} \frac{1}{(\Delta_{\parallel}/\Delta_{\perp})^2 + q}\right)}{(1+q)^2 ((\Delta_{\parallel}/\Delta_{\perp})^2 + q)^{1/2}} dq, \\ B_{\parallel} &= \int_0^{\infty} \frac{\exp\left(-\frac{V_{\perp}^2}{2\Delta_{\perp}^2} \frac{1}{1+q} - \frac{V_{\parallel}^2}{2\Delta_{\perp}^2} \frac{1}{(\Delta_{\parallel}/\Delta_{\perp})^2 + q}\right)}{(1+q) ((\Delta_{\parallel}/\Delta_{\perp})^2 + q)^{3/2}} dq. \end{aligned} \quad (3.28)$$

In the case of uniform Maxwellian distribution (when $\Delta_{\parallel} = \Delta_{\perp} = \Delta_e$) the integrals (3.28) coincide with each other and reproduce Chandrasekhar's formula leading to Budker's formula for cooling time. In Budker's notation the friction force is presented in the following form:

$$\vec{F} = -\frac{\vec{V}}{V^3} \frac{4\pi n_e e^4 Z^2 L_C}{m} \varphi\left(\frac{V}{\Delta_e}\right), \text{ where}$$

$$\varphi(x) = \sqrt{\frac{2}{\pi}} \int_0^x e^{-y^2/2} dy - \sqrt{\frac{2}{\pi}} x e^{-x^2/2}. \quad (3.29)$$

The formulae (3.22) give the same result when the logarithm is removed from the integrals.

3.1.3. Asymptotic representations at flattened velocity distribution

For fast simulation of the cooling process one can use different asymptotic formulae. For instance, on the basis of Coulomb analogy the asymptotic formulae were derived by I. Meshkov in [2], Ya. Derbenev derived the asymptotic formulae for the longitudinal component of the friction force at zero transverse velocity of the ion.

In the case, when transverse velocity spread of electrons is substantially larger than longitudinal one the friction force can be approximated in three ranges of the ion velocity. In accordance with Meshkov's asymptotes the force components are calculated with the following formulae.

I. High velocity $V \geq \Delta_{\perp}$, here longitudinal and transverse components of the friction force are equal:

$$\vec{F} = -\frac{4\pi Z^2 e^4 n_e L_C}{m} \frac{\vec{V}}{V^3}, \quad (3.30)$$

and in this range the friction force shape coincides with formula (3.29).

II. Low velocity $\Delta_{\parallel} \leq V < \Delta_{\perp}$. Here the transverse component of the friction force is given by the following expression:

$$F_{\perp} = -\frac{4\pi Z^2 e^4 n_e L_C}{m} \cdot \frac{V_{\perp}}{\Delta_{\perp}^3}, \quad (3.31)$$

and longitudinal one:

$$F_{\parallel} = -\frac{4\pi Z^2 e^4 n_e L_C}{m} \frac{V_{\parallel}}{|V_{\parallel}| \Delta_{\perp}^2}. \quad (3.32)$$

III. Superlow velocity $V < \Delta_{\parallel}$. Here the transverse component of the friction force is equal to zero, the longitudinal component is given by:

$$F_{\parallel} = -\frac{4\pi Z^2 e^4 n_e L_C}{m} \frac{V_{\parallel}}{\Delta_{\parallel} \Delta_{\perp}^2}. \quad (3.33)$$

The minimal impact parameter in the Coulomb logarithm is equal to:

$$\rho_{\min} = \frac{Ze^2}{m} \frac{1}{V^2 + \Delta_e^2}, \quad (3.34)$$

where Δ_e is given by the formula (3.20).

The asymptotes by Ya. Derbenev for the longitudinal component of the force have the following form:

$$F_{\parallel} = -\frac{4\pi Z^2 e^4 n_e L(V_{\parallel})}{m} \frac{V_{\parallel}}{\Delta_{\parallel} \Delta_{\perp}^2} \sqrt{\frac{2}{\pi}}, \text{ if } V \ll \Delta_{\parallel}. \quad (3.35)$$

$$F_{\parallel} = -\frac{4\pi Z^2 e^4 n_e}{m} \left[L(V_{\parallel}) \frac{V_{\parallel}}{|V_{\parallel}| \Delta_{\perp}^2} - \sqrt{\frac{\pi}{2}} L(\Delta_{\perp}) \frac{V_{\parallel}}{\Delta_{\perp}^3} \right], \text{ if } \Delta_{\perp} > V \gg \Delta_{\parallel}. \quad (3.36)$$

Here the Coulomb logarithms are calculated in accordance with the following formulae:

$$L(V_{\parallel}) = \ln \left(\sqrt{\frac{V_{\parallel}^2 m}{4\pi n_e e^2}} / \rho_{\min} \right), \quad (3.37)$$

$$L(\Delta_{\perp}) = \ln \left(\sqrt{\frac{\Delta_{\perp}^2 m}{4\pi n_e e^2}} / \rho_{\min} \right). \quad (3.38)$$

In order to provide uniform usage of the formulae in the program the friction force calculation is realized in three ranges of the ion velocity similarly to Meshkov's asymptotes.

I. High velocity $V \geq \Delta_{\perp}$, here longitudinal and transverse components of the friction force are equal:

$$F_{\perp} = -\frac{4\pi Z^2 e^4 n_e L_C}{m} \frac{V_{\perp}}{V^3}, \quad (3.39)$$

$$F_{\parallel} = -\frac{4\pi Z^2 e^4 n_e}{m} \left(L_C \frac{V_{\parallel}}{V^3} - \sqrt{\frac{2}{\pi}} L(\Delta_{\perp}) \frac{1}{V_{\parallel}^2} \right). \quad (3.40)$$

II. Low velocity $\Delta_{\parallel} \leq V < \Delta_{\perp}$. Here the transverse component of the friction force is given by the following expression:

$$F_{\perp} = -\frac{4\pi Z^2 e^4 n_e L_C}{m} \cdot \frac{V_{\perp}}{\Delta_{\perp}^3}, \quad (3.41)$$

and longitudinal one:

$$F_{\parallel} = -\frac{4\pi Z^2 e^4 n_e}{m} \left(L_C \frac{V_{\parallel}}{\sqrt{V_{\parallel}^2 + \Delta_{\parallel}^2} \Delta_{\perp}^2} - \sqrt{\frac{2}{\pi}} L(\Delta_{\perp}) \frac{V_{\parallel}}{\Delta_{\perp}^3} \right). \quad (3.42)$$

III. Superlow velocity $V < \Delta_{\parallel}$. Here the transverse component of the friction force is equal to zero, the longitudinal component is given by:

$$F_{\parallel} = -\frac{4\pi Z^2 e^4 n_e}{m} L_C \frac{V_{\parallel}}{\sqrt{V_{\parallel}^2 + \Delta_{\parallel}^2 \Delta_{\perp}^2}}. \quad (3.43)$$

These formulae in the case $V_{\perp} = 0$ give the correct result for longitudinal component of the friction force (3.45), (3.46) and have a correct asymptotes at high ion velocity. The transverse component of the force is calculated in accordance with Meshkov's representation.

3.2. Magnetized electron beam. Derbenev-Skrinsky-Meshkov formulae

In the magnetized electron beam, when the maximum impact parameter (3.14) is larger than radius of electron Larmor rotation the magnetized collisions between ion and electron take place. In this case the electron is attracted by the ion, which pulls it along the magnetic field line forth or back, depending on the ion position [3]. In different ranges of the ion velocity and impact parameter three type of collisions are possible: fast, adiabatic and magnetized.

3.2.1. Magnetized collisions

At ion collisions with electrons at the impact parameter higher than the mean radius of electron Larmor rotation

$$\rho_{\perp} = \frac{cm\Delta_{\perp}}{eB} \quad (3.44)$$

the friction force in the particle rest frame can be expressed as follows [3]:

$$\bar{F} = \frac{2\pi Z^2 e^4 n_e}{m} \frac{\partial}{\partial \vec{V}} \int \left[\frac{V_{\perp}^2}{U^3} L_M + \frac{2}{U} \right] f(v_e) dv_e, \quad (3.45)$$

where $U = \sqrt{V_{\perp}^2 + (V_{\parallel} - v_e)^2}$ - the relative velocity of the ion and electron "Larmor circle". $f(v_e)$ is the electron distribution over longitudinal velocity, in the case of Maxwellian distribution with rms velocity spread of Δ_{\parallel} it is expressed as

$$f(v_e) = \frac{1}{\sqrt{2\pi}\Delta_{\parallel}} \exp\left(-\frac{v_e^2}{2\Delta_{\parallel}^2}\right). \quad (3.46)$$

Maximum impact parameter in the Coulomb logarithm for magnetized collisions

$$L_M = \ln\left(\frac{\rho_{\max}}{\rho_{\perp}}\right) \quad (3.47)$$

is calculated as usual (3.14).

The formula (3.55) has asymptotes in the region of small and large ion velocities. When $V \gg \Delta_{\parallel}$ the electron distribution can be approximated by delta-function $f(v_e) = \delta(v_e)$, and integration in (3.55) gives:

$$F_{\parallel} = -V_{\parallel} \frac{2\pi Z^2 e^4 n_e}{m V^3} \left(\frac{3V_{\perp}^2}{V^2} L_M + 2 \right), \quad (3.48)$$

$$F_{\perp} = -V_{\perp} \frac{2\pi Z^2 e^4 n_e L_M}{m V^3} \frac{V_{\perp}^2 - 2V_{\parallel}^2}{V^2}. \quad (3.49)$$

When the ion velocity is sufficiently less than electron velocity spread $V \ll \Delta_{\parallel}$ the friction force can be expressed as [3]:

$$F_{\parallel} \approx -2\sqrt{2\pi} \frac{Z^2 e^4 L_M}{m \Delta_{\parallel}^3} V_{\parallel}, \quad (3.50)$$

$$F_{\perp} \approx -2\sqrt{2\pi} \frac{Z^2 e^4 L_M}{m \Delta_{\parallel}^3} \ln \left(\frac{\Delta_{\parallel}}{V_{\perp}} \right) V_{\perp}. \quad (3.51)$$

In the general case the friction force components can be calculated numerically as the following 1-dimensional integrals:

$$F_{\perp}(V_{\perp}, V_{\parallel}) = -\frac{2\pi Z^2 e^4 n_e L_M}{m} \int \frac{V_{\perp} (V_{\perp}^2 - 2(V_{\parallel} - v_e)^2)}{(V_{\perp}^2 + (V_{\parallel} - v_e)^2)^{5/2}} f(v_e) dv_e, \quad (3.52)$$

$$F_{\parallel}(V_{\perp}, V_{\parallel}) = -\frac{2\pi Z^2 e^4 n_e}{m} \int \left(L_M \frac{3V_{\perp}^2 (V_{\parallel} - v_e)}{(V_{\perp}^2 + (V_{\parallel} - v_e)^2)^{5/2}} + 2 \frac{V_{\parallel} - v_e}{(V_{\perp}^2 + (V_{\parallel} - v_e)^2)^{3/2}} \right) f(v_e) dv_e. \quad (3.53)$$

The non-logarithmic term in (3.63) describes the radiation of plasma waves by the ion. It should be taken into account only at large ion velocity $V \gg \Delta_{\parallel}$. In the region of small ion velocity the longitudinal component of the friction force is

$$F_{\parallel}(V_{\perp}, V_{\parallel}) = -\frac{2\pi Z^2 e^4 n_e L_M}{m} \int \frac{3V_{\perp}^2 (V_{\parallel} - v_e)}{(V_{\perp}^2 + (V_{\parallel} - v_e)^2)^{5/2}} f(v_e) dv_e. \quad (3.54)$$

General problem in numerical integration of (3.52, 3.53, 3.54) is singularity of the integrands at $V_{\perp}, V_{\parallel} \rightarrow 0$. In the integral (3.54) V_{\perp} can be moved out from the integration, however the integral

$$\int \frac{(V_{\parallel} - v_e)}{(V_{\perp}^2 + (V_{\parallel} - v_e)^2)^{5/2}} \exp \left(-\frac{v_e^2}{2\Delta_{\parallel}^2} \right) dv_e \quad (3.55)$$

has singularity at $V_{\perp} = 0$. As result the friction force at zero ion transverse velocity has a finite value given by the formula:

$$F_{\parallel}(0, V_{\parallel}) = -V_{\parallel} \frac{4\pi Z^2 e^4 n_e L_M}{m \sqrt{2\pi} \Delta_{\parallel}^3} \exp \left(-\frac{V_{\parallel}^2}{2\Delta_{\parallel}^2} \right). \quad (3.56)$$

To avoid these difficulties the integrals (3.62, 3.64) can be replaced by their asymptotes (3.50, 3.51) at the ion velocity region $V \ll \Delta_{\parallel}$ and integral (3.64) can be replaced by its accurate value (3.56) at $V_{\perp} \ll \Delta_{\parallel}$.

One can avoid numerical problems in integration of (3.52, 3.54) at small ion velocity and provide calculations without usage of analytic asymptotes using algorithm proposed by D.Pestrikov. The integral (3.55) can be rewritten in the following form:

$$F_{\parallel}(V_{\perp}, V_{\parallel}) = -\frac{2\pi Z^2 e^4 n_e L_M}{m} \int \frac{V_{\perp}^2}{(V_{\perp}^2 + (V_{\parallel} - v_e)^2)^{3/2}} \frac{df(v_e)}{dv_e} dv_e, \quad (3.57)$$

$$F_{\perp}(V_{\perp}, V_{\parallel}) = -\frac{2\pi Z^2 e^4 n_e L_M}{m} \int \frac{V_{\perp}(V_{\parallel} - v_e)}{(V_{\perp}^2 + (V_{\parallel} - v_e)^2)^{3/2}} \frac{df(v_e)}{dv_e} dv_e. \quad (3.58)$$

At distribution function (3.56) and using substitutions $x = \frac{v_e}{\Delta_{\parallel}}$, $y = \frac{V_{\parallel}}{\Delta_{\parallel}}$, $z = \frac{V_{\perp}}{\Delta_{\parallel}}$ these integrals has the following form:

$$F_{\parallel} = -\frac{2\pi Z^2 e^4 n_e L_M}{m\sqrt{2\pi}\Delta_{\parallel}^2} \int_{-\infty}^{\infty} \frac{z^2 x}{(z^2 + (y-x)^2)^{3/2}} \exp\left(-\frac{x^2}{2}\right) dx, \quad (3.59)$$

$$F_{\perp} = -\frac{2\pi Z^2 e^4 n_e L_M}{m\sqrt{2\pi}\Delta_{\parallel}^2} \int_{-\infty}^{\infty} \frac{zyx}{(z^2 + (y-x)^2)^{3/2}} \exp\left(-\frac{x^2}{2}\right) dx, \quad (3.60)$$

Changing the integration variable by $x = y + |z|\tan\alpha$ one can reduce these integrals to the form with nonsingular integrant:

$$F_{\parallel} = -\frac{2\pi Z^2 e^4 n_e L_M}{m\sqrt{2\pi}\Delta_{\parallel}^2} \int_{-\pi/2}^{\pi/2} (y \cos\alpha + |z|\sin\alpha) \exp\left(-\frac{(y + |z|\tan\alpha)^2}{2}\right) d\alpha, \quad (3.61)$$

$$F_{\perp} = -\text{sgn}(z) \frac{2\pi Z^2 e^4 n_e L_M}{m\sqrt{2\pi}\Delta_{\parallel}^2} \int_{-\pi/2}^{\pi/2} \tan\alpha (y \cos\alpha + |z|\sin\alpha) \exp\left(-\frac{(y + |z|\tan\alpha)^2}{2}\right) d\alpha. \quad (3.62)$$

Integral (3.61) at $z = 0$ can be calculated analytically and gives the formula (3.56).

3.2.2. Friction force at small impact parameters

When the impact parameter is less than the radius of the electron rotation $\rho < \rho_{\perp}$ the influence of the magnetic field can be neglected and the friction force can be calculated in accordance with:

$$\vec{F} = -\frac{4\pi n_e e^4 Z^2}{m} \int (L_F + N_{coll} L_A) \frac{\vec{V} - \vec{v}_e}{|\vec{V}_i - \vec{v}_e|^3} f(v_e) d^3 v_e. \quad (3.63)$$

The range of impact parameters from ρ_{\min} to ρ_{\perp} in (3.63) is divided by two regions: the region where

$$\rho_{\min} < \rho < \rho_F$$

corresponds to so called “fast collisions” and in the region of

$$\rho_F < \rho < \rho_{\perp}$$

the ion can collide with the same electron a few times during its movement through the cooling section. The last region corresponds to so called “adiabatic” or “cycling” collisions. The intermediate impact parameter ρ_F is equal to:

$$\rho_F = \rho_{\perp} \frac{\sqrt{V^2 + \Delta_{\parallel}^2}}{\Delta_{\perp}}, \quad (3.64)$$

and corresponding Coulomb logarithms are:

$$L_A = \ln \frac{\rho_{\perp}}{\rho_F}, \quad L_F = \ln \frac{\rho_F}{\rho_{\min}}. \quad (3.65)$$

The number of multiple adiabatic collisions of the ion with the same electron is [4]:

$$N_{coll} = 1 + \frac{\Delta_{\perp}}{\pi \sqrt{V^2 + \Delta_{\parallel}^2}}. \quad (3.66)$$

The minimum impact parameter is calculated as usual:

$$\rho_{\min} = \frac{Ze^2}{m} \frac{1}{|\vec{V} - \vec{v}_e|^2}. \quad (3.67)$$

Numerical evaluation of the integral (3.63) is discussed in the chapter 3.1.2.

3.2.3. Asymptotic representation by I.Meshkov

Summarizing asymptotic presentations for all types of collisions one can obtain analytical formulae for friction force derived in [2]:

$$F_{\perp} \approx -\frac{2\pi Z^2 e^4 n_e}{m} v_{\perp} \left\{ \begin{array}{l} \frac{1}{v^3} \left(2L_F + \frac{V_{\perp}^2 - 2V_{\parallel}^2}{V^2} L_M \right), \{I\} \\ \frac{2}{\Delta_{\perp}^3} (L_F + N_{col} L_A) + \frac{V_{\perp}^2 - 2V_{\parallel}^2}{V^2} \frac{L_M}{V^3}, \{II\} \\ \frac{2}{\Delta_{\perp}^3} (L_F + N_{col} L_A) + \frac{L_M}{\Delta_{\parallel}^3}, \{III\} \end{array} \right. \quad (3.68)$$

$$F_{\parallel} \approx -\frac{2\pi Z^2 e^4 n_e}{m} v_{\parallel} \left\{ \begin{array}{l} \frac{1}{v^3} \left(2L_F + \frac{3V_{\perp}^2}{V^2} L_M + 2 \right), \{I\} \\ \frac{2}{\Delta_{\perp}^2 V_{\parallel}} (L_F + N_{col} L_A) + \left(\frac{3V_{\perp}^2}{V^2} L_M + 2 \right) \frac{1}{V^3}, \{II_a\} \\ \frac{2}{\Delta_{\perp}^2 \Delta_{\parallel}} (L_F + N_{col} L_A) + \frac{L_M}{\Delta_{\parallel}^3}, \{II_b, III\} \end{array} \right. \quad (3.69)$$

Ion velocity domains I , $II = II_a + II_b$, and III are shown in Fig. 3.3.

In these formulae the Coulomb logarithms are defined as follows:

$$L_M = \ln \frac{R}{k\rho_{\perp}}, \quad L_A = \ln \frac{k\rho_{\perp}}{\rho_F}, \quad L_F = \ln \frac{\rho_F}{\rho_{\min}}. \quad (3.70)$$

Note that if argument of a logarithm is less than 1, then the logarithm value has to be set to zero. It means that the corresponding type of collisions is absent at given parameters. The minimum impact parameter is given by the formula

$$\rho_{\min} = \frac{Ze^2}{m_e} \frac{1}{V^2 + \Delta_{\parallel}^2}, \quad (3.71)$$

and dynamic shielding radius in the formula (3.12) for the maximum impact parameter is determined by the electron longitudinal velocity spread:

$$\rho_{sh} = \frac{\sqrt{V^2 + \Delta_{\parallel}^2}}{\omega_p}. \quad (3.72)$$

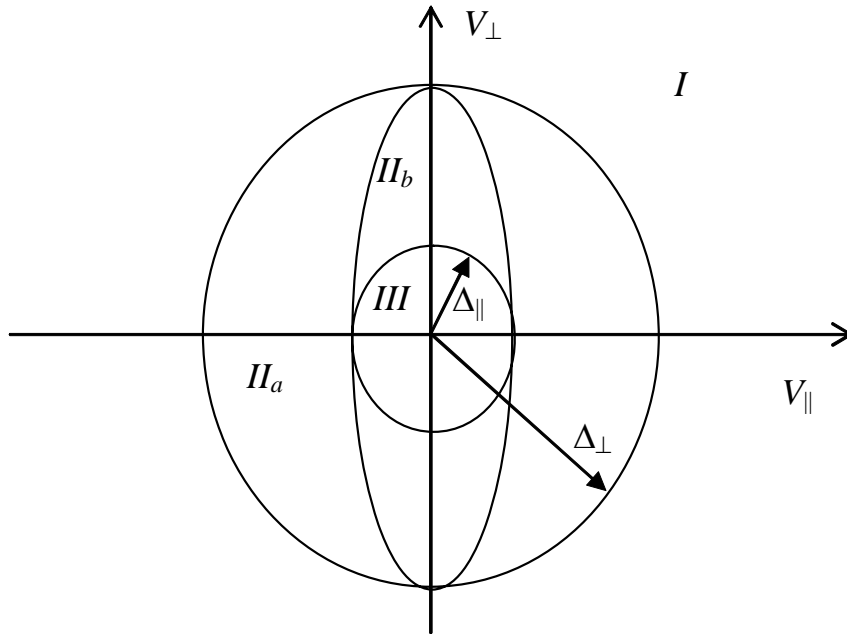


Fig.3.3. Domains in the velocity space for the friction force calculation. V_{\perp} , V_{\parallel} are the ion velocity components in PRF; Δ_{\perp} is the transverse electron velocity spread, Δ_{\parallel} is the longitudinal one.

Coefficient k in the formulae (3.70) was introduced to smooth the friction force shape. In the original paper it was chosen to be 2, in the program now it is used as an additional input parameter.

3.3. Magnetized electron beam. Semi-empirical formula by Parkhomchuk

In [5] was proposed a semi-empirical formula for calculation of the friction force in magnetized electron beam:

$$\vec{F} = -\vec{V} \frac{4Z^2 e^4 n_e L_p}{m} \frac{1}{(V^2 + \Delta_{e,eff}^2)^{3/2}}, \quad (3.73)$$

where $\Delta_{e,eff}$ is the effective electron velocity spread with taking into account variations of the magnetic field line position in the transverse direction. The Coulomb logarithm is given by the expression:

$$L_p = \ln \left(\frac{\rho_{\max} + \rho_{\min} + \rho_{\perp}}{\rho_{\min} + \rho_{\perp}} \right). \quad (3.74)$$

Where the minimum impact parameter is calculated in accordance with

$$\rho_{\min} = \frac{Ze^2}{m} \frac{1}{V^2 + \Delta_{e,eff}^2}. \quad (3.75)$$

Maximum impact parameter in accordance with original formula is calculated as:

$$\rho_{\max} = \frac{v_i}{1/\tau_{flight} + \omega_p}, \quad (3.76)$$

where τ_{flight} is the ion time of flight the cooling section (3.15), ω_p is the plasma frequency (3.10).

This formula presumes that

$$\Delta_{e,eff} \ll \Delta_{\perp}.$$

3.4. Model of electron cooling friction force developed by Erlangen University

In [B.Mollers et al, Drag force on ions in magnetized electron plasmas, NIM B 207 (2003) 462-481] the friction force was calculated in the frame of binary collision model under assumption that the ion velocity stays constant in a collision with an electron. The unperturbed motion of electron is a helix with the Larmor radius:

$$\rho_{\perp} = \frac{cmv_{\perp}}{eB} \quad (3.77)$$

and the pitch determined by longitudinal velocity. The ion velocity variation is calculated iteratively and at impact parameters larger than the Larmor radius one can obtain solution in a closed form for two limiting cases:

$$\delta = \frac{cm\sqrt{V_{\perp}^2 + (V_{\parallel} - v_{\parallel})^2}}{eB} \gg \rho_{\perp}$$

and $\delta \ll \rho_{\perp}$, where δ is the pitch of the helix as seen from the ion.

Correspondingly, the friction force includes three components related to different types of collision:

- fast collisions at impact parameters less than radius of electron rotation,

- collisions with “tight” helices,
- collisions with “stretched” helices.

In the case of axial symmetry the electron distribution function can be written in the following form:

$$f(v_e) = \left(\frac{1}{2\pi}\right)^{3/2} \frac{1}{\Delta_\perp^2 \Delta_\parallel} \exp\left(-\frac{v_\perp^2}{2\Delta_\perp^2} - \frac{v_\parallel^2}{2\Delta_\parallel^2}\right), \quad (3.78)$$

where Δ_\perp and Δ_\parallel are the electron rms velocity spreads in the transverse and longitudinal direction correspondingly.

For the fast collisions the formula is analogous to non-magnetized collisions. The components of the friction force at fast collisions can be calculated in cylindrical co-ordinate system as follows:

$$F_{\perp,f} = -\sqrt{\frac{2}{\pi}} \frac{Z^2 e^4 n_e}{m \Delta_\perp^2 \Delta_\parallel} \int_0^\infty \int_{-\infty}^\infty \int_0^{2\pi} \ln\left(\frac{\rho_{\max}}{\rho_{\min}}\right) \frac{(V_\perp - v_\perp \cos \varphi) \exp\left(-\frac{v_\perp^2}{2\Delta_\perp^2} - \frac{v_\parallel^2}{2\Delta_\parallel^2}\right)}{\left((V_\parallel - v_\parallel)^2 + (V_\perp - v_\perp \cos \varphi)^2 + v_\perp^2 \sin^2 \varphi\right)^{3/2}} v_\perp d\varphi dv_\parallel dv_\perp,$$

$$F_{\parallel,f} = -\sqrt{\frac{2}{\pi}} \frac{Z^2 e^4 n_e}{m \Delta_\perp^2 \Delta_\parallel} \int_0^\infty \int_{-\infty}^\infty \int_0^{2\pi} \ln\left(\frac{\rho_{\max}}{\rho_{\min}}\right) \frac{(V_\parallel - v_\parallel) \exp\left(-\frac{v_\perp^2}{2\Delta_\perp^2} - \frac{v_\parallel^2}{2\Delta_\parallel^2}\right)}{\left((V_\parallel - v_\parallel)^2 + (V_\perp - v_\perp \cos \varphi)^2 + v_\perp^2 \sin^2 \varphi\right)^{3/2}} v_\perp d\varphi dv_\parallel dv_\perp. \quad (3.79)$$

But here both impact parameters – minimum and maximum – are the functions of the electron velocity:

$$\rho_{\min} = \frac{Ze^2}{m_e} \frac{1}{(V_\parallel - v_\parallel)^2 + (V_\perp - v_\perp \cos \varphi)^2 + v_\perp^2 \sin^2 \varphi}. \quad (3.80)$$

$$\rho_{\max} = \rho_\perp = \frac{cmv_\perp}{eB}.$$

The friction force in collisions with tight helices

$$F_{\parallel,t}(V_\perp, V_\parallel) = -\frac{4\pi Z^2 e^4 n_e}{m} \frac{1}{\Delta_\perp^2 \sqrt{2\pi} \Delta_\parallel} \int \frac{V_\perp^2 (V_\parallel - v_\parallel)}{(V_\perp^2 + (V_\parallel - v_\parallel)^2)^{5/2}} \exp\left(-\frac{v_\parallel^2}{2\Delta_\parallel^2}\right) \int_0^\infty \ln\left(\frac{\rho_{\max}}{\max(\rho_\perp, \delta)}\right) \exp\left(-\frac{v_\perp^2}{2\Delta_\perp^2}\right) v_\perp dv_\perp dv_\parallel, \quad (3.81)$$

$$F_{\perp,t}(V_\perp, V_\parallel) = -\frac{4\pi Z^2 e^4 n_e}{m} \frac{1}{\Delta_\perp^2 \sqrt{2\pi} \Delta_\parallel} \int \frac{V_\perp (V_\perp^2 - (V_\parallel - v_\parallel)^2)}{2(V_\perp^2 + (V_\parallel - v_\parallel)^2)^{5/2}} \exp\left(-\frac{v_\parallel^2}{2\Delta_\parallel^2}\right) \int_0^\infty \ln\left(\frac{\rho_{\max}}{\max(\rho_\perp, \delta)}\right) \exp\left(-\frac{v_\perp^2}{2\Delta_\perp^2}\right) v_\perp dv_\perp dv_\parallel, \quad (3.82)$$

where

$$\delta = \frac{cm\sqrt{V_{\perp}^2 + (V_{\parallel} - v_{\parallel})^2}}{eB}. \quad (3.83)$$

For stretched helices

$$F_{\parallel,s}(V_{\perp}, V_{\parallel}) = -\frac{4\pi Z^2 e^4 n_e}{m} \frac{1}{\Delta_{\perp}^2 \sqrt{2\pi} \Delta_{\parallel}} \int \frac{V_{\parallel} - v_{\parallel}}{(V_{\perp}^2 + (V_{\parallel} - v_{\parallel})^2)^{3/2}} \exp\left(-\frac{v_{\parallel}^2}{2\Delta_{\parallel}^2}\right) \int_0^{\infty} \ln\left(\frac{\min(\delta, \rho_{\max})}{\min(\rho_{\perp}, \rho_{\max})}\right) \exp\left(-\frac{v_{\perp}^2}{2\Delta_{\perp}^2}\right) v_{\perp} dv_{\perp} dv_{\parallel}, \quad (3.84)$$

$$F_{\perp,s}(V_{\perp}, V_{\parallel}) = -\frac{4\pi Z^2 e^4 n_e}{m} \frac{V_{\perp}}{\Delta_{\perp}^2 \sqrt{2\pi} \Delta_{\parallel}} \int \frac{1}{(V_{\perp}^2 + (V_{\parallel} - v_{\parallel})^2)^{3/2}} \exp\left(-\frac{v_{\parallel}^2}{2\Delta_{\parallel}^2}\right) \int_0^{\infty} \ln\left(\frac{\min(\delta, \rho_{\max})}{\min(\rho_{\perp}, \rho_{\max})}\right) \exp\left(-\frac{v_{\perp}^2}{2\Delta_{\perp}^2}\right) v_{\perp} dv_{\perp} dv_{\parallel}. \quad (3.86)$$

When $V \gg \Delta_{\parallel}$ the electron distribution can be approximated by delta-function $f(v_{\parallel}) = \delta(v_{\parallel})$. In this case integration over electron velocity components can be provided independently. The friction force components for tight helices can be expressed in the following form:

$$F_{\parallel} = -V_{\parallel} \frac{4\pi Z^2 e^4 n_e}{mV^3} \frac{V_{\perp}^2}{V^2} L_M, \quad (3.87)$$

$$F_{\perp} = -V_{\perp} \frac{4\pi Z^2 e^4 n_e L_M}{mV^3} \frac{V_{\perp}^2 - V_{\parallel}^2}{V^2}. \quad (3.88)$$

Here the Coulomb logarithm is determined by the expression

$$L_M = \frac{1}{\Delta_{\perp}^2} \int_0^{\infty} \ln\left(\frac{\rho_{\max}}{\max(\rho_{\perp}, \delta)}\right) \exp\left(-\frac{v_{\perp}^2}{2\Delta_{\perp}^2}\right) v_{\perp} dv_{\perp} \approx \ln\left(\frac{\rho_{\max}}{\langle \rho_{\perp} \rangle}\right),$$

at $\delta = \frac{cm\sqrt{V_{\perp}^2 + V_{\parallel}^2}}{eB}$. Within an accuracy to the logarithm definition these formulae coincide with derived in the limit of infinite magnetic field in [doctoral thesis by V.Parkhomchuk].

In the same approximation $V \gg \Delta_{\parallel}$ the formulae for collisions with stretched helices can be rewritten in the form:

$$\vec{F} \approx -\vec{V} \frac{4\pi Z^2 e^4 n_e}{m} \frac{1}{(V^2 + \Delta_{\parallel}^2)^{3/2}} \left(\ln\left(\frac{\rho_{\max}}{\langle \rho_{\perp} \rangle}\right) + \ln\left(\frac{\omega_p}{\omega_B}\right) \right), \quad (3.89)$$

where ω_p , ω_B are the plasma and cyclotron frequencies. This formula is valid at $\frac{V}{\Delta_{\perp}} \gg 1$ and its structure is similar to semi-empirical formula by Parkhomchuk.

Numerical integration of (3.87) has to be provided taking into account peculiarity of the integral at $V_{\perp} \rightarrow 0$.

3.4. Probability of the particle loss

Probability of the electron capture by the ion during its passage in the cooling section is expressed by the following formula:

$$\frac{dP_{loss}}{dt} = \frac{\alpha_r n_e}{\gamma^2}, \quad (3.90)$$

where n_e is the local electron density in LRF. Recombination coefficient α_r calculated under assumption that ion velocity in PRF is substantially less than electron one and at flattened electron velocity distribution is given by the formula [6]:

$$\alpha_r = A \cdot Z^2 \sqrt{\frac{1}{T_{\perp}}} \left[\ln \left(\frac{11.32Z}{\sqrt{T_{\perp}}} \right) + 0.14 \left(\frac{T_{\perp}}{Z^2} \right)^{1/3} \right], \quad A = 3.02 \cdot 10^{-13} \frac{cm^3}{s} \quad (3.91)$$

In the case, when the electron velocity spread depends on position inside the electron beam (for instance, if space charge effects in the electron beam are taken into account, or when for cooling process simulation one uses results of the electron dynamics simulation performed using external program) the recombination coefficient as well as the local electron density is a function of the ion co-ordinates. Correspondingly, the particle loss probability after crossing the cooling section is calculated by numerical integration of the formula (3.77) along the ion trajectory. This integration is performed together with solution of the ion motion equation in the cooling section, which is provided by a model of the electron beam. The algorithm is described in more details in the next chapter.

3.4.1. Simulation of ion-electron recombination in presence of undulator field

Electron cooling at RHIC using non-magnetized electron beam sufficiently simplifies the cooler design. Generation and acceleration of the electron bunch without longitudinal magnetic field permits to reach low value of emittance in the cooling section. General problem of such a scheme is high recombination rate at low electron temperature. Suppression of the ion recombination with electrons in the cooling section using undulator field was proposed for RHIC in [8]. In presence of the undulator field, trajectories of all electrons have the same coherent azimuth angle θ , determined by the undulator period λ and field value B at the axis:

$$\theta = \frac{eB\lambda}{2\pi pc}, \quad (3.92)$$

where p is the electron momentum. Since the recombination cross section is approximately inversely proportional to the electron energy in the ion rest frame, the ion beam life time can be sufficiently improved.

One can expect that at impact parameters significantly larger than electron rotation radius

$$r_0 = \frac{\theta\lambda}{2\pi} = \frac{eB\lambda^2}{4\pi^2 pc} \quad (3.93)$$

kinematics of a binary collision will be similar to Rutherford scattering of free electron. Thus the minimum impact parameter ρ_{min} in presence of the undulator field has to be replaced by r_0 value. At larger impact parameters the friction force can be calculated using formula (3.92) without tacking into account coherent electron velocity.

In difference with the friction force the recombination coefficient, determined via recombination cross section σ as follows

$$\alpha_r = \int (V_i - v_e) \sigma(V_i - v_e) f(v_e) d^3 v_e, \quad (3.94)$$

has to be calculated taking into account the coherent transverse electron velocity. For the recombination rate calculation one should to use a distribution function

$$f(v) d^3 v = \left(\frac{m}{2\pi} \right)^{3/2} \frac{1}{T_{\perp} \sqrt{T_{\parallel}}} e^{-m(v_{\perp} + v_{und})^2 / 2T_{\perp} - mv_{\parallel}^2 / 2T_{\parallel}} 2\pi v_{\perp} dv_{\perp} dv_{\parallel}, \quad (3.95)$$

where v_{und} is the electron azimuth velocity due to rotation in the undulator field:

$$v_{und} = c\beta\gamma\theta. \quad (3.96)$$

The ion beam life time due to recombination in the cooling section is calculated via recombination coefficient α_r by the following formula:

$$\frac{1}{N} \frac{dN}{dt} = - \frac{\alpha_r n_e l_{cool}}{\gamma^2 C}, \quad (3.97)$$

here C is the ring circumference. Under assumption that ion velocity in PRF is substantially less than electron one the α_r is calculated in PRF by averaging of the recombination cross section over electron distribution function:

$$\alpha_r = \langle v \sigma(v) \rangle \quad (3.98)$$

The recombination cross section can be calculated with good accuracy using the following formula [9]:

$$\sigma = A \left(\frac{h\nu_0}{E} \right) \left(\ln \sqrt{\frac{h\nu_0}{E}} + 0.1402 + 0.525 \left(\frac{E}{h\nu_0} \right)^{1/3} \right), \quad (3.99)$$

where $A = 2^4 3^{-3/2} h e^2 / (m_e^3 c^2) = 2.11 \times 10^{-22} \text{ cm}^2$, $h\nu_0 = 13.6 \cdot Z^2 \text{ eV}$ is the ion ground state binding energy. The electron kinetic energy $E = \frac{m_e v_e^2}{2}$. In presence of the undulator field it has to be calculated as:

$$E = \frac{m}{2} \left((v_{\perp} + v_{und})^2 + v_{\parallel}^2 \right), \quad (3.100)$$

The formula (3.98) at flattened distribution can be rewritten in the form adopted for numerical integration:

$$\alpha_r = \frac{1}{Int} \int_0^{3\Delta_{\perp}} \int_{-3\Delta_{\parallel}}^{3\Delta_{\parallel}} \sigma(E) \sqrt{(v_{\perp} + v_{und})^2 + v_{\parallel}^2} \exp \left(-\frac{(v_{\perp} + v_{und})^2}{2\Delta_{\perp}^2} - \frac{v_{\parallel}^2}{2\Delta_{\parallel}^2} \right) v_{\perp} dv_{\parallel} dv_{\perp}. \quad (3.101)$$

The normalization factor is calculated as:

$$Int = \int_0^{3\Delta_{\perp}} \int_{-3\Delta_{\parallel}}^{3\Delta_{\parallel}} \exp \left(-\frac{(v_{\perp} + v_{und})^2}{2\Delta_{\perp}^2} - \frac{v_{\parallel}^2}{2\Delta_{\parallel}^2} \right) v_{\perp} dv_{\parallel} dv_{\perp}. \quad (3.102)$$

To avoid overflow in calculation of the exponents, at $v_{und} > 6 \cdot \Delta_{\perp}$ the recombination coefficient is calculated directly from the coherent velocity:

$$\alpha_r = v_{und} \sigma(v_{und}), \quad (3.103)$$

that corresponds to electron distribution in the form of delta function.

In absents of the undulator field the recombination coefficient α_r calculated at flattened electron velocity distribution is given by the formula (3.91). Correspondingly, at small undulator magnetic field and electron temperature of longitudinal degree of freedom the numerical solution (3.88) has to coincide with (3.91). At large value of the coherent velocity the integral (3.101) has to coincide with solution (3.103).

4. Map of the cooling section

The map of the cooler provides transformation of the ion co-ordinates from the entrance to the end of the cooling section. This transformation is based on the solution of the ion motion equation in the cooling section. The ion motion inside a storage ring is described in the canonically conjugated variables:

$$\vec{X} = \{x, \theta_x, z, \theta_z, s-s_0, \theta_s\}, \quad (4.1)$$

where x, z are the horizontal and vertical co-ordinates, $\theta_{x,z} = \frac{P_{x,z}}{P}$, $\theta_s = \frac{\Delta P}{P}$, $P = \beta\gamma Mc$ is the longitudinal component of the reference particle momentum, $P_{x,z}$ are the transverse components of the ion momentum, ΔP is the longitudinal momentum deviation, $s - s_0$ is the ion longitudinal distance from the bunch center (the reference particle), $\beta = V_0/c$, $\gamma = \sqrt{1 - \beta^2}$, c is the speed of light, V_0 – velocity of the reference particle.

Under assumption, that transverse components of the particle momentum are substantially less than longitudinal one, the ion motion equations can be presented in the following form:

$$\left\{ \begin{array}{l} \frac{dx}{ds} = \theta_x \\ \frac{d\theta_x}{ds} = \frac{F_x}{Mc^2 \beta^2 \gamma} \\ \frac{dz}{ds} = \theta_z \\ \frac{d\theta_z}{ds} = \frac{F_z}{Mc^2 \beta^2 \gamma} \\ \frac{d(s-s_0)}{ds} = \frac{\theta_s}{\gamma^2} \\ \frac{d\theta_s}{ds} = \frac{F_s}{Mc^2 \beta^2 \gamma} \end{array} \right. \quad (4.2)$$

where $F_{x,z,s}$ are the force components in the laboratory reference frame.

The force acting on the ion inside the cooling section is the sum of Lorenz force from solenoid magnetic field, the electron beam space charge force, the friction force and the force randomly distributed around zero value, which determines the diffusion in the electron beam. The influence of the electron beam space charge and longitudinal magnetic field on the ion motion can be described by standard way and here we will discuss only calculation of the friction force.

The friction force components are calculated in PRF using the standard list of parameters. Model of electron beam has to transform the ion velocity components to PRF and calculate all the parameters required for the friction force calculation. After calculation of the friction force in PRF the electron beam model calculates the force components in LRF that can be used in the right hand side of the system (4.2).

In presence of transverse components of the guiding magnetic field at the axis of the cooler solenoid the electron beam is characterized by co-ordinates of it's center position and angle between electron beam axis and ion equilibrium orbit. In this case the ion transverse angles in the frame referenced to the electron beam orbit have to be corrected by the values of the angular misalignment $\delta\theta$ between electron and ion beams:

$$\theta_\alpha^* = \theta_\alpha - \delta\theta_\alpha(s), \alpha = x, z, \quad (4.3)$$

where θ^* is the ion angle in the electron beam reference frame.

The space charge of the electron beam determines the electron average velocity and electron velocity spread as functions of co-ordinates inside the electron beam. Electron beam density in general case is also a function of co-ordinates. To calculate the ion position inside the electron beam one needs to introduce transverse co-ordinates of the electron bunch center (x_c, z_c) and distance between the centers of the electron and ion bunches s_c . Under assumption that $\delta\theta \cdot l_{bunch} \ll a$ the ion co-ordinates inside the electron beam are:

$$x^* = x + x_c, z^* = z + z_c, (s-s_0)^* = (s-s_0) + s_c. \quad (4.4)$$

The transformation of the ion co-ordinates in accordance with the magnetic field line curvature, choice of the numerical algorithm for integration of the system (4.2) and calculation of the particle loss probability are provided by the model of cooler. The particle loss probability is calculated by integration of expression (3.39):

$$P_{loss} = \int_0^{l_{cool}} \frac{\alpha_r n_e}{\gamma^2 \beta c} ds, \quad (4.5)$$

which is performed along the particle trajectory during numerical integration of the ion motion equations.

The model of the cooler is realized as a procedure, which obtain at the entrance the 6D vector of initial particle co-ordinates, transforms components of this vector in accordance with solution of the system (4.2) and returns the value of the ion loss probability.

All stages of the algorithm providing the ion co-ordinate transformation through the cooling section are presented in the Fig. 4.1.

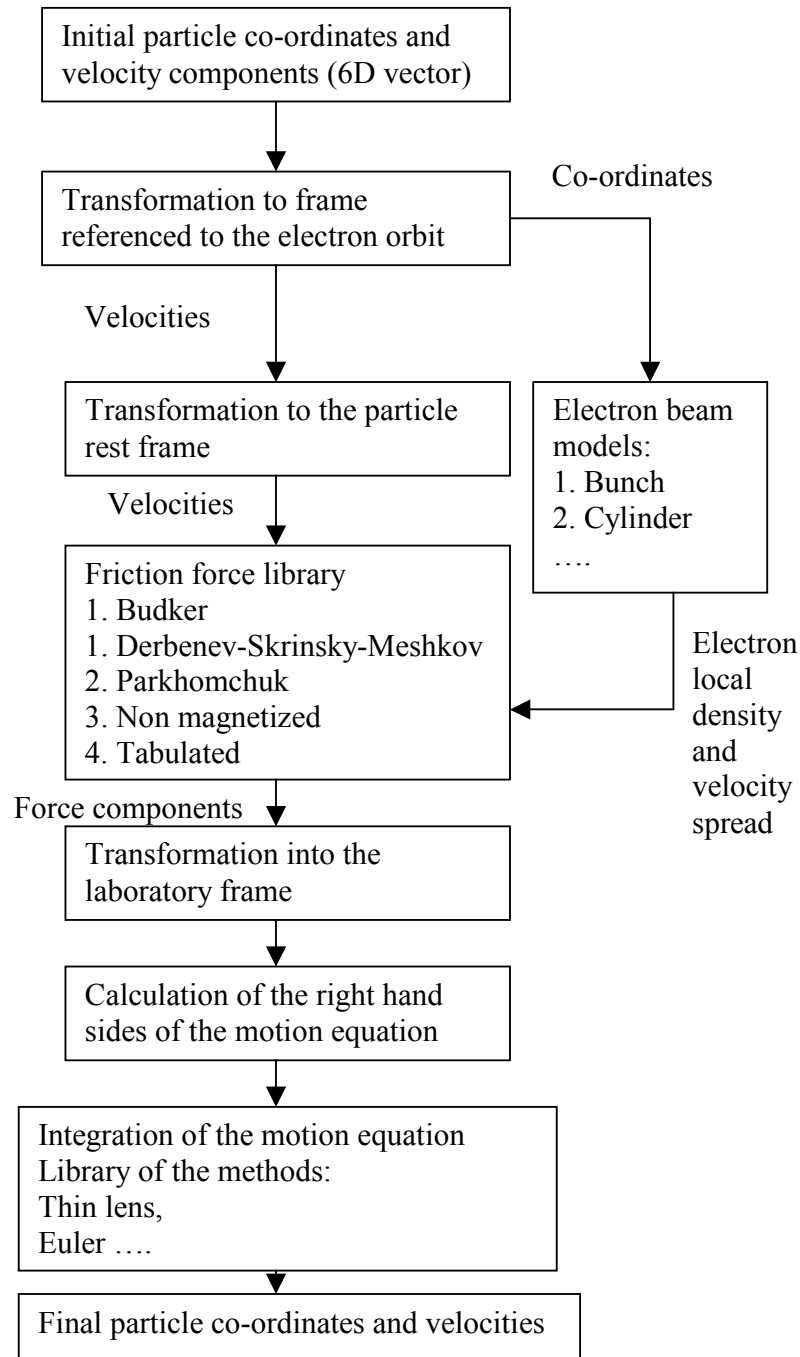


Fig. 4.1. Block scheme of the particle propagation through the cooling section.

4.1. Models of electron beam

The model of electron beam calculates list of parameters required for friction force procedure, transforms the ion velocity from LRF to PRF, makes a choice of the friction force procedure from library and transforms the force components from PRF to LRF. In the list of parameters required for friction force procedure generally there parameters depend on the electron beam model:

the local density of electrons,
the electron velocity spread in transverse plane,
the electron longitudinal velocity spread.

The local electron beam density is determined by geometry of the electron beam. The local velocity spread is the function of co-ordinates inside the electron beam if the space charge effects are taken into account. The space charge effects can also lead to shift of the electron mean velocity. The last effect does not change the beam velocity spread and it is taken into account by required correction of the longitudinal component of the ion velocity.

In the present version of the program four models of the electron beam are realized:

1. Uniform round cylinder,
2. Gaussian bunch of round (or elliptical) cross-section,
3. Uniform bunch,
4. Cylinder with round (or elliptical) cross-section with Gaussian distribution in transverse plane.
5. Parabolic distribution
6. Reading an electron density from file

4.1.1. Uniform cylinder

The first model corresponds to electron beam of usual electron cooling system. For this model the input parameters are electron beam current and radius and electron beam density is assumed to be independent on the ion co-ordinates inside the electron beam. The local electron beam density in LRF is constant determined by the expression:

$$n_e = I_e / (e\pi a^2 \beta c) \quad (4.6)$$

For this model the space charge effects in the electron beam are taken into account as described in the chapter 4.2.

4.1.2. Gaussian bunch

Input parameters for the Gaussian bunch model are the following:

- r.m.s. bunch dimensions,
- offset between electron and ion bunch centres,
- number of electrons in the bunch N_e .

For this model the local electron density in PRF in the point $(x, z, s - s_0)$ is calculated as follows:

$$n_e = \frac{N_e}{(2\pi)^{3/2} \sigma_x \sigma_z \sigma_s \gamma} \exp\left(-\frac{x^2}{2\sigma_x^2} - \frac{z^2}{2\sigma_z^2} - \frac{(s - s_0)^2}{2\sigma_s^2}\right), \quad (4.7)$$

where σ_x σ_z are r.m.s. transverse bunch dimensions, $s - s_0$ is calculated taking into account offset between electron and ion bunch centers.

As an output parameter the program calculates electron peak current as:

$$I_e = \frac{eN_e\beta c}{\sigma_s\sqrt{2\pi}}, \quad (4.8)$$

where σ_s is r.m.s. bunch length.

4.1.3. Uniform bunch

The Uniform bunch model presumes that the electron bunch has a uniform density in transverse direction and Gaussian distribution along longitudinal co-ordinate. Correspondingly the input parameters for are the following:

- the bunch transverse dimensions,
- the rms bunch length,
- offset between electron and ion bunch centres,
- number of electrons in the bunch N_e .

For this model the local electron density in PRF in the point $(s - s_0)$ is determined as follows:

$$n_e = \frac{N_e}{(2\pi)^{1/2} \pi a_x a_z \sigma_s \gamma} \exp\left(-\frac{(s - s_0)^2}{2\sigma_s^2}\right), \quad (4.9)$$

where a_x a_z are the transverse bunch dimensions, $s - s_0$ is calculated taking into account offset between electron and ion bunch centers.

As an output parameter the program calculates electron peak current in accordance with the formula (4.8).

4.1.4. Gaussian cylinder

The model of Gaussian cylinder can be used for cooling time calculation in the case when short electron bunch moves forward and back along a long ion bunch during the time shorter than cooling time. This model is more realistic in the case of electron cooling with magnetized circulating electron beam. The model input parameters are:

- r.m.s. dimensions of the cylinder cross-section,
- number of electrons per unit of length λ_e .

Local electron beam density in PRF in a position (x, z) is calculated in accordance with:

$$n_e = \frac{\lambda_e}{2\pi\sigma_x\sigma_z\gamma} \exp\left(-\frac{x^2}{2\sigma_x^2} - \frac{z^2}{2\sigma_z^2}\right). \quad (4.10)$$

Electron beam current for this model is given by the formula:

$$I_e = e\lambda_e\beta c. \quad (4.11)$$

The last two models of the electron beam do not take into account the space charge effects in the electron beam. However, the expressions for the self-fields of the electron beam are introduced into the program as described in the next chapter and can be introduced into calculation if necessary.

4.1.5. Hollow beam

Hollow beam is an infinite cylinder which has non-uniform radial density distribution. We assume in the code this model to be presented as two cylinders one inside another. Electron density is uniform inside each cylinder (Fig.4.2).

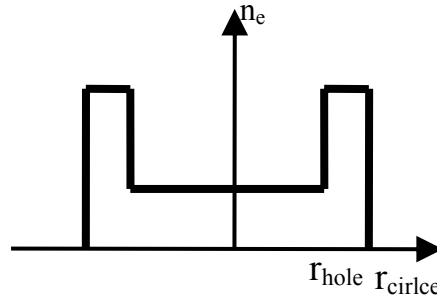


Fig.4.2. Electron density radial distribution in the hollow beam model.

The cross-section of such a beam is presented in the Fig. 4.3, where all the model input parameters are indicated.

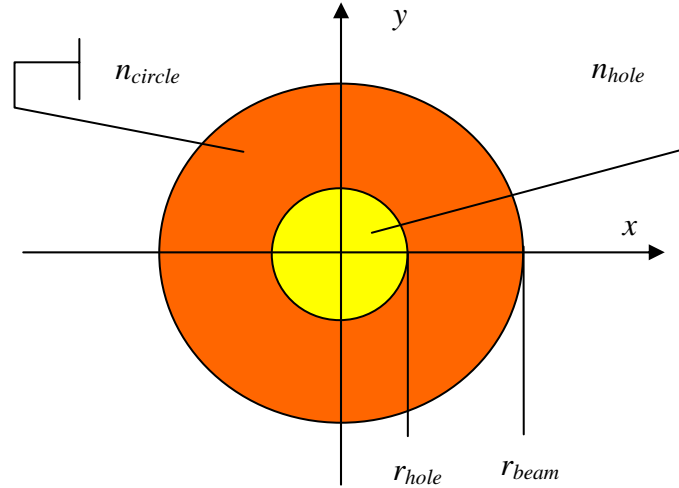


Fig.4.3. Cross-section of the hollow beam.

The input parameters are:

- the hole radius r_{hole} ,
- electron density in the laboratory rest frame (LRF) in the hole n_{hole} ,
- the outer circle radius r_{beam} ,
- density in LRF in the circle n_{circle} .

They are input in the visual form ECOOL | Electron beam in the tab sheet Hollow beam (Fig. 4.4) and are used to calculate the total beam current which is an output parameter.

Fig. 4.4. Visual form for input and output the hollow beam parameters.

The beam current is calculated as

$$I_{beam} = I_{sum} + I_{hole} - I_{hole, n_{circle}}, \quad (4.12)$$

where I_{sum} is the current of the uniform cylinder at density equal to n_{circle} :

$$I_{sum} = en_{circle} \pi r_{beam}^2 \beta c, \quad (4.13)$$

I_{hole} is the current inside the hole:

$$I_{hole} = en_{hole} \pi r_{hole}^2 \beta c, \quad (4.14)$$

and $I_{hole, n_{circle}}$ is the current inside the hole at electron density equal to the density inside outer circle:

$$I_{hole, n_{circle}} = en_{circle} \pi r_{hole}^2 \beta c, \quad (4.15)$$

βc is the electron velocity.

In the current version of the program it is assumed that the electron thermal velocity spread has the same value inside the hole and in the outer circle.

4.1.6. Parabolic beam

The parabolic distribution of the electron beam density was introduced in the BETACOOOL code for simulation of the electron cooling at Recycler. The density in the center of the electron beam is calculated as

$$n_0 = 2 \frac{I_e}{\pi a^2 e \beta c}, \quad (4.16)$$

where I_e – electron current, a electron beam radius, e – electron charge, βc – electron velocity. The dependence of the electron density on radius for parabolic distribution are defined as

$$n_e(r) = n_0 \left(1 - \frac{r^2}{a^2} \right), \quad (4.17)$$

where r – current coordinate of the ion. The BETACOOOL window with parameters of the parabolic distribution of the electron beam is shown on Fig.4.5. The gradient G_{\perp} was introduced for the description of the dependence of the relative transverse velocity on the radius:

$$V_{\perp}^2 = T_{\perp} / m_e + G_{\perp}^2 r^2 \quad (4.18)$$

where V_{\perp} - relative transverse velocity, T_{\perp} - transverse temperature, m_e – electron mass.

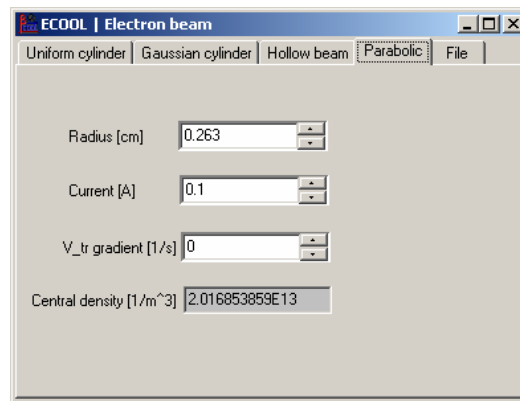


Fig.4.5. Parameters of parabolic distribution of the electron beam.

4.1.7. Distribution of electron density from file

The distribution of the electron beam on the radius can be calculated in other program and result of the calculation can be read into BETACOOOL program as text file. The BETACOOOL window for reading of the external file with radial distribution of electron density and transverse gradient is shown on Fig.4.6. First column of the file is the radial coordinate in mm, second column is the electron density in A/cm², and third column is the transverse gradient G_{\perp} in 1/sec. If the third column is absent in the file then the constant transverse gradient will be used from window (Fig.4.6a). Example of the text file with the electron beam density is shown on Fig.4.6b.

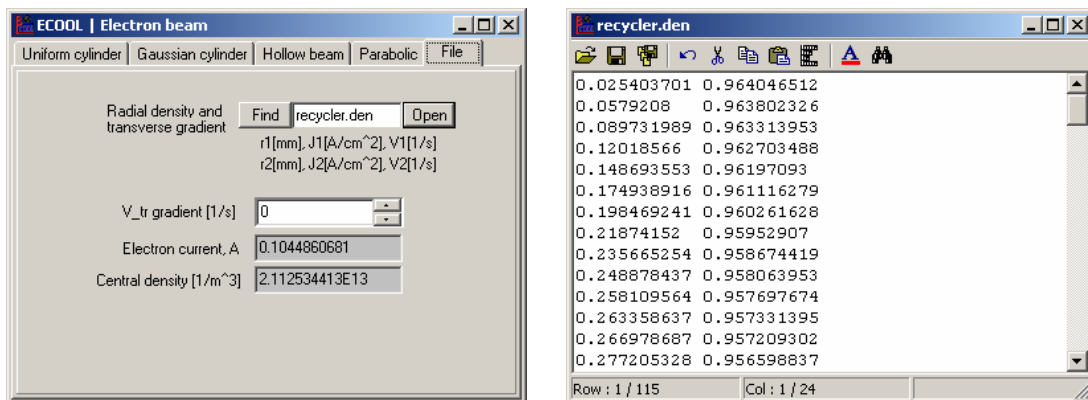


Fig.4.6. (a) Window for the reading of the electron beam density and transverse gradient from external text file. (b) Example of the text file with electron beam density

4.2. Space charge effects of the electron beam

The space charge effects lead to dependence of the mean electron velocity and electron velocity spread on co-ordinates inside the electron beam. There are two general effects related to the space charge of electron beam:

1. Electron longitudinal momentum shift due to potential distribution inside the beam,
2. Drift motion of the electrons in the crossed guiding longitudinal magnetic field of the cooler solenoid and radial electric field of the electron beam.

The electron drift motion leads to two effects: electron beam rotation with the drift velocity around its axis and increase of the transverse velocity spread by the value depending on conditions of the electron beam injection into the magnetic field. In the worst case additional transverse velocity spread is equal to the drift velocity value.

The space charge effects can be calculated accurately for electron beam of uniform density distribution. In this case the relative longitudinal momentum shift of the electrons at the point (x^*, z^*) is calculated in accordance with

$$\delta\theta_s = (1 - \eta_n(r^*)) \frac{eI}{\beta^3 \gamma m_e c^3} \left(\frac{r^*}{a} \right)^2, \quad (4.19)$$

where $r^* = \sqrt{(x^*)^2 + (z^*)^2}$, I , a are electron beam current and radius correspondingly, η_n is the factor of electron beam space charge neutralisation by ions of residual gas. The relative coherent drift velocity is calculated as:

$$\theta_d = (1 - \eta_n(r^*)) \frac{2I}{cB\beta\gamma^2} \frac{r^*}{a^2}, \quad (4.20)$$

where B is the magnetic field value. Both values – (4.19), (4.20) do not depend on longitudinal co-ordinate. These formulae can be used for calculation in the case of standard configuration of the cooler or for cooling of bunched ion beam with bunched electron beam, when electron bunch radius and length are substantially larger than ion one. However, in the second case one needs to substitute in (4.19) the electron density in the central part of the electron bunch instead of electron beam current and radius.

In general case of a bunched electron beam the electron momentum varies across the beam in accordance with the following equation [7]:

$$\delta\theta_s = (1 - \eta_n(r^*)) \frac{2\lambda(s - s_0)r_e}{\beta^2 \gamma} F\left(\frac{r^*}{\sqrt{2}a}\right), \quad (4.21)$$

where r_e is the classical electron radius, $a = \sqrt{\sigma_x^2 + \sigma_z^2}$ is the mean electron bunch radius, σ is r.m.s bunch dimension in the corresponding direction, λ is the electron linear density and $F(t)$ is the function, which describes the electron beam potential distribution across the beam. When the beam density distribution across the beam is Gaussian, the function $F(t)$ can be written as follows:

$$F(t) = \int_0^t \frac{1 - \exp(-u^2)}{u} du, \quad t = \frac{r}{\sqrt{2}a_i} \quad (4.22)$$

For long electron bunch the $\delta\theta_s$ magnitude (4.21) can be calculated under the assumption of uniform density distribution along the beam axis. For short electron bunch one can expect Gaussian distribution in the longitudinal direction:

$$\lambda(s) = \begin{cases} \frac{N_e}{\sqrt{2\pi}\sigma_s} e^{-\frac{(s-s_0)^2}{2\sigma_s^2}}, & \text{Gaussian bunch} \\ \frac{N_e}{l_{bunch}}, & \text{uniform distribution} \end{cases}, \quad (4.23)$$

where N_e is the electron number in the bunch, σ_s is r.m.s bunch length, l_{bunch} is the total bunch length in the case of uniform density distribution in the longitudinal direction.

For Gaussian bunch the relative coherent drift velocity is described with formula:

$$\theta_d = (1 - \eta_n(r^*)) \frac{e\lambda(s-s_0)}{\beta\gamma^2 B} F_2(r^*), \quad (4.24)$$

where B is the longitudinal magnetic field value and the radial dependence of the bunch field is given by the expression:

$$F_2(r^*) = 2 \frac{1 - \exp\left(-\frac{r^{*2}}{2a^2}\right)}{r^*}. \quad (4.25)$$

The coherent part of the drift velocity has to be added to the ion angle in the electron beam. Finally the ion angles in the frame referenced to the electron beam are:

$$\begin{aligned} \theta_x^* &= \theta_x - \delta\theta_x + \text{sign}(B)\theta_d \frac{z^*}{r^*} \\ \theta_z^* &= \theta_z - \delta\theta_z - \text{sign}(B)\theta_d \frac{x^*}{r^*} \end{aligned} \quad (4.26)$$

Here $\text{sign}(B)$ is positive, when the magnetic field has the same direction as electron velocity and negative in the opposite case.

The drift velocity has also to be included into calculation of the friction force as an addition to the electron transverse velocity spread:

$$\theta_{\perp} = \sqrt{\theta_T^2 + (k\theta_d)^2}, \quad (4.27)$$

where k is some coefficient less than unit, θ_T is the electron angular spread on the electron beam axis corresponding to the electron thermo-velocity:

$$\theta_T = \frac{1}{\beta\gamma} \sqrt{\frac{T_\perp}{m_e c^2}}, \quad (4.28)$$

where T_\perp is the electron temperature of the transverse degree of freedom determined by the electron gun cathode temperature in the case of electrostatic acceleration of the electron beam.

At arbitrary density distribution of the electron beam one needs to solve numerically the Poisson equation. This procedure can be realized in future development of the program. At this stage the simulation of electron cooling at arbitrary shape of density distribution will be performed neglecting to the electron beam space charge. Calculation of the electron beam space charge effects decreases significantly the calculation speed. More preferable way is to calculate its influence in the frame of a simplest model of the electron beam and to use this result as an estimation of the mistake in the cooling time calculation.

If the electron beam parameters in the cooling section is calculated using external program, for instance PARMELA, the electron beam model can be build on the basis of these results. For this aim one needs to prepare procedures returning local electron beam density and velocity spread as function of co-ordinates inside the electron beam.

4.2.1. Space charge effect in the hollow electron beam

The space charge effects lead to dependence of the mean electron velocity and electron velocity spread on co-ordinates inside the electron beam. There are two general effects related to the space charge of electron beam:

1. Electron longitudinal momentum shift due to potential distribution inside the beam,
2. Drift motion of the electrons in the crossed guiding longitudinal magnetic field of the cooler solenoid and radial electric field of the electron beam.

In difference with usual electron cooling system at the moment there is no realistic model of the beam neutralization by residual gas ions. For the electron beam at uniform density it was experimentally proved at a few coolers, that the distribution of the residual gas ions inside the electron beam is closed to uniform. Therefore the space charge neutralization can be taken into account with analytical expressions for the beam self fields. For the hollow beam one can expect overcompensation of the electron space charge inside the hole and sufficiently non uniform ion distribution in the outer circle. To develop realistic model of the electron beam neutralization for the hollow beam detailed experimental investigations are necessary. Thus in the current version of the model the space charge effects can be taken into account correctly at zero neutralization degree only. The space charge effects are simulated in the program when the check box “Space Charge” (Fig. 4.5) is checked.

The electron momentum shift as a function of radial co-ordinate repeats the shape of potential distribution. It is assumed that at the beam axis the electron momentum corresponds to the ion one. In this case for instance in the electron beam at uniform distribution the shift in relative momentum is

$$\delta\theta_s = \frac{eI}{\beta^3 \gamma m_e c^3} \left(\frac{r}{a} \right)^2, \quad (4.29)$$

where I is the beam current and a – its radius.

For the hollow beam the potential distribution can be found as a superposition of potentials of two beams: negatively charged beam at density n_{circle} and radius r_{beam} and positively charged beam at density $n_{circle} - n_{hole}$ and radius r_{hole} (Fig.4.7).

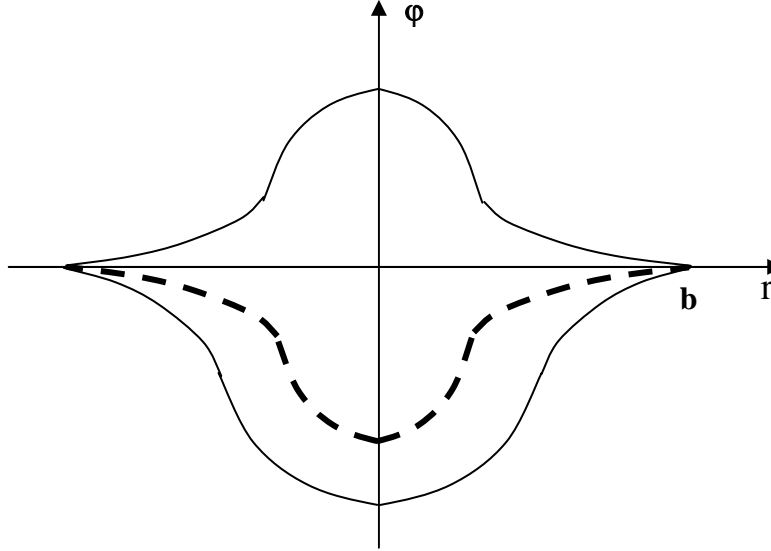


Fig.4.7. The potential distribution in the vacuum chamber of radius b . Dashed line corresponds to potential distribution of the hollow beam.

The relative momentum shift in the negatively charged beam is given by the same formula. The potential distribution of the positively charged beam (under assumption that the potential at the beam axis is zero) is given by the formula:

$$\varphi(r) = -\frac{I}{\beta c} \begin{cases} \frac{r^2}{r_{hole}^2}, & 0 < r \leq r_{hole} \\ 1 + 2 \ln \frac{b}{r_{hole}} - 2 \ln \frac{b}{r}, & r > r_{hole} \end{cases}, \quad (4.30)$$

where the beam current is calculated as

$$I = e(n_{circle} - n_{hole})\pi r_{hole}^2 \beta c. \quad (4.31)$$

The relative coherent drift velocity (drift angle) for uniform cylinder is calculated as:

$$\theta_d = \frac{2I}{cB\beta\gamma^2} \frac{r}{a^2}, \quad (4.32)$$

where B is the magnetic field value. The electric field in this formula is obtained as a derivative of the beam potential. In the case of hollow beam the drift angle is a linear function of the radial coordinate inside the hole, and superposition of linear and inversely proportional functions in the outer circle. For the space charge simulation in the hollow beam an additional input parameter is required – the vacuum chamber radius in the cooler.

4.3. Model of the cooler

The model of electron cooler provides a choice of the numerical method for the system (4.2) integration and takes into account mistakes of the electron beam position in the cooling section. The system can be solved in the frame of two different models of the cooler:

1. Electron cooler as a thin length,
2. Electron cooler as a system of non-zero length.

In the case, when the friction force variation along the cooling section is negligible and relative change of the particle momentum is small, the electron cooling section can be treated as a thin lens. This model presumes also that the ion transverse co-ordinates do not change during motion inside the cooler. Thus, the ion angle variation is calculated as following

$$\Delta\theta = \frac{F}{Mc^2\beta^2\gamma} l_{cool}, \quad (4.33)$$

where l_{cool} is the cooling section length, F is the friction force in LRF. The ion co-ordinates are not changed inside cooler.

At non-zero length of the cooler the ion motion equation can be solved using one of the numerical methods: Euler or Runge-Kutta. Numerical integration of the ion motion equations is necessary also in the case, when electron beam trajectory does not coincide with the ion equilibrium orbit. Herewith the cooler model provides the ion co-ordinates transformation from the frame referenced to the ion equilibrium orbit to the frame referenced to the electron beam trajectory.

Now in the program the electron beam trajectory position is introduced from additional file. In this file the transverse co-ordinates of the electron trajectory are specified in a few points along the cooling section. By this way the cooling section is divided by a few sub intervals in longitudinal direction. In each interval the electron trajectory assumed to be a straight line displaced from the ion trajectory and having some angle with it. Position of the electron beam trajectory is determined by its transverse co-ordinates at the entrance and at the exit of the sub interval.

The ion transverse co-ordinates relatively to the electron beam trajectory are calculated as functions of its longitudinal co-ordinate (independent variable in the system 4.2) in accordance with the angles between electron and ion beam axis:

$$\theta_{e,i,x} = \frac{x_f - x_0}{l_{SI}}, \quad \theta_{e,i,z} = \frac{z_f - z_0}{l_{SI}}, \quad (4.34)$$

where x_f, x_0 is initial and final horizontal co-ordinate of the electron beam trajectory in the sub interval correspondingly, calculated from the ion equilibrium orbit. l_{SI} is the length of corresponding sub interval. The same is for vertical position. The ion velocity components in the frame referenced to the electron beam trajectory are corrected by these angles. We assume that the angles between the electron beam trajectory and the ion equilibrium orbit are sufficiently less than unity. In this case correction of the ion longitudinal velocity is not necessary.

Under assumption that the both angles are sufficiently less than the ion angle the ion co-ordinates in the sub interval are calculated as:

$$\begin{aligned}
x &= x + x_0 + \theta_{e,i,x} s \\
z &= z + z_0 + \theta_{e,i,z} s \\
\theta_x &= \theta_x + \theta_{e,i,x} \\
\theta_z &= \theta_z + \theta_{e,i,z},
\end{aligned} \tag{4.35}$$

where co-ordinate s is calculated from the entrance of corresponding sub interval.

5. Kick of the ion momentum components in the electron cooling section

The Model Beam algorithm presumes that the ion geometrical co-ordinates do not changed after crossing the cooling section and action of the cooling leads to change of the ion momentum components only. The kick in the ion beam momentum after crossing the cooler is calculated on the base of the map of the cooling section. The map transforms the initial ion co-ordinates in 6D phase space to the final ones:

$$\vec{X}_{in} = \{x_{in}, \theta_{x,in}, z_{in}, \theta_{z,in}, (s-s_0)_{in}, \theta_{s,in}\} \rightarrow \vec{X}_f = \{x_f, \theta_{x,f}, z_f, \theta_{z,f}, (s-s_0)_f, \theta_{s,f}\}, \tag{5.1}$$

The Model Beam algorithm ignores the ion geometry co-ordinate variation ($x, z, s-s_0$) and multiplies the ion momentum components by the factor:

$$\theta_\xi = \theta_{\xi,0} \times \exp\left(\left(\theta_{\xi,f} - \theta_{\xi,in}\right) \frac{\Delta t}{T_{rev}}\right), \tag{5.2}$$

where $\xi = x, z, s - s_0$, Δt – step over time in the dynamics simulation.

The particle losses after crossing the cooler are calculated separately for total beam and for Model Beam. In the total beam the ion number is decreased in accordance with:

$$N = N_0 \times \exp\left(-\frac{P_{loss}}{N_{MB}} \frac{\Delta t}{T_{rev}}\right), \tag{5.3}$$

where P_{loss} is the particle loss probability calculated by the map of the cooling section in accordance with (4.5), N_{MB} is the particle number in the Model Beam. For the particle in the Model Beam the program generates random number uniformly distributed in the range from 0 to 1, if this number is smaller than P_{loss} for this particle new co-ordinates are generated in accordance with current ion distribution as it described in the chapter 2. If the random number is larger than P_{loss} the particle is alive and its co-ordinates are not changed.

6. Algorithm of the electron cooling time calculation

For rms dynamics simulation one needs to calculate characteristic cooling times and the lifetime due to recombination in the cooling section. In the present version of the program the cooling times can be calculated for two models of the ion beam. In the frame of the first model the ion beam is presented by an ion having invariants of the motion corresponded to r.m.s. beam emittances. In this case a change of the ion motion invariants after crossing the cooling section is averaged over the phases of the ion betatron and synchrotron oscillations in the ring. In the second model the ion beam

is presented as an array of particles. The particle distribution over co-ordinates is Gaussian at corresponding r.m.s. parameters and matched with the lattice parameters of the ring in the cooling section. The beam is propagated through the cooling section particle by particle and r.m.s. parameters of the particle distribution function at the exit of the cooler are used for the cooling time calculation.

6.1. Calculation of the characteristic times of the ion motion invariant changing

The ion co-ordinates at the entrance of the cooling section can be expressed as functions of the motion invariants and phases of the betatron and synchrotron oscillations. The ion "betatron" coordinates and momentum inside the cooling section can be calculated in accordance with

$$x_\beta = \sqrt{I_x \beta_x} \sin \varphi, \quad x'_\beta = \sqrt{\frac{I_x}{\beta_x}} (\cos \varphi + \alpha_x \sin \varphi). \quad (6.1)$$

where φ - is the phase of the horizontal betatron oscillation, α_x and β_x are alpha and beta functions at the entrance of the cooling section. The same expressions are used for z co-ordinate with substitution of corresponding alpha and beta function values. Where we introduced the notation $x' = \frac{p_x}{p}$. For r.m.s. particle the mean square of the co-ordinates have to be equal corresponding standard deviations:

$$\sigma_x = \sqrt{\varepsilon_x \beta_x}, \quad \sigma_{x'} = \sqrt{\varepsilon_x \gamma_x}, \quad (6.2)$$

where ε_x is r.m.s. emittance and gamma function is calculated as usual $\gamma_x = \frac{1 + \alpha_x^2}{\beta_x}$. To satisfy this equation the invariant of the motion I_x is to be equal to two sigma emittance $I_x = 2\varepsilon_x$.

Longitudinal emittance of the ion beam is determined in the program as a mean square of the particle momentum deviation:

$$\varepsilon_l = \langle \delta^2 \rangle, \quad (6.3)$$

here to simplify the notation the ion relative longitudinal momentum deviation is denoted as $\delta = \frac{\Delta p}{p}$. In the case of coasting beam the cooling time is calculated by averaging over two values of the momentum deviation:

$$\delta = \pm \sqrt{\varepsilon_l}. \quad (6.4)$$

For the bunched ion beam one can express the particle momentum deviation and its longitudinal co-ordinate (distance from the bunch center) as a function of the phase of synchrotron oscillations:

$$\delta = \sqrt{I_l} \cos \psi, \quad s - s_0 = \beta_l \sqrt{I_l} \sin \psi, \quad (6.5)$$

here the "synchrotron function" is determined as:

$$\beta_l = \frac{R|\eta|}{Q_s}, \quad (6.6)$$

where R is the mean ring radius, η - off momentum factor, Q_s is the synchrotron tune. The standard deviations for longitudinal degree of freedom are calculated in accordance with the longitudinal emittance definition:

$$\sigma_\delta = \sqrt{\varepsilon_l}, \quad \sigma_s = \beta_l \sigma_\delta \quad (6.7)$$

and as in the case of transverse motion to satisfy this equation the invariant of the motion I_l is to be equal to two sigma emittance $I_l = 2\varepsilon_l$.

The total values of the ion x -co-ordinates are equal to:

$$x = x_\beta + D_x \delta, \quad x' = x'_\beta + D'_x \delta, \quad (6.8)$$

where D and D' are dispersion and its derivative in the cooling section. For the vertical plane all the procedures are provided by the same way.

Using these formulae at given values of the phases of betatron and synchrotron oscillations one can calculate particle co-ordinates and velocity components at the entrance of the cooling section. The map of the electron cooling section transforms the ion coordinates to the exit of the cooler and returns the probability of the ion loss. New values of the particle motion invariants are calculated in accordance with the following formulae. Invariant of the particle longitudinal motion for a coasting beam is calculated simply as a square of the relative momentum deviation, for a bunched beam

$$I_l = \left(\delta^2 + \left(\frac{(s - s_0)}{\beta_l} \right)^2 \right). \quad (6.9)$$

The Courant – Snider invariants of the particle betatron motion are calculated from the "betatron" particle co-ordinates:

$$x_\beta = x - D_x \delta, \quad x'_\beta = x' - D'_x \delta. \quad (6.10)$$

The invariant calculated in accordance with

$$I_x = \left(\beta_x x'^2_\beta + 2\alpha_x x_\beta x'_\beta + \gamma_x x^2_\beta \right) \quad (6.11)$$

corresponds to 2-sigma emittance of the beam. The invariant of vertical motion is calculated with substitution z instead x .

When the electron cooler is treated as a thin lens, the lattice parameters at the exit of the cooler coincide with that ones at the entrance. For the cooler model taking into account finite length of the cooling section the tracking of the lattice parameters through the cooler is necessary. Neglecting the influence of the cooler magnetic field on the ion motion the lattice parameters at the exit of the cooling section are calculated as:

$$\beta_{f,x} = \beta_x - 2\alpha_x L_{cool} + \gamma_x L_{cool}^2, \quad \alpha_{f,x} = \alpha_x - \gamma_x L_{cool}. \quad (6.12)$$

The characteristic time of change of the rms particle invariant is calculated in accordance with:

$$\frac{1}{\tau_{cool}} = \frac{1}{I} \frac{\langle \delta I \rangle}{T_{rev}}, \quad (6.13)$$

where T_{rev} is the particle revolution period in the storage ring, the brackets mean averaging over the phases of betatron and synchrotron oscillations:

$$\langle \delta I \rangle = \frac{1}{8\pi^3} \int_0^{2\pi} \int \int \delta I(\vec{I}, \varphi_x, \varphi_z, \varphi_s) d\varphi_x d\varphi_z d\varphi_s. \quad (6.14)$$

The formula (6.13) gives the cooling time for single particle, which invariants of the motion correspond to the beam r.m.s. emittances.

The ion beam life time is calculated by averaging over the phases the ion loss probability:

$$\frac{1}{\tau_{life}} = \frac{\langle P_{loss} \rangle}{T_{rev}}, \quad (6.15)$$

where the averaging is performed by the same way as for invariants:

$$\langle P_{loss} \rangle = \frac{1}{8\pi^3} \int_0^{2\pi} \int \int P_{loss}(\vec{I}, \varphi_x, \varphi_z, \varphi_s) d\varphi_x d\varphi_z d\varphi_s. \quad (6.16)$$

6.2. Calculation of the characteristic times of emittance variation using Monte Carlo method

Calculation of the characteristic times of the beam emittance variation is performed in the program using Monte Carlo method, which includes the following steps.

1. Generation the beam as an array of the particles matched with the optics structure of the ring at the entrance of the cooler.
2. Propagation the beam through the cooler particle by particle using the map of the cooling section.
3. Calculation the new values of the beam emittances after crossing the cooler.
4. Calculation the cooling time in accordance with the formula:

$$\frac{1}{\tau_{cool}} = \frac{1}{\varepsilon} \frac{\Delta \varepsilon}{T_{rev}}. \quad (6.17)$$

The beam generation is performed as described in the chapter 2. For the beam emittance calculation one can use one of the procedures described in the chapter 2. The result of the calculation can slightly depends one the procedure used for the emittance calculation. This fact can be illustrated on example of simplest model of the cooler. Really, one can treat the cooling section as a thin lens – in this case the particle co-ordinates keep their initial values and components of momentum are changed in accordance with the friction force value. Therefore the beam Twiss parameters are changed in the same time when the lattice parameters are constant due to zero length of the cooler in the frame of this model. This leads to mismatch the beam with the ring optics structure and as

result to additional emittance growth if the emittance is calculated through rms co-ordinates of the beam.

When the electron cooler is treated as a system of non-zero length the program provides tracking of the lattice parameters through the cooling section as in the case of single particle cooling time calculation.

The ion beam lifetime is calculated with the same formula as in this case of single particle model:

$$\frac{1}{\tau_{life}} = \frac{\langle P_{loss} \rangle}{T_{rev}}, \quad (6.18)$$

however, here the averaging of the loss probability is provided over the particles.

References

- [1] G.Budker, Proc. Intern. Symp. Electron and Positron Storage Rings, Saclay, 1966.
- [2] I.Meshkov, Electron cooling: Status and Perspectives, Phys. Part. Nucl., 25, (6), 1994, 631.
- [3] Derbenev Ya.S., Skrinsky A.N., Fyzika plasmy, 1978. v.4, p.492
- [4] I.Meshkov, Physics and Technique of Electron Cooling, RIKEN-AF-AC-2, 1997
- [5] V.Parkhomchuk, New insights in the theory of electron cooling, NIM A 441 (2000) 9-17, p.9
- [6] A.Wolf, et al., Recombination in electron coolers, NIM A 441(2000), 183
- [7] A. Sidorin, I.Meshkov, T.Katayama, P.Zenkevich "Ion Bunch Stability in the Double Storage Ring", RIKEN-AF-AC-19, Febr. 2000
- [8] Ya. Derbenev, "Electron cooling of heavy ions in solenoid with undulator", TJNAL, 13.02.2001, unpublished.
- [9] M.Bell, J.S.Bell, Capture of cooling electrons by cool protons, Particle accelerators, 1982 Vol.12 pp.49-52.

III. Intrabeam scattering

1. Introduction

Intrabeam scattering (IBS) in the ion beam causes two processes: relaxation of the beam to a thermal equilibrium between degrees of freedom and diffusion growth of 6D phase volume of the beam due to variation of lattice parameters along ring circumference.

All usually used numerical algorithms of IBS growth rate calculation are based on the model of the collisions proposed by A. Piwinski.

Four models for IBS calculation – Piwinski, Martini (extended Piwinski), Bjorken-mtingwa and Jie Wei models are realized in new version of BETACOOOL program for Gaussian distribution of ions over velocity. The Martini model does not require additional assumptions for calculation of the beam emittance growth times. Piwinski model can be deduced from Martini model neglecting a variation of dispersion and beta function along the ring orbit (uniform optics). In the model proposed by Jie Wei characteristic times of emittance variation are calculated for real lattice parameters of the ring under a few additional assumptions, which correspond to storage rings at ion energy over the transition energy (for instance RHIC). The description of the models is presented in this chapter in accordance with notation in original papers [1 – 3].

2. Structure of the effect

Simulation of the intrabeam scattering (IBS) process is based on calculation of the particle momentum variation due to coulomb interactions with other particles of the beam. In the BETACOOOL the particle momentum variation can be calculated using analytical expressions for diffusion coefficients or, for coasting ion beam, using Molecular Dynamics (MD) technique. On the basis of both approaches each optic element of the ring is presented as a map for IBS process.

The map of the IBS process based on direct calculation of the ion coulomb interaction can be combined with the transformation map of optic element calculated from external focusing fields. In such a form the IBS process is simulated in the frame of tracking algorithm based on MD technique. This algorithm uses as input parameters the particle array presenting the ion beam and characteristics of external focusing fields.

The map of IBS process based on analytical theory calculates the growth rates for three degrees of freedom by numerical evaluation of integrals over ion distribution function assuming that the distribution function has Gaussian shape. The values of the growth rates are used for calculation of the individual particle momentum variation. The calculation of the growth rates requires as input parameters the rms beam emittance and lattice functions of the ring in given optic element.

In the frame of rms dynamics simulation the growth rates calculated in each optic element are averaged over the ring circumference. This procedure requires as input parameters the rms beam emittances and description of the ring optic structure. The ring optic structure can be presented in both variants: as a specification of the optic elements or as dependencies of the lattice functions on the longitudinal co-ordinate along the ring circumference. In the first case the program initially provides tracking of Twiss parameters along the ring and transforms the ring model to the form of the lattice functions.

In the frame of a few models for the IBS growth rates calculation one needs mean parameters of the ring only. In this case detail description of the ring optic structure is not necessary and the IBS process can not be presented by a transformation map. Such models of the IBS can be used only in Model Beam algorithm and rms dynamics simulation.

For Model Beam algorithm a few “detailed” models of the IBS process were developed. In the “detailed” models the kick of the particle momentum components is calculated as a function of the particle co-ordinates in 6D phase space.

3. Models of IBS

When particles in a beam scatter within each other one needs to consider both large and small angle scattering. The effect when particles can be lost as a result of a single collision event (large-angle scattering) is called Touschek effect. When the scattering angles are small, random addition of such small scattering events can lead to a growth of beam dimensions. Such a multiple Coulomb scattering was first applied to explain emittance growth in electron beams (Bruck, Le Duff) and was called "multiple Touschek effect".

Typically, in electron machines the longitudinal beam temperature is much smaller than the transverse, an assumption which was used in original studies of the Touschek effect. Multiple Coulomb scattering was later generalized by Piwinski for proton machines without making any restrictions on the magnitude of beam temperatures, thus making it possible to transfer energy from the longitudinal into transverse via collisions. The generalized treatment of multiple small-angle Coulomb scattering was then renamed as the Intrabeam Scattering (IBS). The IBS theory was later extended to include variations of the betatron functions and momentum dispersion function along the lattice, and was summarized by Martini (typically referred to as Martini's model).

The different approach to IBS using the scattering matrix formalism from quantum electrodynamics was used by Bjorken and Mtingwa (B-M model). Both B-M and Martini's models are in good agreement with one another. In what way IBS in particle beams is different from similar scattering of gas molecules? In circular accelerators, the curvature of the orbit produces a dispersion. Because of the dispersion, a change of energy leads to change in the betatron amplitude. In other words, we have coupling of the longitudinal and transverse motion.

Another consequence of this curvature effect is the negative-mass behavior of particles so that conservation law of beam temperature leads to a simple conclusion that below transition energy one can have an equilibrium between the transverse and longitudinal temperatures while above transition (in the "negative-mass" regime) there is a continuous emittance increase in both transverse and longitudinal directions. Is this coupling effect always important in circular accelerator and one always needs to use standard IBS approach rather than the gas-relaxation formula?

This question was studied in detail by Sorensen. He found that the IBS growth rates can be simply represented by a universal curve. When plotted against parameter $\varepsilon/(\Delta p/p)^2$ (where ε is the rms beam emittance) such a universal curve shows a minimum ("brake-up") point. To the left of such a minimum the transverse growth rate dominates, while to the right - the growth rate is dominated by the longitudinal growth rate. This was explained by a collapse of the longitudinal velocity distribution with energy. The longitudinal and transverse velocities spread in the beam rest frame are given by:

$$\Delta v_{\parallel} = \frac{\Delta p}{\gamma m}, \quad \Delta v_x = \frac{1}{m} \sqrt{\frac{\varepsilon}{\beta_x}} p,$$

which gives

$$\frac{\varepsilon}{(\Delta p / p)^2} = \frac{\varepsilon}{\gamma^2}$$

As a result, for a high energy $\gamma > \gamma_{tr}$, the effect of collapsed velocity distribution dominates over coupling, and the longitudinal IBS can be described by the gas-relaxation formula, independent of the ring lattice.

3.1. Analytical model of the multiple particle collisions

According to Piwinski [1], the relative changes of momenta after a collision between two particles labeled by 1 and 2 are (for the longitudinal and radial axis):

$$\begin{aligned} \frac{\delta p}{p} &= \frac{1}{2} (2\alpha\gamma \sin \bar{\psi} \sin \bar{\phi} + \gamma\xi(\cos \bar{\psi} - 1)) \\ \frac{\delta p_x}{p} &= \frac{1}{2} \left(\left[\varsigma \sqrt{1 + \frac{\xi^2}{4\alpha^2}} \cos \bar{\phi} - \frac{\xi\theta}{2\alpha} \sin \bar{\phi} \right] \sin \bar{\psi} + \theta(\cos \bar{\psi} - 1) \right), \end{aligned} \quad (3.1)$$

with the notation

$$\gamma\xi = \frac{\Delta p_1}{p} - \frac{\Delta p_2}{p}, \quad \theta = x'_1 - x'_2, \quad \varsigma = z'_1 - z'_2 \quad (3.2)$$

γ - is the particle Lorenz factor.

$\bar{\psi}$ and $\bar{\phi}$ denote the scattering axial and azimuthal angles in the center of mass (C.M.) between the particles after the collision.

$2\alpha \ll 1$ is the angle between the momentum vectors of the colliding particles in the laboratory reference frame; this angle can be evaluated by taking the scalar product of the particle momentum vectors (Fig. 3.1).



Fig. 3.1. Two particles collision scheme (non-relativistic case)
a) – LRF; b) C.M. reference frame

The change of particle momentum after collision leads to the corresponding change of the particle motion invariant. It can be calculated under assumption that the radial position of the particle is not changed during the interaction, which is sufficiently short [4.1].

The radial displacement of the particle from the closed orbit is equal to the sum of the betatron and momentum change contributions, which is, to the first order in $\Delta p/p$, described as:

$$x = x_\beta + D \left(\frac{\Delta p}{p} \right), \quad (3.3)$$

where $D(s)$ is the dispersion function. The derivative of x with respect to the co-ordinate s along the equilibrium orbit is equal to the small angle the particle makes with s -axis:

$$x' \equiv \frac{P_x}{P} = x'_\beta + D' \left(\frac{\Delta p}{p} \right) \quad (3.4)$$

where p_x is the x-component of the momentum.

The Courant and Snyder invariant of a particle transverse motion is described as the following:

$$I_x = \gamma_x x_\beta^2 + 2\alpha_x x_\beta x'_\beta + \beta_x x'^2_\beta, \quad (3.5)$$

where $\beta_x \gamma_x - \alpha_x^2 = 1$ and $\beta'_x = -2\alpha_x$.

The change of the Courant and Snyder invariant I is given by:

$$\beta_x \delta I_x = (1 + \alpha_x^2) (2x_\beta \delta x_\beta + \delta x_\beta^2) + 2\alpha_x \beta_x (x'_\beta \delta x_\beta + x_\beta \delta x'_\beta + \delta x_\beta \delta x'_\beta) + \beta_x^2 (2x'_\beta \delta x'_\beta + \delta x'^2_\beta). \quad (3.6)$$

In accordance with the assumption $x = \text{constant}$ we find from (4.3) and (4.4):

$$\delta x_\beta = -D \left(\frac{\delta p}{p} \right), \quad \delta x'_\beta = (\delta p_x / p) - D' (\delta p / p), \quad (3.7)$$

since $\delta \Delta p / p = \delta p / p$, where δp is the full particle momentum change in the collision, it means that variation of the longitudinal component of the particle momentum leads to a change of the horizontal motion invariant, when dispersion is not equal to zero:

$$\begin{aligned} \frac{\delta I_x}{\beta_x} = & -\frac{2}{\beta_x} \left(x_\beta \left(\frac{(1 + \alpha_x^2)}{\beta_x} D + \alpha_x D' \right) + x'_\beta \tilde{D} \right) \frac{\delta p}{p} + \frac{(D^2 + \tilde{D}^2)}{\beta_x^2} \left(\frac{\delta p}{p} \right)^2 + 2 \left(x'_\beta + \frac{\alpha_x}{\beta_x} x_\beta \right) \frac{\delta p_x}{p} + \\ & + \left(\frac{\delta p_x}{p} \right)^2 - \frac{2\tilde{D}}{\beta_x} \frac{\delta p}{p} \frac{\delta p_x}{p}, \end{aligned} \quad (3.8)$$

where $\tilde{D} = \alpha_x D + \beta_x D'$. The changes of vertical and longitudinal invariants are equal:

$$\begin{aligned} \delta I_z = & 2(\beta_z \theta_{z,\beta} + \alpha_x z_\beta) \frac{\delta p_z}{p} + \beta_z \left(\frac{\delta p_z}{p} \right)^2, \\ \delta I_s = & 2m \frac{\delta p}{p} \frac{\Delta p}{p} + m \left(\frac{\delta p}{p} \right)^2, \end{aligned} \quad (3.9)$$

Here we assume that D and D' have zero value in the vertical plane. In this case $z_\beta = z$.

The dependence of the horizontal invariant changes on a longitudinal momentum change leads to heating of the ion beam due to the multiple particle collisions: the particle momentum components

are changed in accordance with momentum conservation law, however in presence of dispersion the sum of the particle motion invariants can increase or decrease depending on collision parameters. Therefore in the frame of this model, IBS in a linear transport line leads only to relaxation between freedom degrees of the ion beam, where as six dimensional phase space is constant (the energy source producing the heating is large value of the longitudinal component of the ion momentum in LRF). In cycling accelerators IBS leads to two effects: relaxation between degrees of freedom and change of six dimensional phase space volume of the beam in presence of dispersion.

The variation of the beam phase space volume can be calculated by averaging of the particle invariant change over the collisions in accordance with particle distribution function. A. Piwinski introduces the time derivative in the C.M. system of the average radial emittance for all particles (denoted $\langle \varepsilon \rangle$) by means of the integral:

$$\left\langle \frac{d}{dt} \frac{\langle \varepsilon \rangle}{\beta_x} \right\rangle = \int 2c \bar{\beta} \bar{P} \int_{\bar{\Psi}_m}^{\pi} d\bar{\Psi} \int_0^{2\pi} d\bar{\Phi} \frac{d\bar{\sigma}}{d\bar{\Omega}} \frac{\delta I_1}{\beta_x} \sin \bar{\Psi} d\bar{\tau} \quad (3.10)$$

where the outer brackets $\langle \dots \rangle$ indicate the average value around the ring. The first integral extends over all phase space betatron co-ordinates, momentum spread values and azimuthal location of two interacting particles (denoted 1 and 2). \bar{P} is the probability density function for the betatron amplitudes and angles, the momentum errors and the azimuthal positions of the interacting particles. \bar{P} is the probability written in terms of the C.M. variables, while P is the same probability written for the laboratory frame variables. Henceforth the bar indicates the values in the C.M. reference frame. $d\bar{\sigma}/d\bar{\Omega}$ is the differential cross-section in the C.M. system for the scattering into the element of solid angle $d\bar{\Omega}$ at given angles $\bar{\Psi}$ and $\bar{\Phi}$. $d\bar{\tau}$ is the C.M. time interval which is related to the laboratory time by the equation $dt = \gamma \cdot d\bar{\tau}$. P may be written according to independent probability density law:

$$P = \rho_{x_\beta x'_\beta}(x_{\beta_1} x'_{\beta_1}) \cdot \rho_{x_\beta x'_\beta}(x_{\beta_2} x'_{\beta_2}) \cdot \rho_{z z'}(z_1 z'_1) \cdot \rho_{z z'}(z_2 z'_2) \cdot \rho_\eta\left(\frac{\Delta p_1}{p}\right) \cdot \rho_\eta\left(\frac{\Delta p_2}{p}\right) \cdot \rho_s(s_1) \cdot \rho_s(s_2), \quad (3.11)$$

$d\bar{\tau}$ is the infinitesimal element of the phase space $dx_{\beta_1} dx'_{\beta_1} \dots ds_1 ds_2$.

At the time when the interaction takes place we have $s_1 = s_2 = s$, $z_1 = z_2$ and $x_1 = x_2$ where $x_{1,2}$ satisfies the equation (3.4).

The collision cross-section can be calculated by the following way. We approximately find for $\alpha \ll 1$:

$$2\alpha \approx \left((x'_2 - x'_1)^2 + (z'_1 - z'_2)^2 \right)^{1/2}. \quad (3.12)$$

Let's consider now the distribution of the scattering angle $\bar{\Psi}$, which results from the Coulomb interaction of two charged particles considering the case of non-relativistic particles in the C.M. system one can use the Rutherford formula:

$$\frac{d\bar{\sigma}(\bar{\Psi})}{d\bar{\Omega}} = \frac{1}{4} \left(\frac{Z^2 e^2}{T} \right)^2 \frac{1}{\sin^4(\bar{\Psi}/2)}, \quad d\bar{\Omega} = \sin \bar{\Psi} \cdot d\bar{\Psi} \cdot d\bar{\Phi} \quad (3.13)$$

T is the kinetic energy of each colliding particle in the C.M. system.

Let $\bar{\psi}_m$ be the smallest scattering angle, its corresponding impact parameter \bar{b} is given by the equation:

$$\bar{b} = \frac{e^2}{2T} \text{ctg} \frac{\bar{\psi}_m}{2}. \quad (3.14)$$

Alternatively, equation (3.13) may be expressed as follows:

$$\frac{d\sigma(\bar{\psi})}{d\Omega} = \left(\frac{\frac{Z^2}{A} r_p}{4\bar{\beta}^2} \right) \frac{1}{\sin^4(\bar{\psi}/2)}, \quad (3.15)$$

where $r_p = \frac{Z^2 e^2}{A m_p c^2}$ is the ion classical radius, m_p is the proton mass, Z and A are the ion charge and atomic numbers, $\bar{\beta}c$ is the particle velocity in the C.M. system and $\bar{\beta} \ll 1$ by our assumption. In a similar fashion one gets:

$$\text{tg} \bar{\psi}_m = \frac{r_i}{2\bar{\beta}^2 \bar{b}}. \quad (3.16)$$

To evaluate $\bar{\beta}$ we express the two particle momenta difference, which is roughly equal to $2m_i \bar{\beta}c$, in terms of their components in the C.M. reference frame. Then, using the Lorentz transformation for the momenta, we come back to the LRF. With all the calculations done we find in a first approximation:

$$\bar{\beta} \approx \frac{1}{2} \beta \gamma \left(\frac{1}{\gamma^2} \left(\frac{\Delta p_1}{p} - \frac{\Delta p_2}{p} \right)^2 + (x'_1 - x'_2)^2 + (z'_1 - z'_2)^2 \right)^{1/2}, \quad \Delta P_{1,2} = (\bar{P}_{1,2} - \bar{P}_0)_s \quad (3.17)$$

where βc is the average particle velocity in the LRF and γ is the associated Lorenz factor, P corresponds to the particle with the velocity of βc . The integral required for calculation of formula (3.10) can be written as following:

$$Int = \int_{\bar{\psi}_m}^{\pi} d\bar{\psi} \int_0^{2\pi} d\bar{\phi} \frac{\delta \varepsilon}{\beta_x} \frac{d\sigma}{d\Omega} \sin \bar{\psi}. \quad (3.18)$$

It is evaluated by substitution of the expressions given in equations (4.1, 4.2, 4.8, 4.15), which leads to the following result:

$$Int = \frac{\pi r_o^2}{16\bar{\beta}^4} \int_{\bar{\psi}_m}^{\pi} d\bar{\psi} \frac{\sin \bar{\psi}}{\sin^4(\bar{\psi}/2)} \left\{ (1 - \cos \bar{\psi}) \left(\frac{2x_\beta}{\beta_x} \left(\frac{(1 + \alpha_x^2)}{\beta_x} D\gamma\xi + \alpha_x (D'\gamma\xi - \theta) \right) + \right. \right. \\ \left. \left. + 2x'_\beta \left(\frac{\bar{D}\gamma\xi}{\beta_x} - \theta \right) + \frac{(D^2 + \bar{D}^2)}{\beta_x^2} \gamma^2 \xi^2 + \theta^2 - \frac{2\bar{D}}{\beta_x} \gamma\xi\theta \right) + \right. \quad (3.19)$$

$$+ \sin^2 \bar{\Psi} \left(\frac{(D^2 + \bar{D}^2)}{4\beta_x^2} \gamma^2 (\theta^2 + \varsigma^2 - 2\xi^2) + \frac{1}{4} (\xi^2 + \varsigma^2 - 2\theta^2) + \frac{3\bar{D}}{2\beta_x} \gamma \xi \theta \right) \Bigg\}.$$

The definite integrals over the scattering angle $\bar{\Psi}$ can be calculated analytically:

$$\int_{\bar{\Psi}_m}^{\pi} \frac{\sin \bar{\Psi} (1 - \cos \bar{\Psi})}{\sin^4 (\bar{\Psi}/2)} d\bar{\Psi} = -4 \ln \left(\frac{1 - \cos \bar{\Psi}}{2} \right) \Bigg|_{\bar{\Psi}_m}^{\pi} = 4 \ln \left(1 + \frac{4\bar{\beta}^4 \bar{b}^2}{r_i^2} \right), \quad (3.20)$$

since $1 - \cos \bar{\Psi} = 2tg^2(\bar{\Psi}/2)/(1 + tg^2(\bar{\Psi}/2))$ and $tg \bar{\Psi}_m$ with the Formula (3.16).

In a similar way we find:

$$\int_{\bar{\Psi}_m}^{\pi} \frac{\sin^3 \bar{\Psi}}{\sin^4 (\bar{\Psi}/2)} d\bar{\Psi} = -8 \left(\cos^2 (\bar{\Psi}/2) + \ln \left(\frac{1 - \cos \bar{\Psi}}{2} \right) \right) \Bigg|_{\bar{\Psi}_m}^{\pi} = 8 \ln \left(1 + \frac{4\bar{\beta}^4 \bar{b}^2}{r_0^2} \right), \quad (3.21)$$

under the assumption $4\bar{\beta}^4 \bar{b}^2 / r_0^2 \gg 1$.

Taking advantage of these results we arrive, after simple formal transformations, at the expression:

$$\begin{aligned} Int = \frac{\pi \cdot r_i^2}{8\bar{\beta}^4} & \left\{ \frac{4x_{\beta}}{\beta_x} \left(\frac{(1 + \alpha_x^2)}{\beta_x} D\gamma\xi + \alpha_x (D'\gamma\xi - \theta) \right) + 4x'_{\beta} \left(\frac{\bar{D}}{\beta_x} \gamma\xi - \theta \right) + \xi^2 + \varsigma^2 + \right. \\ & \left. + \frac{(D^2 + \bar{D}^2)}{\beta_x^2} \gamma^2 (\theta^2 + \varsigma^2) + \frac{2\bar{D}}{\beta_x} \gamma\xi\theta \right\} \ln \left(1 + \frac{4\bar{\beta}^4 \bar{b}^2}{r_i^2} \right). \end{aligned} \quad (3.22)$$

Let us perform the substitutions into (3.22) (in full accordance with Formula (3.2)):

$$x_{\beta_{1,2}} = x_{\beta} \pm \frac{D\gamma \cdot \xi}{2}, \quad x'_{\beta_{1,2}} = x'_{\beta} \pm \frac{\theta - D'\gamma \cdot \xi}{2}, \quad z'_{1,2} = z' \pm \frac{\xi}{2}, \quad \left(\frac{\Delta p}{p} \right)_{1,2} = \eta \pm \frac{\gamma \cdot \xi}{2} \quad (3.23)$$

(Note that η is not here the usual eta function $-(\Delta f / f) / (\Delta p / p)$).

Hence, by virtue of the theorem on functions of random variables, the joint probability density law P expressed in terms of these new variables takes the following form:

$$P(x_{\beta}, x'_{\beta}, z, z', \eta, s, \xi, \theta, \zeta) = |J| \cdot P(x_{\beta_1}, x'_{\beta_1}, x'_{\beta_2}, z_1, z'_1, z'_2, \frac{\Delta p_1}{p}, \frac{\Delta p_2}{p}, s) \quad (3.24)$$

and $|J| = \gamma$, where J is the Jacobian of the transformation (3.23).

In accordance with calculations carried out earlier (eq.3.22), we obtain:

$$\begin{aligned}
\frac{d}{d\bar{t}} \cdot \frac{\langle \varepsilon \rangle}{\beta_x} = & \frac{\pi}{4} \cdot c r_0^2 \gamma \int \bar{P} \left\{ \frac{4x_{\beta_1}}{\beta_x} \left(\frac{(1 + \alpha_x^2)}{\beta_x} \cdot D \cdot \gamma \cdot \xi + \alpha_x (D' \cdot \gamma \cdot \xi - \theta) \right) + \right. \\
& 4x'_{\beta_1} (D' \cdot \gamma \cdot \xi - \theta) + \xi^2 + \zeta^2 - 2\theta^2 + \frac{(D^2) + \tilde{D}^2}{\beta_x^2} \gamma^2 (\zeta^2 + \theta^2 - 2\xi^2) + \frac{6\gamma}{\beta_x} \tilde{D} \xi \cdot \theta \Big\} \cdot \\
& \cdot \ln \left(1 + \frac{4\bar{\beta}^4 \bar{b}^2}{r_0^2} \right) \frac{d\bar{\tau}}{\bar{\beta}^3}
\end{aligned} \quad (3.25)$$

where $d\bar{\tau} = dx_\beta dx'_\beta dz dz' d\eta \cdot ds \cdot d\xi \cdot d\theta \cdot d\zeta$.

Clearly, P is symmetrical with respect to ξ, θ and ζ . Therefore, the integral vanishes for the linear terms in ξ, θ, ζ of the integrand. Consequently, we are left with:

$$\begin{aligned}
\frac{d}{d\bar{t}} \cdot \frac{\langle \varepsilon \rangle}{\beta_x} = & \frac{\pi}{4} \cdot c r_0^2 \gamma \int \bar{P} \left\{ \xi^2 + \zeta^2 - 2\theta^2 + \frac{(D^2) + \tilde{D}^2}{\beta_x^2} \gamma^2 (\zeta^2 + \theta^2 - 2\xi^2) + \frac{6\gamma}{\beta_x} \tilde{D} \xi \cdot \theta \right\} \cdot \\
& \cdot \ln \left(1 + \frac{4\bar{\beta}^4 \bar{b}^2}{r_0^2} \right) \frac{d\bar{\tau}}{\bar{\beta}^3}
\end{aligned} \quad (3.26)$$

This formula is obtained without an assumption about particle distribution, hence this integral can be calculated for arbitrary distribution function. All the analytical models described below are based under assumption that all betatron amplitudes and angles as well as the momentum deviations obey a Gaussian distribution, while the particle distribution in the longitudinal direction is assumed to be uniform if the beam is unbunched, otherwise it is assumed to be Gaussian as well.

3.2. Molecular Dynamics techniques

The particle momentum variation due to IBS process can be calculated by numerical solution of the particle motion equation in the real optic structure taking into account interactions between particles.

Since the calculation of the space-charge effect is time consuming, one can use two possibilities to reduce required particle number:

- molecular dynamics (MD),
- macro particle simulation.

In the present BETACOOOL version MD simulation of the IBS process is realized. In the frame of this algorithm the ion beam is presented by array of real particles. For solution of the particle motion equation one uses specification of the ring optic structure included basic parameters of all optic elements.

The equations of the particle motion in external fields are solving in the following canonical conjugated variables. Transverse motion is described in the traditional variables: co-ordinate and transverse momentum normalised on the longitudinal momentum. Longitudinal motion is defined by the “scaled arrival time” and the longitudinal momentum deviation. The vector of canonical variables is

$$X = \left(x, p_x = \frac{P_x}{P_s}, y, p_y = \frac{P_y}{P_s}, z = -(t - t_0)\beta_0 c, p_z = \frac{E - E_0}{P_s \beta_0 c} \right), \quad (3.27)$$

where x, y are the horizontal and vertical positions, p_x, p_y are the corresponding normalized momenta, z is the “arrival time” of the particle multiplied by $-c\beta_0$, p_z is the normalized momentum deviation $p_z = \Delta P / P_s$.

Including space charge the Hamiltonian is expressed as:

$$H = -\frac{xp_z}{\rho} + \frac{p_z^2}{2\gamma_0^2} + \frac{p_x^2 + p_y^2}{2} + \frac{x^2}{2\rho^2} + \frac{K_1}{2}(x^2 - y^2) + \frac{r_{ion}}{\gamma_0^2 \beta_0^2} \sum_i \frac{1}{\sqrt{(x - x_i)^2 + (y - y_i)^2 + \gamma_0^2(z - z_i)^2}}, \quad (3.28)$$

where ρ is the curvature radius of the reference orbit. The effect of quadrupole components of the magnets is included with the parameters K_1 which is defined as

$$K_1 \equiv \frac{1}{B\rho} \frac{\partial B_y}{\partial x}, \quad (3.29)$$

where $B\rho = p_0 / q$ is the magnetic rigidity. The last term of Eq. (3.28) corresponds to the space charge effect.

Required values of the bending radius and bending angle in a dipole magnet, quadrupole strength and length are input into the program from input MAD file. The force acting on the particle inside an optic element is calculated as a sum of the forces corresponded to different types of the fields included in this element. The drift components are included into each element of non zero length.

Besides the components of the field, each optic element includes also procedures describing action of the fringe fields at the entrance and at the exit of element. Different types of the optic elements are collected in the optic library. The ring structure in the input file includes an array of the pointer to the optic element type and values of all the field components for each concrete element.

For solution of the motion equations three integration methods can be used: Runge-Kutta, symplectic integrator of the 1st order and linear transformation of the particle co-ordinates between points of IBS calculation. Runge-Kutta method is well-known and reliable. A shortcoming is that this method does not satisfy to symplecticity condition i.e. energy conservation. So, the step value Δs should be given properly in order to do not have large energy error. Symplectic integrator as well as the linear transformation provides the energy conservation. In the case of the linear transformation the optic element is divided by slices in accordance with the integration step. For each slice a transformation matrix is calculated from the right-hand parts of the particle motion equations. Thereafter at each step of the motion equations

In the frame of MD technique, the beam is divided into several cells and the motion equations are solved for the particles from one cell only. Other particles are taking into account using a periodic boundary condition for the distribution function in the longitudinal degree of freedom (Fig. 3.2). MD technique is described in {TASK.3.3}.

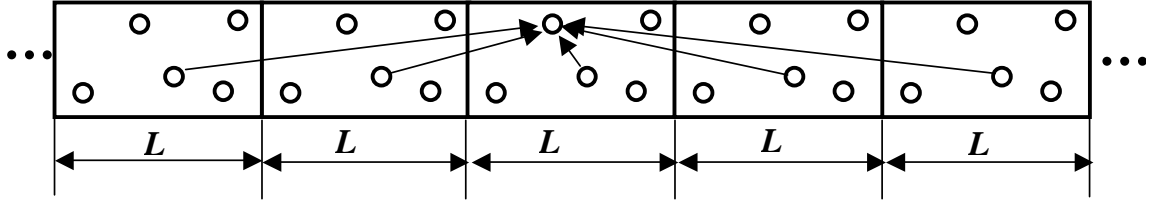


Fig. 3.2. The beam model used in Molecular Dynamics simulation.

4. Analytical models of IBS

4.1. Piwinski model

In his model [1], A. Piwinski derives the formulae for the variations of the mean radial and vertical emittances and the mean momentum spread per time unit due to a scattering event, neglecting the derivative of the beta and dispersion functions with respect to the longitudinal beam axis. For the smoothed focusing approximation only the mean values of the lattice functions are used and they are determined as follows:

$$\beta_{h,v} = \frac{R}{Q_{h,v}}, \quad D = \frac{R}{Q_h^2}, \quad \alpha_{h,v} = 0, \quad D' = 0, \quad (4.1)$$

where R is the ring mean radius, $Q_{h,v}$ are horizontal and vertical betatron tunes. In the frames of this model the growth rates are calculated in accordance with the following expressions:

$$\begin{aligned} \frac{1}{\tau_p} &= \frac{1}{2\sigma_p^2} \frac{d\sigma_p^2}{dt} = nA \frac{\sigma_h^2}{\sigma_p^2} f(a,b,c), \\ \frac{1}{\tau_x} &= \frac{1}{2\sigma_{x\beta}^2} \frac{d\sigma_{x\beta}^2}{dt} = A \left[f\left(\frac{1}{a}, \frac{b}{a}, \frac{c}{a}\right) + \frac{D^2 \sigma_p^2}{\sigma_{x\beta}^2} f(a,b,c) \right], \\ \frac{1}{\tau_z} &= \frac{1}{2\sigma_z^2} \frac{d\sigma_z^2}{dt} = Af\left(\frac{1}{b}, \frac{a}{b}, \frac{c}{b}\right), \end{aligned} \quad (4.2)$$

where $n = 1$ for a bunched beam and $n = 2$ for an coasting beam,

$$A = \frac{r_i^2 c N_b}{64\pi^2 \sigma_s \sigma_p \sigma_{x\beta} \sigma_z \sigma_{x'} \sigma_{z'} \beta^3 \gamma^4} \quad \text{- for a bunched beam} \quad (4.3)$$

For coasting beam one has to use the substitution $\frac{N_b}{\sigma_s} \rightarrow \frac{2\sqrt{\pi}N}{C}$.

The standard deviations are determined here as follows:

$$\sigma_{x\beta,z} = \sqrt{\epsilon_{x,z} \beta_{x,z}}, \quad \sigma_{x\beta',z'} = \sqrt{\frac{(1 + \alpha_{x,z}^2) \epsilon_{x,z}}{\beta_{x,z}}}, \quad (4.4)$$

and σ_p is the r.m.s. momentum spread. The function $f(a,b,c)$ is the following integral:

$$f(a, b, c) = 8\pi^2 \int_0^1 \left[\ln \left(\frac{c^2}{2} \left(\frac{1}{\sqrt{p}} + \frac{1}{\sqrt{q}} \right) \right) - 0.577 \right] (1 - 3x^2) \frac{dx}{\sqrt{pq}}. \quad (4.5)$$

The following relations determine normalized parameters used in the Formula (4.5):

$$a = \frac{\sigma_h}{\gamma\sigma_{x'}}, \quad b = \frac{\sigma_h}{\gamma\sigma_{z'}}, \quad c = \beta\sigma_h \sqrt{2 \frac{\rho_{\max}}{r_i}}, \quad \frac{1}{\sigma_h^2} = \frac{1}{\sigma_p^2} + \frac{D^2}{\sigma_{x\beta}^2}, \quad p = a^2 + x^2(1 - a^2),$$

$$q = b^2 + x^2(1 - b^2),$$

and the maximum impact parameter ρ_{\max} is about 0.5 beam vertical size. Integral (4.5) is calculated numerically.

In the article [2] it was shown that the integrals (4.9) under assumptions (4.1) are reduced to the Piwinski integral (4.5) and Piwinski model is one of possible simplification of Martini model.

4.2. Martini model

In accordance with the Martini model [2] for Gaussian probability law the r.m.s parameter growth rates can be inserted into the calculations in the form of the corresponding characteristic times:

$$\frac{1}{\tau_p} = \left\langle \frac{nA}{2} (1 - d^2) f_1 \right\rangle$$

$$\frac{1}{\tau_{x'}} = \left\langle \frac{A}{2} [f_2 + (d^2 + \tilde{d}^2) f_1] \right\rangle \quad (4.6)$$

$$\frac{1}{\tau_{z'}} = \left\langle \frac{A}{2} f_3 \right\rangle$$

where angular brackets mean averaging over the ring circumference, $n = 1$ for a bunched beam and $n = 2$ for coasting beam,

$$A = \frac{\sqrt{1 + \alpha_x^2} \sqrt{1 + \alpha_z^2} c r_i^2 \lambda}{16\pi \sqrt{\pi} \sigma_{x\beta} \sigma_{x\beta} \sigma_z \sigma_{z'} \sigma_p \beta^3 \gamma^4} \quad (4.7)$$

λ is the linear ion density:

$$\lambda = \begin{cases} N/L, & \text{for coasting beam} \\ N_b / (2\sqrt{\pi} \sigma_s), & \text{for a bunched beam} \end{cases} \quad (4.8)$$

The functions f_i are integrals of the following form:

$$f_i = k_i \int_0^\infty \int_0^\pi \int_0^{2\pi} \sin \mu g_i(\mu, \nu) \exp[-D(\mu, \nu)z] \ln(1 + z^2) d\nu d\mu dz, \quad (4.9)$$

with the coefficients $k_1 = 1/c^2$, $k_2 = a^2/c^2$, $k_3 = b^2/c^2$, and

$$D(\mu, \nu) = \frac{\left[\sin^2 \mu \cos^2 \nu + \sin^2 \mu (a \sin \nu - \tilde{d} \cos \nu)^2 + b^2 \cos^2 \mu \right]}{c^2}, \quad (4.10)$$

$$g_1(\mu, \nu) = 1 - 3 \sin^2 \mu \cos^2 \nu, \quad (4.11)$$

$$g_2(\mu, \nu) = 1 - 3 \sin^2 \mu \sin^2 \nu + 6 \tilde{d} \sin \mu \sin \nu \cos \nu / a, \quad (4.12)$$

$$g_3(\mu, \nu) = 1 - 3 \cos^2 \mu. \quad (4.13)$$

The normalized parameters are to be calculated from the following expressions:

$$a = \frac{\sigma_y}{\sigma_{x_\beta}} \sqrt{1 + \alpha_x^2}, \quad b = \frac{\sigma_y}{\sigma_{z'}}, \quad c = q \sigma_y, \quad d = \frac{\sigma_p}{\sigma_x} D, \quad \tilde{d} = \frac{\sigma_p}{\sigma_x} \tilde{D},$$

where $\tilde{D} = \alpha_x D + \beta_x D'$, $\sigma_x^2 = \sigma_{x_\beta}^2 + D^2 \sigma_p^2$, $\sigma_y = \frac{\sigma_p \sigma_{x_\beta}}{\gamma \sigma_x}$ and $q = 2\beta\gamma \sqrt{\frac{\sigma_z}{r_i}}$.

The integration over z - variable can be performed numerically or one can use one of the simplified results. If the integration is approximately performed as:

$$\int_0^\infty \exp[-D(\mu, \nu)z] \ln(1 + z^2) dz \approx \frac{2L_C}{D(\mu, \nu)}, \quad (4.14)$$

where L_C is the Coulomb logarithm, which is approximately equal to 20, this model is reduced to the Bjorken – Mtingwa model [3]. Other possible way is to use a few first terms of the integral expansion into series. For instance in accordance with the book by Abramowitz & Stegun the integral:

$$\int_0^\infty \exp[-D(\mu, \nu)z] \ln(1 + z^2) dz \approx$$

at $D \geq 1$ can be approximated by the expression

$$\approx \frac{2 \left(\left(\left(\left(\frac{a_4}{D^2} + a_3 \right) \frac{1}{D^2} + a_2 \right) \frac{1}{D^2} + a_1 \right) \frac{1}{D^2} + 1 \right)}{D^3 \left(\left(\left(\left(\frac{b_4}{D^2} + b_3 \right) \frac{1}{D^2} + b_2 \right) \frac{1}{D^2} + b_1 \right) \frac{1}{D^2} + 1 \right)}, \quad (4.15)$$

here $a_1 = 42.242855$, $a_2 = 302.757865$, $a_3 = 352.018498$, $a_4 = 21.821899$, $b_1 = 48.196927$, $b_2 = 482.485984$, $b_3 = 1114.978885$, $b_4 = 449.690326$.

And at $D < 1$

$$\approx \left(\left(\left(\left(\left(a_6 D + a_5 \right) D + a_4 \right) D + a_3 \right) D + a_2 \right) D + a_1 \right) D + a_0 + \frac{a_m}{D} + \left(\left(\left(b_5 D^2 + b_3 \right) D^2 + b_1 \right) D + \frac{b_m}{D} \right) \ln D, \quad (4.16)$$

here $a_m = -2.0E$, $a_0 = \pi$, $a_1 = -1.5 + E$, $a_2 = -\pi/6.0$, $a_3 = (25.0 - 12.0E)/144.0$, $a_4 = \pi/120.0$, $a_5 = (-49.0 + 20.0 * E)/7200.0$, $a_6 = -0.818\pi/5040.0$, $b_m = -2.0$, $b_1 = 1.0$, $b_3 = -12.0/144.0$, $b_5 = 20.0/7200.0$ and $E = 0.57721566490153286061$ is the Euler constant.

In any cases the integral is approximately proportional to $1/D(\mu, \nu)$ and numerical integration over μ and ν - variables has to be performed accurately because the $D(\mu, \nu)$ value at some beam parameters can be close to zero. Correspondingly, number of the integration step required to obtain good accuracy of the calculations depends on concrete task.

4.3. Jie Wei model

The model proposed by Jie Wei [4.4] is based on the same model of the interparticle collisions as Piwinski and Martini models (section {4.1}). In the notation of [4.4] the characteristic times of r.m.s. beam parameter variation are expressed as follows [4.5]:

$$\begin{bmatrix} \frac{1}{\sigma_p} \frac{d\sigma_p}{dt} \\ \frac{1}{\sigma_x} \frac{d\sigma_x}{dt} \\ \frac{1}{\sigma_z} \frac{d\sigma_z}{dt} \end{bmatrix} = \frac{A_0}{2} \int e^{-Dz} \ln(1 + C^4 z^2) \begin{bmatrix} n_b(1-d^2)g_1 \\ a^2 g_2 + (d^2 + \bar{d}^2)g_1 \\ b^2 g_3 \end{bmatrix} \sin \theta d\theta d\varphi dz, \quad (4.17)$$

where $A_0 = \frac{cr_p^2 NZ^4 \beta_x \beta_z}{32\pi A^2 \sigma_x^2 \sigma_z^2 \sigma_p \sigma_s \beta^3 \gamma^4}$, for a bunched beam N is the number of particles per bunch, σ_s

is the rms bunch length. For coasting beam N is the total number of particles and $\sigma_s = C/2\sqrt{\pi}$,

where C is the ring circumference. $r_p = \frac{e^2}{m_p c^2}$, $d = \frac{D_p \sigma_p}{\sqrt{\sigma_x^2 + D_p^2 \sigma_p^2}}$ is the effective ratio of the

“dispersion” amplitude $D_p \delta_p$ to the horizontal total one, D_p is horizontal dispersion, $\bar{d} = \frac{\bar{D}_p d}{D_p}$,

$$\bar{D}_p = \alpha_x D_p + \beta_x D'_p, \quad a = \frac{\beta_x d}{D_p \gamma}, \quad b = \frac{\beta_z \sigma_x}{\beta_x \sigma_z} a,$$

$$D = \cos^2 \theta + b^2 \sin^2 \theta \sin^2 \varphi + (a \sin \theta \cos \varphi - \bar{d} \cos \theta)^2,$$

$$C = 2\beta \sigma_p \left[\sigma_z (1-d^2) / r_p \right]^{1/2},$$

$$g_1 = 1 - 3 \cos^2 \theta,$$

$$g_2 = \cos^2 \theta - 2 \sin^2 \theta \cos^2 \varphi + \sin^2 \theta \sin^2 \varphi + 6\bar{d} \cos \theta \sin \theta \cos \varphi / a,$$

$$g_3 = \cos^2 \theta + \sin^2 \theta \cos^2 \varphi - 2 \sin^2 \theta \sin^2 \varphi.$$

The actual growth rate, observed over a time long compared with the revolution period, is calculated by averaging over the circumference.

With accuracy to notations the expression (4.17) coincides with the expression (4.6). The following simplifications of the (4.17) are proposed in [4]:

- the quantity $\ln(1 + C^4 z^2)$ can be substituted by a constant $2L_C$, where L_C is about 20 (this simplification is common for Jie Wei and Bjorken – Mtingwa models),
- for accelerator consisting of regular cells the variation in $D_p / \beta_x^{1/2}$ is small along the ring circumference, thus the terms including \bar{D}_p and \bar{d} can be neglected,
- for simplification of the integration over θ and ϕ the $\sin^2 \phi$ and $\cos^2 \phi$ are replaced by their average value of 1/2.

Then the formula (4.43) can be reduced to the following form:

$$\begin{bmatrix} \frac{1}{\sigma_p} \frac{d\sigma_p}{dt} \\ \frac{1}{\sigma_x} \frac{d\sigma_x}{dt} \\ \frac{1}{\sigma_z} \frac{d\sigma_z}{dt} \end{bmatrix} = 4\pi A_0 L_C F(\chi) \begin{bmatrix} n_b(1-d^2) \\ -a^2/2 + d^2 \\ -b^2/2 \end{bmatrix}, \quad (4.18)$$

where $\chi = (a^2 + b^2)/2 \geq 0$,

$$F(\chi) = \frac{-3 + (1 + 2\chi)I(\chi)}{1 - \chi}, \quad (4.19)$$

$$I(\chi) = \begin{cases} \frac{1}{\sqrt{\chi(\chi-1)}} \operatorname{Arth} \sqrt{\frac{\chi-1}{\chi}}, & \chi \geq 1, \\ \frac{1}{\sqrt{\chi(1-\chi)}} \arctan \sqrt{\frac{1-\chi}{\chi}}, & \chi < 1. \end{cases} \quad (4.20)$$

To calculate characteristic times one needs to average the expressions (4.18) over the ring circumference.

In terms of normalized transverse emittance and longitudinal bunch area $S = \pi m_0 c^2 \gamma \sigma_s \sigma_p / \beta^3 c A$ in phase space, Eq.(4.18) can be rewritten

$$\begin{bmatrix} \frac{1}{\sigma_p} \frac{d\sigma_p}{dt} \\ \frac{1}{\sigma_x} \frac{d\sigma_x}{dt} \\ \frac{1}{\sigma_y} \frac{d\sigma_y}{dt} \end{bmatrix} = \frac{Z^4 N}{A^2} \frac{r_0^2 m_0 c^2 L_c}{8\beta^4 \gamma \epsilon_x \epsilon_y S} F(\chi) \begin{bmatrix} n_b(1-d^2) \\ -a^2/2 + d^2 \\ -b^2/2 \end{bmatrix} \quad (4.21)$$

Except for the beam factors χ , d , a and b that depend on the ratio of the beam amplitudes in different dimension, the rates are linearly proportional to the density in the six-dimensional phase space, and are strongly dependent on the charge state of the particle.

The coupling between the horizontal and vertical motion averages the growth rates in the transverse dimension. If the motion is fully coupled within time periods much shorter than the IBS diffusion time, the average rates become:

$$\begin{bmatrix} \frac{1}{\sigma_p} \frac{d\sigma_p}{dt} \\ \frac{1}{\sigma_{x,y}} \frac{d\sigma_{x,y}}{dt} \end{bmatrix} = \frac{Z^4 N}{A^2} \frac{r_0^2 m_0 c^2 L_c}{8\beta^4 \gamma \epsilon_x \epsilon_y S} F(\chi) \begin{bmatrix} n_b(1-d^2) \\ (-\chi + d^2)/2 \end{bmatrix} \quad (4.22)$$

In a typically circular accelerator, the transition energy γ_T is approximately equal to the average value of β_x / D_p in the regular cells. When the beam energy is high $\gamma \gg \gamma_T$, the growth in horizontal direction results mostly from the variation of the betatron closed orbit during the exchange of the particle momentum ($a^2 \ll d^2$). The growths in horizontal and longitudinal amplitudes are therefore proportional to each other.

When the vertical amplitude is no longer small so that $\chi > 1$ and $F(\chi) < 0$. According to equation (4.44), both horizontal and longitudinal amplitudes grow.

In a typical storage ring like the Relativistic Heavy Ion Collider (RHIC) the beams are stored at energies much higher than the transition energy. Due to the coupling and injection conditions, the horizontal and vertical betatron amplitudes are about the same. The growth rates can be explicitly written from Eq. (4.18) using the expression for $F(\chi)$:

$$\begin{bmatrix} \frac{1}{\sigma_p} \frac{d\sigma_p}{dt} \\ \frac{1}{\sigma_{x,y}} \frac{d\sigma_{x,y}}{dt} \end{bmatrix} = \frac{Z^4 N}{A^2} \frac{r_0^2 m_0 c^2 L_c}{16\beta^4 \gamma_T \epsilon_x \epsilon_y S} F(\chi) \begin{bmatrix} n_b(1-d^2)/d \\ d/n_c \end{bmatrix} \quad (4.23)$$

Their dependence on the energy of the beam, which appears only in the form factor d , is usually weak. After the initial stage of the storage, the asymptotic configuration

$$n_b n_c \sigma_x^2 \approx D_p^2 \sigma_p^2, \quad \gamma \gg \gamma_T \quad (4.24)$$

will be approximately reached ($d \approx n_b n_c / (1 + n_b n_c)$).

4.4. Bjorken – Mtingwa model

To take into account dispersion in vertical plane as well as in horizontal the IBS growth rates are calculated in accordance with [4]:

$$\begin{cases} \frac{1}{\tau_x} = \left\langle \frac{H_x}{\epsilon_x} \gamma_0^2 I_{zz} - 2 \frac{\beta_x \phi_{Bx}}{\epsilon_x} \gamma_0 I_{xz} + \frac{\beta_x}{\epsilon_x} I_{xx} \right\rangle_s \\ \frac{1}{\tau_y} = \left\langle \frac{H_y}{\epsilon_y} \gamma_0^2 I_{zz} - 2 \frac{\beta_y \phi_{By}}{\epsilon_y} \gamma_0 I_{yz} + \frac{\beta_y}{\epsilon_y} I_{yy} \right\rangle_s \\ \frac{1}{\tau_z} = \left\langle \frac{1}{2} \frac{\gamma_0^2}{\sigma_p^2} I_{zz} \right\rangle_s \end{cases} \quad (4.25)$$

where $\phi_{Bi} = D_i' + \alpha_i D_i / \beta_i$, $H_i = \beta_i D_i'^2 + 2\alpha_i D_i D_i' + \gamma D_i^2$ and $\alpha_i, \beta_i, \gamma_i$ - lattice functions in the horizontal ($i=x$) and vertical ($i=y$) plane, $\varepsilon_{x,y}$ are the horizontal and vertical emittances, σ_p - rms momentum spread. Angular brackets mean averaging over the ring circumference. At zero vertical dispersion these formulae coincide with original Bjorken-Mtingwa theory. The diffusion coefficients I_{ij} are calculated in each position of the ring by numerical evaluation of the following integrals

$$I_{ij} = A \int_0^\infty d\lambda \frac{\lambda^{1/2}}{\sqrt{\det \Lambda}} (\delta_{ij} \text{Tr} \Lambda^{-1} - 3\Lambda_{ij}^{-1}), \quad (4.26)$$

where the matrix $A = I\lambda + L$, I - unit matrix, and matrix L is calculated via beam rms parameters and ring lattice functions in accordance with:

$$L = \begin{bmatrix} \frac{\beta_x}{\varepsilon_x} & 0 & -\gamma_0 \frac{\beta_x \phi_{Bx}}{\varepsilon_x} \\ 0 & \frac{\beta_y}{\varepsilon_y} & -\gamma_0 \frac{\beta_y \phi_{By}}{\varepsilon_y} \\ -\gamma_0 \frac{\beta_x \phi_{Bx}}{\varepsilon_x} & -\gamma_0 \frac{\beta_y \phi_{By}}{\varepsilon_y} & \frac{\gamma_0^2 H_x}{\varepsilon_x} + \frac{\gamma_0^2 H_y}{\varepsilon_y} + \frac{\gamma_0^2}{\sigma_p^2} \end{bmatrix}. \quad (4.27)$$

The IBS constant A is determined as in other IBS models:

$$A = \frac{cr_i^2 N L_c}{8\pi\beta^3 \gamma_0^2 \varepsilon_x \varepsilon_y \sigma_p \sigma_s}. \quad (4.28)$$

Here β and γ_0 are the Lorenz parameters, r_i is the ion classical radius, N is the ion number, L_c is the Coulomb logarithm, which is introduced as an input parameter.

4.5.1. High energy approach

Diffusion coefficients for a spatially uniform gas of density n and isotropic Maxwellian distribution are well known. The rate of such diffusion can be written as

$$\tau^{-1} = \frac{4\pi n (Ze)^4}{m^2} \frac{\Lambda}{\Delta^3} \quad (4.29)$$

where Δ is the one-dimensional rms velocity and Λ is the Coulomb logarithm. Equation (4.29) shows that the heating rate is determined by the 6-D phase-space density of the gas $\mu = n/(m^3 \Delta^3)$, where n is the spatial density. Similarly, the diffusion coefficients can be derived for a longitudinally collapsed velocity distribution ("at distribution"):

$$f(\vec{r}, \vec{v}) = \frac{n}{\pi \sqrt{\pi} \Delta_\perp^2 \Delta_\parallel} e^{-(v_x^2 + v_y^2)/\Delta_\perp^2} e^{-v_z^2/(2\Delta_\parallel^2)}, \quad (4.30)$$

with $\Delta_\parallel \ll \Delta_\perp$. The resulting coefficient is:

$$D_{zz} = \frac{4\pi n(Ze)^4}{m^2} \frac{\Lambda}{\Delta_{\perp}} \left[\sqrt{\pi} e^{-u^2/(2\Delta_{\perp}^2)} I_0 \left(\frac{u^2}{2\Delta_{\perp}^2} \right) \right] \quad (4.31)$$

Due to a slow decrease of function in the square brackets with its argument, one can replace expression in the square brackets by 1. As a result, one gets

$$D_{zz} \approx \frac{4\pi n(Ze)^4}{m^2} \frac{\Lambda}{\Delta_{\perp}}, \quad (4.32)$$

The growth rate in the longitudinal directions is then given by

$$\tau_{\parallel}^{-1} = \frac{1}{\Delta_{\parallel}^2} \frac{d\bar{v}_z^2}{dt} = 4\pi m(Ze)^4 \mu \Lambda \frac{\Delta_{\perp}}{\Delta_{\parallel}}, \quad (4.33)$$

where the 6-D phase-space density μ is defined as $\mu = n/(m^3 \Delta_{\perp}^2 \Delta_{\parallel})$

4.5.2. Kinetic model of IBS on the basis of Bjorken-Mtingwa theory

Kinetic simulation of IBS process presumes a solution of Langevin equation for each model particle. The drift and diffusion terms of the equation has to be calculated for each particle independently as a function of its co-ordinates, velocity components and distribution function of all other particles in the Model Beam.

To benchmark the algorithm reducing friction and diffusion to Langevin force components the simplified kinetic model for IBS simulation proposed by P.Zenkevich and O.Boine-Frankenheim was introduced into the code and tested preliminary at parameters typical for gold-gold collisions at RHIC. This model is based on analytical formulae for friction and diffusion components and presumes that only the friction depends on the particle velocity. The diffusion tensor in the frame of this model does not depend on the particle momentum and has a simplified structure.

Accurate benchmarking the code presumes simulation of IBS process at different lattice structures and at different parameters of the ion distribution function. For instance, RHIC is operated over transition energy and longitudinal temperature of the ion bunch is sufficiently less than transverse one. At these conditions the growth of the phase volume of the bunch is determined by longitudinal diffusion mainly. All other terms (friction and transverse diffusion components) are less as minimum by about one order of magnitude. Therefore the obtained good coincidence of the kinetic simulations with rms dynamics predictions for RHIC parameters indicates that the D_{zz} component of the diffusion tensor are calculated correctly and overall algorithm structure was developed properly. To benchmark all the parts of the code one needs to provide simulations below transition (or as for HESR – at imaginary transition energy) at bunch parameters closed to thermal equilibrium, which permits to test other components of the diffusion tensor. The friction force plays a leading role in the relaxation process. Therefore the benchmarking of this part of algorithm presumes simulation of IBS process for a bunch at sufficiently different temperatures of different degrees of freedom. It is preferable to perform the simulations for a ring working below transition energy (for instance, NESR).

Another effect which has to be taken into account by the kinetic IBS model is residual coupling between transverse degrees of freedom. In the frame of rms dynamics model the simulations are providing at the following assumptions:

- during single revolution of the beam in the ring the coupling can be neglected, and IBS growth rates are calculated in accordance with uncoupled ring lattice structure;
- at a long step of integration over time the residual coupling leads to equality of the horizontal and vertical growth rates:

$$\frac{1}{\tau_{x,coupled}} = \frac{1}{\tau_{y,coupled}} = \frac{1}{2} \left(\frac{1}{\tau_x} + \frac{1}{\tau_y} \right)_{uncoupled}. \quad (4.34)$$

In the frame of the kinetic model motion of each model particle is simulated depending on its momentum components, correspondingly the mean heating rates can not be used for the simulations directly. The long term coupling in this case can be simulated as a beam rotation in the (x, y) plane at some angle after each integration step. Simplest version of this algorithm was realized in the code, it requires further development and an accurate benchmarking.

At ion distribution function closed to Gaussian one the kinetic simulation of IBS process in the frame of Model Beam algorithm is realized on the basis of the following simplifications:

- the components of the friction force are a linear functions of the ion momentum
 $F_i = -K_i P_i$, where K_i are the constants,
- the components of the diffusion tensor $D_{i,j}$ do not depend on the ion momentum.

The model particle momentum variation after crossing an optic element of length l_k are calculated in accordance with Langevin equation:

$$P_i(t + \Delta t) = P_i(t) - K_i P_i(t) \Delta t \frac{l_k}{C} + \sqrt{\Delta t \frac{l_k}{C}} \sum_{j=1}^3 C_{i,j} \xi_j, \quad (4.35)$$

where ξ_j are three Gaussian random numbers with unit dispersion. The coefficients $C_{i,j}$ have to be calculated from diffusion and friction coefficients. Total momentum variation is calculated in cycle over optic elements along the ring circumference C .

The diffusion tensor men components in the frame of Bjorken –Mtingwa model are calculated as the following integrals:

$$D_{i,j} = A \int_0^\infty d\lambda \frac{\lambda^{1/2}}{\sqrt{\det \Lambda}} (\delta_{ij} Tr \Lambda^{-1} - \Lambda_{ij}^{-1}). \quad (4.36)$$

The collision coefficients can be expressed via friction and diffusion components as follows:

$$\left\langle \frac{d(P_i P_j)}{dt} \right\rangle = -(K_i + K_j) \langle P_i P_j \rangle + D_{i,j}, \quad (4.37)$$

where triangular brackets mean averaging over the particles. $\delta_{i,j}$ is the Kronecker-Kapelli symbol.

Comparing (4.26) and (4.37) one can find expressions for the friction coefficients:

$$K_i = \frac{A}{\langle P_i^2 \rangle} \int_0^\infty d\lambda \frac{\lambda^{1/2}}{\sqrt{\det \Lambda}} \Lambda_{ii}^{-1}. \quad (4.38)$$

To find expressions for $C_{i,j}$ lets multiply the momentum variation for i and j -th particles:

$$\begin{aligned} P_i(t + \Delta t)P_j(t + \Delta t) &= \left(P_i(t) - K_i P_i(t)\Delta t + \sqrt{\Delta t} \sum_{k=1}^3 C_{i,k} \xi_k \right) \left(P_j(t) - K_j P_j(t)\Delta t + \sqrt{\Delta t} \sum_{k=1}^3 C_{j,k} \xi_k \right) = \\ &= P_i(t)P_j(t) - (K_i + K_j)P_i(t)P_j(t)\Delta t + K_i K_j P_i(t)P_j(t)(\Delta t)^2 + P_i(t)\sqrt{\Delta t} \sum_{k=1}^3 C_{j,k} \xi_k + \\ &\quad + P_j(t)\sqrt{\Delta t} \sum_{k=1}^3 C_{i,k} \xi_k + \sum_{k=1}^3 C_{i,k} \xi_k \sum_{k=1}^3 C_{j,k} \xi_k \Delta t \end{aligned}$$

and average this expression over the particles. Neglecting the term $(\Delta t)^2$ and taking into account that

$$\begin{aligned} \left\langle P_j(t) \sqrt{\Delta t} \sum_{k=1}^3 C_{i,k} \xi_k \right\rangle &= 0, \\ \langle \xi_i \xi_j \rangle &= \delta_{i,j}, \end{aligned}$$

we obtain

$$\frac{\langle \Delta P_i P_j \rangle}{\Delta t} = -(K_i + K_j) \langle P_i P_j \rangle + \sum_{k=1}^3 C_{i,k} C_{j,k}. \quad (4.39)$$

The coefficients $C_{i,k}$ have to be chosen to obtain the same values of collision integrals (4.37), that gives the following system of equations:

$$-(K_i + K_j) \langle P_i P_j \rangle + \sum_{k=1}^3 C_{i,k} C_{j,k} = -(K_i + K_j) \langle P_i P_j \rangle + D_{i,j}. \quad (4.40)$$

Due to diagonal symmetry of the diffusion tensor the system consists of the following 6 independent equations for 9 unknown coefficients:

$$\begin{aligned} C_{x,1} C_{y,1} + C_{x,2} C_{y,2} + C_{x,3} C_{y,3} &= D_{x,y} \\ C_{x,1} C_{z,1} + C_{x,2} C_{z,2} + C_{x,3} C_{z,3} &= D_{x,z} \\ C_{y,1} C_{z,1} + C_{y,2} C_{z,2} + C_{y,3} C_{z,3} &= D_{y,z} \\ C_{x,1}^2 + C_{x,2}^2 + C_{x,3}^2 &= D_{x,x} \\ C_{y,1}^2 + C_{y,2}^2 + C_{y,3}^2 &= D_{y,y} \\ C_{z,1}^2 + C_{z,2}^2 + C_{z,3}^2 &= D_{z,z} \end{aligned} \quad (4.41)$$

This system has an infinite number of solutions and can be simplified, when the diffusion tensor has a zero components. In our case $D_{x,y} = 0$ and $\langle P_x P_y \rangle = 0$, the solution can be build by the following

way. Lets assume, that the random number ξ_1 correspond to scattering in horizontal plane, ξ_2 – in vertical and put $C_{x,2} = C_{y,1} = 0$. From the first equation of the system (4.40) follows that $C_{x,3}C_{y,3} = 0$. Lets put $C_{x,3} = 0$. In this case

$$C_{x,1} = \sqrt{D_{x,x}} . \quad (4.42)$$

From the second equation of (4.10) follows

$$C_{z,1} = \frac{D_{x,z}}{\sqrt{D_{x,x}}} . \quad (4.43)$$

Then, for simplicity put

$$C_{y,2} = C_{y,3} = \sqrt{D_{y,y}/2} . \quad (4.44)$$

From the third equation of (4.10):

$$C_{z,2} = \frac{D_{y,z}}{\sqrt{D_{y,y}/2}} - C_{z,3} . \quad (4.45)$$

Substituting (4.13) and (4.15) into the last equation of (4.10) we obtain quadratic equation about $C_{z,3}$:

$$C_{z,3}^2 - \frac{D_{y,z}}{\sqrt{D_{y,y}/2}} C_{z,3} + \frac{(D_{x,z})^2}{2D_{x,x}} + \frac{(D_{y,z})^2}{D_{y,y}} - \frac{D_{z,z}}{2} = 0 .$$

In absence of vertical dispersion ($D_{y,z} = 0$, $\langle P_y P_z \rangle = 0$) it gives

$$C_{z,3} = \sqrt{\frac{D_{z,z}}{2} - \frac{(D_{x,z})^2}{2D_{x,x}}} . \quad (4.46)$$

In the general case

$$C_{z,3} = \frac{D_{y,z}}{\sqrt{2D_{y,y}}} \pm \sqrt{\frac{D_{z,z}}{2} - \frac{(D_{x,z})^2}{2D_{x,x}} - \frac{(D_{y,z})^2}{2D_{y,y}}} . \quad (4.47)$$

Fixing the sign plus in the last expression one can write total set of the coefficients:

$$\begin{aligned} C_{x,1} &= \sqrt{D_{x,x}} , \\ C_{y,2} &= C_{y,3} = \sqrt{D_{y,y}/2} , \\ C_{z,1} &= \frac{D_{x,z}}{\sqrt{D_{x,x}}} , \end{aligned} \quad (4.48)$$

$$C_{z,2} = \frac{D_{y,z}}{\sqrt{D_{y,y}/2}} - \sqrt{\frac{DetD}{2D_{x,x}D_{y,y}}},$$

$$C_{z,3} = \frac{D_{y,z}}{\sqrt{2D_{y,y}}} + \sqrt{\frac{DetD}{2D_{x,x}D_{y,y}}},$$

all the other are equal to zero. Here $DetD$ is the determinant of the matrix

$$\begin{pmatrix} D_{x,x} & 0 & D_{x,z} \\ 0 & D_{y,y} & D_{y,z} \\ D_{x,z} & D_{y,z} & D_{z,z} \end{pmatrix}, \quad (4.49)$$

D_{ij} are calculated in accordance with (4.46).

Taking into account that the diffusion and friction components are determined for the following momentum components:

$$\left(x' - D'_x \frac{\Delta p}{p}, y' - D'_y \frac{\Delta p}{p}, \frac{1}{\gamma} \frac{\Delta p}{p} \right), \quad (4.50)$$

the variations of the ion momentum components inside k -th optic element are given by

$$\Delta x'_n = -F_x \frac{\left(x'_n - D'_x \frac{\Delta p}{p_n} \right) \beta_{x,k}}{\varepsilon_x (1 + \alpha_{x,k}^2)} \Delta t \frac{l_k}{C} + \sqrt{D_{x,x} \Delta t \frac{l_k}{C}} \xi_1, \quad (4.51)$$

$$\Delta y'_n = -F_y \frac{\left(y'_n - D'_y \frac{\Delta p}{p_n} \right) \beta_{y,k}}{\varepsilon_y (1 + \alpha_{x,k}^2)} \Delta t \frac{l_k}{C} + \sqrt{\frac{D_{y,y}}{2} \Delta t \frac{l_k}{C}} \xi_1 + \sqrt{\frac{D_{y,y}}{2} \Delta t \frac{l_k}{C}} \xi_2, \quad (4.52)$$

$$\Delta \frac{\Delta p}{p_n} = -F_z \frac{\gamma \frac{\Delta p}{p_n}}{\varepsilon_{long}} \Delta t \frac{l_k}{C} + \sqrt{\Delta t \frac{l_k}{C}} \gamma C_{z,1} \xi_1 + \sqrt{\Delta t \frac{l_k}{C}} \gamma C_{z,2} \xi_2 + \sqrt{\Delta t \frac{l_k}{C}} \gamma C_{z,3} \xi_3, \quad (4.53)$$

here n is the number of the particle, $\varepsilon_{x,y}$ – horizontal and vertical emittances, α_k, β_k, D'_k – lattice parameters, longitudinal emittance is determined as $\varepsilon_{long} = \sigma_p^2$, γ is Lorentz factor, the friction coefficients F_i are calculated in accordance with:

$$F_{x,y} = \frac{\beta_{x,y}}{\varepsilon_{x,y} (1 + \alpha_{x,y}^2)} A \int_0^\infty d\lambda \frac{\lambda^{1/2}}{\sqrt{\det \Lambda}} \Lambda_{ii}^{-1}, \quad (4.54)$$

$$F_z = \frac{1}{\varepsilon_{long}} A \int_0^\infty d\lambda \frac{\lambda^{1/2}}{\sqrt{\det \Lambda}} \Lambda_{ii}^{-1}. \quad (4.55)$$

To test a possibility to simulate the IBS process in presence of a residual coupling between transverse planes the simplest algorithm was implemented into program. After each step of integration over time the beam is rotated by 90^0 around longitudinal axis. For each particle its co-ordinates are changed in accordance with the following equation:

$$\begin{pmatrix} x \\ y \end{pmatrix} = \begin{pmatrix} 0 & -1 \\ 1 & 0 \end{pmatrix} \begin{pmatrix} x \\ y \end{pmatrix}_0. \quad (4.56)$$

For Gaussian distribution the described kinetic model has to coincide with Rms dynamics simulation using Bjorken-Mtingwa model. Comparison of the kinetic model and Rms dynamics simulations are presented in the Fig. 4.1, 4.2. The simulations were performed at RHIC parameters, corresponding to gold-gold collisions at 100 GeV/u.

Even at model particle number of 2000 the coincidence is satisfactory. The simulations were provided at ideal RHIC lattice and the vertical dispersion was assumed to be zero along the total ring circumference. At the typical gold bunch parameters (rms emittance of about $2.5 \cdot 10^{-8} \pi \cdot \text{m} \cdot \text{rad}$ in both planes and rms momentum spread of $5 \cdot 10^{-4}$) general term determining the IBS growth is z - z component of the diffusion tensor. The friction and other components of the diffusion are negligible in comparison with mistakes of the simulations. Therefore the collision integral consists of only one significant term $-I_{zz}$, which coincides practically with the corresponding diffusion component. At uncoupled motion, in accordance with (4.25) the I_{zz} component determines the momentum spread and horizontal emittance growth. At absence of vertical diffusion the vertical emittance growth rate is determined by I_{yy} component of the collision integral and from Fig. 4.1 we can see that this component is comparable with the noise of the algorithm. The I_{xx} and I_{xz} have the same order of magnitude as I_{yy} and the horizontal emittance growth is caused by the longitudinal diffusion mainly.

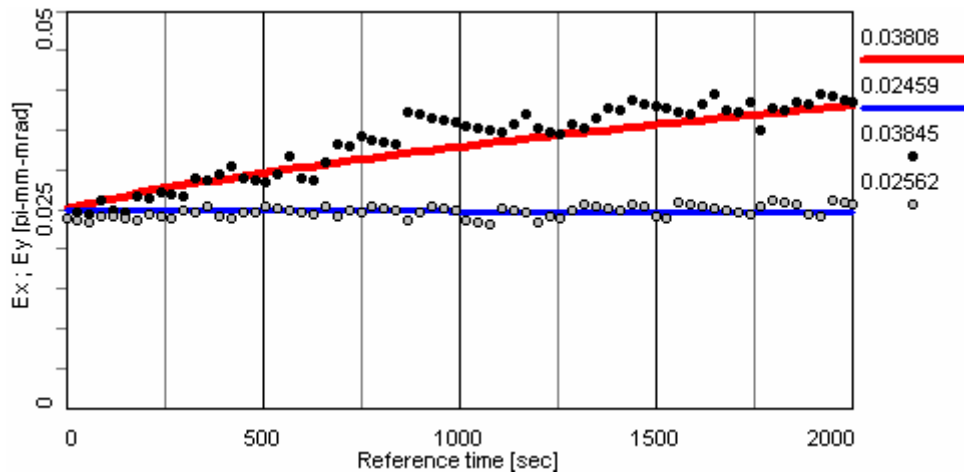


Fig. 4.1. Horizontal emittance time dependence. RMS dynamics – red solid line, kinetic model (2000 particles) – black dots. Vertical emittance time dependence. RMS dynamics – blue solid line, kinetic model (2000 particles) – gray dots.

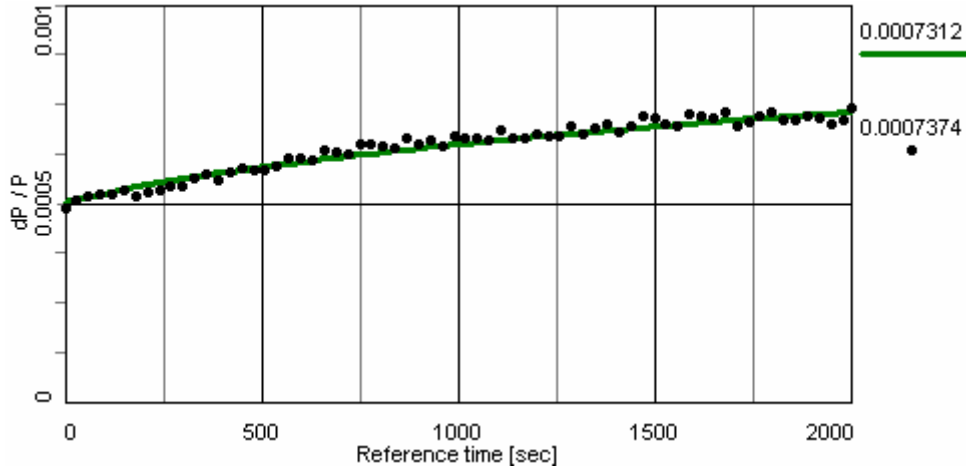


Fig. 4.2. Momentum spread time dependence. RMS dynamics solid line, kinetic model (2000 particles) – black dots.

Good agreement of the momentum spread evolution (Fig. 4.2) between exact theory result and kinetic model indicates that the diffusion due to the component D_{zz} is simulated correctly. Good agreement in the horizontal emittance evolution indicates that the algorithm structure is built correctly. All other components of the collision integral are calculated correctly by the order of magnitude (as minimum they are not overestimated) that leads to very small variation of vertical emittance in time (Fig. 4.1). Accurate benchmarking the algorithm requires more extensive simulations in a wide range of a storage ring and beam parameters.

4.5. Gas Relaxation model

Diffusion coefficients for a spatially uniform gas of density n and isotropic Maxwellian distribution are well known. The rate of such diffusion can be written as

$$\tau^{-1} = \frac{4\pi n(Ze)^4}{m^2} \frac{\Lambda}{\Delta^3} \quad (4.57)$$

where Δ is the one-dimensional rms velocity and Λ is the Coulomb logarithm. The heating rate is determined by the 6-D phase-space density of the gas $\mu = n/(m^3\Delta^3)$, where n is the spatial density. Similarly, the diffusion coefficients can be derived for a longitudinally collapsed velocity distribution ("at distribution"):

$$f(\vec{r}, \vec{v}) = \frac{n}{\pi\sqrt{\pi}\Delta_{\perp}^2\Delta_{\parallel}} e^{-(v_x^2+v_y^2)/\Delta_{\perp}^2} e^{-v_z^2/(2\Delta_{\parallel}^2)}, \quad (4.58)$$

with $\Delta_{\parallel} \ll \Delta_{\perp}$. The resulting coefficient is:

$$D_{zz} = \frac{4\pi n(Ze)^4}{m^2} \frac{\Lambda}{\Delta_{\perp}} \left[\sqrt{\pi} e^{-u^2/(2\Delta_{\perp}^2)} I_0\left(\frac{u^2}{2\Delta_{\perp}^2}\right) \right] \quad (4.59)$$

Due to a slow decrease of function in the square brackets with its argument, one can replace expression in the square brackets by 1. As a result, one gets

$$D_{zz} \approx \frac{4\pi n(Ze)^4}{m^2} \frac{\Lambda}{\Delta_{\perp}}, \quad (4.60)$$

The growth rate in the longitudinal directions is then given by

$$\tau_{\parallel}^{-1} = \frac{1}{\Delta_{\parallel}^2} \frac{d\bar{v}_z^2}{dt} = 4\pi m(Ze)^4 \mu \Lambda \frac{\Delta_{\perp}}{\Delta_{\parallel}}, \quad (4.61)$$

where the 6-D phase-space density μ is defined as $\mu = n/(m^3 \Delta_{\perp}^2 \Delta_{\parallel})$.

One can rewrite diffusion coefficient

$$D_{zz} \approx \frac{4\pi n(Ze)^4}{m^2} \frac{\Lambda}{\Delta_{\perp}} \quad (4.62)$$

in terms of beam parameters. In the laboratory system it becomes:

$$D_{zz} = \frac{2r_i^2 c N_i \Lambda}{\beta^3 \gamma^3 \epsilon_{\perp}^{3/2} \beta_{\perp}^{1/2} C} \quad (4.63)$$

where for the 6-D phase-space density we used $\mu = n/(m^3 \Delta_{\perp}^2 \Delta_{\parallel}) = N/V_6$, with the 6-D volume being $V_6 = (2\pi)^3 (\beta\gamma)^3 m^3 \epsilon_x \epsilon_y \epsilon_z$. Here, the formula is written for coasting beam with C being the ring circumference. Note that the normalization factor in velocity space was already taken into account in the derivation of (4.62). One then needs only the 3-D spatial contribution to the normalization coefficient to get from (4.62) to (4.63). Expression given in (4.40) was used in the original version of the SimCool code to represent diffusion rate due to the IBS. The longitudinal heating rate for a bunched beam with C being replaced by $2\sqrt{\pi}\sigma_s$ (following the standard definition in the IBS theory, which corresponds to 92% of a Gaussian beam in longitudinal direction) is then

$$\tau_{\parallel}^{-1} = \frac{1}{\sigma_p^2} \frac{d\sigma_p^2}{dt} = \frac{r_i^2 c N_i \Lambda}{8\beta^3 \gamma^3 \epsilon_x^{3/2} \langle \beta_{\perp}^{1/2} \rangle \sqrt{\pi/2} \sigma_s \sigma_p^2} \quad (4.64)$$

The transverse growth rate can be simply expressed through the longitudinal growth rate as

$$\tau_{\perp}^{-1} = \frac{\sigma_p^2}{\epsilon_x} \left\langle \frac{D_x^2 + (D_x' \beta_x + \alpha_x D_x)^2}{\beta_x} \right\rangle \tau_{\parallel}^{-1}, \quad (4.65)$$

where $\langle \rangle$ is an average value of the ring lattice. For the RHIC lattice the contribution of the term with dispersion derivatives and alpha-function is small (smooth lattice) and can be neglected so that only $\langle D_x^2 / \beta_x \rangle$ may be considered. Recently, the transverse heating rate based on (4.65) was implemented in the SimCool code.

4.5.1. High energy approach

For high energies at RHIC (when approximation of at velocity distribution in the beam rest frame becomes valid), simple gas-relaxation formula gives reasonable approximation for description of the longitudinal heating rate, compared to the involved IBS treatment with complicated dependence on the lattice parameters.

This simple formula based on the diffusion coefficient in a gas for a at velocity distribution was also used in the original version of the SimCool code. The standard IBS formulas can be simplified for high-energy case. For example, Bjorken-Mtingwa (B-M) model can be approximated for a round beam at high-energy as

$$\tau_{\parallel}^{-1} = \frac{r_i^2 c N_i \Lambda}{8\beta^3 \gamma^3 \epsilon_x^{3/2} \langle \beta_{\perp}^{1/2} \rangle \sigma_s \sigma_p^2} \quad (4.66)$$

The high-energy approximation of B-M agrees very well with the one obtained using the Gas-Relaxation model. This confirms that the main effect in IBS diffusion at high energy is determined by a degree of a collapse of velocity distribution in the beam moving frame of reference. Treatment of the IBS in such a case is then extremely simplified. To describe applicability region of the high-energy approximation one typically introduces parameter g_f which describes a degree of a collapse

of ion velocity distribution, and is defined as $g_f = \left(\frac{\Delta_{\parallel}}{\Delta_{\perp}} \right)^2 = \frac{\langle \beta_{\perp} \rangle \sigma_p^2}{\gamma^2 \epsilon_{\perp}}$.

For typical parameters of Au ions at RHIC store energy g_f is in the range 0.1-0.2 which justifies the use of high-energy approximation treatment of the IBS for simple estimates.

4.7. Calculations of IBS in the case of transverse coupling

In the case when transverse motion is completely coupled within one revolution over the ring the invariant change after interparticle collision has to be calculated using bilinear forms of the lattice in the collision position instead of formulae (3.8) and (3.9). Theory of the IBS for coupled motion was done by Piwinski in [6]. When transverse coupling in the ring has small value the IBS rates can be calculated using formulae for uncoupled motion. At RHIC parameters IBS growth times are rather long - a few tens of minutes. At such a long time the transverse emittances are connected together even at a small coupling. If the motion is completely coupled within time period much shorter than IBS diffusion time Jie Wei proposed [3] to use average value of the transverse rates for both degrees of freedom:

$$\frac{1}{\tau_{x,z,coupled}} = \frac{1}{2} \left(\frac{1}{\tau_x} + \frac{1}{\tau_z} \right)_{uncoupled} \quad (4.67)$$

Such a manner of the coupling insertion into calculation is used in our code for all the models of IBS. For instance, in Jie Wei model the average rates become:

$$\left[\begin{array}{c} \frac{1}{\sigma_p} \frac{d\sigma_p}{dt} \\ \frac{1}{\sigma_{x,z}} \frac{d\sigma_{x,z}}{dt} \end{array} \right] = 4\pi A_0 L_C F(\chi) \left[\begin{array}{c} n_b(1-d^2) \\ (-\chi + d^2)/2 \end{array} \right]. \quad (4.68)$$

5. Kick of the ion momentum components due to IBS

5.1. Mean growth rates

In the case of IBS calculation using mean growth rates, the mean growth rates are calculated in accordance with one of the analytical model developed in BETACOOOL and the ring structure loaded from output MAD file. When the growth rates are known one can calculate mean square of the scattering angle taking into account multiplication factor. The mean square angle after one revolution in the ring can be calculated under assumption that the alpha function and dispersion in the position of calculation are zero. In this case initial beam emittance is equal to:

$$\varepsilon_x = \sqrt{\langle (x - \langle x \rangle)^2 \rangle \langle (x' - \langle x' \rangle)^2 \rangle}. \quad (5.1)$$

After the scattering of all the particles on the randomly distributed angle θ the new emittance value is

$$\varepsilon_{x,new} = \sqrt{\langle (x - \langle x \rangle)^2 \rangle \langle (x' - \langle x' \rangle + \theta)^2 \rangle}. \quad (5.2)$$

New r.m.s. angular spread value can be calculated as follows

$$\langle (x' - \langle x' \rangle + \theta)^2 \rangle = \langle (x' - \langle x' \rangle)^2 \rangle + 2\langle (x' - \langle x' \rangle)\theta \rangle + \langle \theta^2 \rangle.$$

The second is equal zero because x' and θ are independent random values, therefore the emittance can be expressed as:

$$\varepsilon_{x,new} = \varepsilon_{x,0} \sqrt{1 + \frac{\langle \theta^2 \rangle}{\langle (x' - \langle x' \rangle)^2 \rangle}}. \quad (5.3)$$

Assuming that the square scattering angle is less than the beam r.m.s. angular spread one can expand this expression into Taylor series with accuracy to the first term. It gives for the scattering angle such an equality:

$$\langle \theta^2 \rangle = 2 \frac{\Delta \varepsilon_x}{\varepsilon_{x,0} \beta_x}. \quad (5.4)$$

Using the rate value definition one can writes for the scattering angle:

$$\langle \theta^2 \rangle = 2 \frac{\varepsilon}{\beta} \frac{T_{rev}}{\tau}, \quad (5.5)$$

where β is the beta function in the point of the particle array generation, τ is characteristic growth time in corresponding degree of freedom. Here the angular deviation of the particle trajectory means relative momentum components: $\theta_{x,y} = \frac{p_{x,y}}{p}$, $\theta_s = \frac{\Delta p}{p}$. After N_{turn} revolutions in the ring the square of the scattering angle is equal to the sum of the square angles at each revolution:

$$\langle \theta^2 \rangle = 2 \frac{\varepsilon}{\beta} \frac{T_{rev}}{\tau} N_{turn}. \quad (5.6)$$

The variation of the particle trajectory angular deviation is calculated in accordance with

$$\Delta\theta = \sqrt{\langle \theta^2 \rangle} \xi \quad (5.7)$$

where ξ is the random value with Gaussian distribution at unit dispersion.

5.2. Detailed calculation of the momentum kick

5.2.1. Burov's model

In the case of detailed calculation of the growth rates the algorithm is similar to the previous case. However, the characteristic times are calculated for each particle individually. For this aim one needs to know not only r.m.s. parameters of the particle array distribution function, but the amplitudes of the betatron and synchrotron oscillations of the particle. The inverse growth times for each particle can be calculated by numerical evaluation of the scattering integrals. Under some additional assumption the integration can be performed analytically in one degree of freedom. For instance, in the frame of Burov's model of detailed IBS calculation, the longitudinal IBS rate is presented as [8]:

$$\Lambda_i^{\parallel} \equiv \frac{1}{V_{zm}^2} \frac{d}{dt} V_{zm}^2 = \sqrt{\frac{2}{\pi}} \frac{N_i r_i^2 c L_i}{\gamma^2 V_{zm}^2 \sigma_x^2 \sigma_z u_x} \exp\left(-\frac{z_m^2}{4\sigma_z^2}\right) I_0\left(\frac{z_m^2}{4\sigma_z^2}\right) \Phi\left(\frac{V_{xm}}{u_x}, \frac{V_{ym}}{u_y}\right) \left(1 - \sqrt{\frac{V_{zm}}{u_x \sqrt{2}}}\right) \quad (5.8)$$

Here u_x are rms velocities in PRF, $s_{x,y}$ – rms beam sizes. z_m – amplitude of the ion oscillations over longitudinal co-ordinate, $V_{xm,ym}$ are the amplitudes of oscillations over transverse velocities, I_0 – modified Bessel function. The form-factor Φ is given by the expression:

$$\Phi(x, y) \equiv \frac{2}{\pi} \exp\left(-\frac{x^2 + y^2}{2}\right) \iint_0^{\sqrt{x^2 + y^2}} \frac{d\xi d\eta}{\sqrt{\xi^2 + \eta^2}} \exp\left(-\frac{\xi^2 + \eta^2}{2}\right) I_0(\xi x) I_0(\eta y) \quad (5.9)$$

Horizontal IBS rate relates to the longitudinal one as:

$$\Lambda_i^x / \Lambda_i^{\parallel} = \frac{\overline{D^2 + (D'\beta_x + \alpha_x D)^2}}{x_m^2} V_{zm}^2 \quad (5.10)$$

where the bar stays for the orbit-averaging.

The formula (5.8) is derived on the basis of plasma relaxation model and does not contain averaging over the ring lattice parameters. The formula is based under assumption of Gaussian distribution of the ions flattened in velocity space. To test the model at the same model of IBS process at initial

step of the simulations in the program the following combination of r.m.s. rates calculation and detailed formula is used. Square of the particle scattering angle is calculated as

$$\langle \theta^2 \rangle = \langle \theta_{mean}^2 \rangle F(V_{zm}, V_{xm}, V_{ym}), \quad (5.11)$$

where $\langle \theta_{mean}^2 \rangle$ is calculated using analytical model of IBS in accordance with expression (2.24). The form factor F is calculated accordingly to (5.8) as

$$F(V_{zm}, V_{xm}, V_{ym}) = \exp\left(-\frac{z_m^2}{4\sigma_z^2}\right) I_0\left(\frac{z_m^2}{4\sigma_z^2}\right) \Phi\left(\frac{V_{xm}}{u_x}, \frac{V_{ym}}{u_y}\right) \left(1 - \sqrt{\frac{V_{zm}}{u_x \sqrt{2}}}\right) \times C. \quad (5.12)$$

Normalization constant C is calculated numerically to satisfy the condition: variation of r.m.s. beam parameters with time has no depends on the way of IBS calculation – mean or detailed.

5.2.2. Bi-Gaussian model

Model Beam algorithm can simulate the beam dynamics with ordinary distribution of model particles. The most number of physical effects in the BETACOOOL program make kicks on the ion beam in the single particle approximation. It means that particle distribution does not influence on the kick value from each effects.

Another situation exists for IBS effect when heating rates are calculated as the collective effect. Standard model of IBS is assumed that the particles have the Gaussian distribution. In the case of Model Beam algorithm the particles can have the ordinary distribution. To resolve this problem the special Bi-Gaussian approximation was elaborated. The distribution function can be presented as summary of two Gaussian functions for core and tail particles:

$$f(x_i) = f^{tail}(x_i) + f^{core}(x_i) = a_i^{tail} \exp\left[-\frac{1}{2}\left(\frac{x_i}{\sigma_i^{tail}}\right)^2\right] + a_i^{core} \exp\left[-\frac{1}{2}\left(\frac{x_i}{\sigma_i^{core}}\right)^2\right], \quad (5.13)$$

where a^{tail} , a^{core} , σ^{tail} , σ^{core} – amplitudes and widths of beam profile, i – corresponds to degrees of freedom: 1 – horizontal, 2 - vertical, 3 - longitudinal. Powell method [9] is used in the code to find of Gaussian function parameters. This method minimizes the deviation between the model beam profile and Bi-Gaussian distribution:

$$\sum_{i=1}^N [y_i - f(x_i)]^2 \rightarrow Minimum, \quad (5.14)$$

where (x_i, y_i) – points of the beam profile distribution, N is the total particle number. RMS parameters of ion beam E_i^{rms} (emittances and momentum spread) are calculated in the suggestion that distribution of model particles has Gaussian shape. Beam parameters and particle number for Bi-Gaussian distributions are:

$$E_i^{tail} = E_i^{rms} (\sigma_i^{tail})^2, \quad E_i^{core} = E_i^{rms} (\sigma_i^{core})^2, \quad N_i^{core} = N \times \left[1 + \frac{\sigma_i^{tail}}{\sigma_i^{core}} \cdot \frac{a_i^{tail}}{a_i^{core}}\right]^{-1}, \quad N_i^{tail} = 1 - N_i^{core}. \quad (5.15)$$

Heating growth rates $\tau_i^{tail}(E_i^{tail}, N)$ and $\tau_i^{core}(E_i^{core}, N)$ of Bi-Gaussian distributions are calculated with standard procedure as described above in section {4} on the base of choosing IBS model for Gaussian distribution. Model particles in the tail get the kick with standard procedure as described in section {5.1} using of tail heating growth rates.

$$\Delta\theta_{1,2}^{tail} = \sqrt{2 \frac{\varepsilon_{1,2}^{tail}}{\beta_{1,2}} \frac{T_{rev}}{\tau_{1,2}^{tail}} N_{turn}} \times \xi, \quad \Delta\theta_3^{tail} = \sqrt{\left(\frac{\Delta p^{tail}}{p}\right)^2 \frac{T_{rev}}{\tau_3^{tail}} N_{turn}} \times \xi, \quad (5.16)$$

where $\varepsilon_{1,2}$ – horizontal and vertical emittances, $\beta_{1,2}$ – horizontal and vertical beta-functions, $(\Delta p/p)$ – momentum spread, T_{rev} – revolution period, N_{turn} – number of turns, ξ – the random value with Gaussian distribution at unit dispersion. Particles in the core get the summary kick from core and tail heating rates:

$$\begin{aligned} \frac{1}{\tau_i^{sum}} &= \frac{1}{\tau_i^{core}} \left(\frac{N_i^{core}}{N} \right)^2 + \frac{1}{\tau_i^{tail}} \left(\frac{N_i^{tail}}{N} \right)^2 \frac{E_i^{tail}}{E_i^{core}}. \\ \Delta\theta_{1,2}^{core} &= \sqrt{2 \frac{\varepsilon_{1,2}^{core}}{\beta_{1,2}} \frac{T_{rev}}{\tau_{1,2}^{sum}} N_{turn}} \times \xi \\ \Delta\theta_3^{core} &= \sqrt{\left(\frac{\Delta p^{core}}{p}\right)^2 \frac{T_{rev}}{\tau_3^{sum}} N_{turn}} \times \xi \end{aligned} \quad (5.17)$$

5.2.3. Parzen's model for bi-Gaussian distribution

The model for IBS growth rates calculation proposed by G.Parzen [10] is based on presentation of the ion distribution function as a sum of two Gaussian distributions. $N f(x, p)$ gives the number of particles in $d^3 x d^3 p$, where N is the number of particles in a bunch. For a bi-gaussian distribution, $f(x, p)$ is given by

$$f(x, p) = \frac{N_c}{N} \frac{1}{\Gamma_c} \exp[-S_c(x, p)] + \frac{N_t}{N} \frac{1}{\Gamma_t} \exp[-S_t(x, p)]. \quad (5.18)$$

Here N_c and N_t are the particle number in the first (corresponding to the core of total distribution) and second Gaussian (describing the tail of the total distribution). $\Gamma_{c,t} = \int \exp(-S_{c,t}(x, p)) d^3 x d^3 p$ are the corresponding normalization factors,

$$S = S_x + S_y + S_s, \quad (5.19)$$

where

$$S_i = \frac{I_i}{\varepsilon_i}, \quad i = x, y, s \quad (5.20)$$

is the ratio of the particle invariant of the motion I to 2-sigma emittance ε in the corresponding plane.

Because of $N_c + N_t = N$ the distribution (5.18) is described by 7 independent parameters: $\epsilon_{x,c}, \epsilon_{y,c}, \epsilon_{s,c}, \epsilon_{x,t}, \epsilon_{y,t}, \epsilon_{s,t}$ and N_c . To find these parameters for arbitrary array of particles one needs to solve 7-D optimization problem, which looks unrealistic. To avoid this difficulty the 7-D optimization problem was replaced by solution of 3 independent 3-D optimization problem. For each degree of freedom from smoothed beam profile the program calculates rms emittances for core and tail of distribution function using Powel method [9]. As result of the calculations one has a set of 9 parameters:

$$\begin{aligned} \epsilon_{x,c}, \epsilon_{x,t}, N_{x,c}, \\ \epsilon_{y,c}, \epsilon_{y,t}, N_{y,c}, \\ \epsilon_{s,c}, \epsilon_{s,t}, N_{s,c}, \end{aligned} \quad (5.21)$$

the emittances are used as corresponding parameters of Bi-Gaussian distribution, and intensity of core Gaussian is calculated as:

$$N_c = \frac{N_{x,c} + N_{y,c} + N_{s,c}}{3}. \quad (5.22)$$

Thereafter the program calculates additional four parameters, required for evaluation of growth rates for total beam:

$$\epsilon_{x,ct} = \frac{\epsilon_{x,c} \epsilon_{x,t}}{\epsilon_{x,c} + \epsilon_{x,t}}, \quad \epsilon_{y,ct} = \frac{\epsilon_{y,c} \epsilon_{y,t}}{\epsilon_{y,c} + \epsilon_{y,t}}, \quad \epsilon_{s,ct} = \frac{\epsilon_{s,c} \epsilon_{s,t}}{\epsilon_{s,c} + \epsilon_{s,t}} \quad \text{and} \quad N_{ct} = \frac{N_c N_t}{N^2}. \quad (5.23)$$

The diffusion coefficients for core and tail Gaussians are calculated in accordance with Bjorken-Mtingwa model:

$$I_{ij,c} = A_c \int_0^\infty d\lambda \frac{\lambda^{1/2}}{\sqrt{\det \Lambda_c}} (\delta_{ij} \text{Tr} \Lambda_c^{-1} - 3\Lambda_{ij,c}^{-1}), \quad (5.24)$$

$$I_{ij,t} = A_t \int_0^\infty d\lambda \frac{\lambda^{1/2}}{\sqrt{\det \Lambda_t}} (\delta_{ij} \text{Tr} \Lambda_t^{-1} - 3\Lambda_{ij,t}^{-1}), \quad (5.25)$$

$$I_{ij,ct} = A_{ct} \int_0^\infty d\lambda \frac{\lambda^{1/2}}{\sqrt{\det \Lambda_{ct}}} (\delta_{ij} \text{Tr} \Lambda_{ct}^{-1} - 3\Lambda_{ij,ct}^{-1}), \quad (5.26)$$

where matrixes $\Lambda_c, \Lambda_t, \Lambda_{ct}$ are calculated in accordance with (4.27) with substitution of corresponding emittances. The IBS constants are calculated as usual:

$$A_i = \frac{c r_i^2 N_i L_c}{8\pi\beta^3 \gamma_0^2 \epsilon_{x,i} \epsilon_{y,i} \sigma_{p,i} \sigma_{s,i}}. \quad (5.27)$$

Diffusion coefficients for the total beam are calculated as:

$$I_{ij} = I_{ij,c} \frac{N_c}{N} + I_{ij,t} \frac{N_t}{N} + 2I_{ij,ct}. \quad (5.28)$$

And finally the heating rates are calculated with the same formula (3.54). This procedure is repeated in each optic element of the ring and resulting heating rates are averaged over the ring circumference.

The described algorithm does not coincide exactly with original paper [10]. However it uses the same final formula (5.28) and based on the same modification of the Bjorken-Mtingwa model, which simplifies benchmarking of the model.

References

- [1] A.Piwinski, Proc. 9th Int. Conf. on High Energy Accelerators, p. 105, 1974.
- [2] M. Martini "Intrabeam scattering in the ACOOL-AA machines", CERN PS/84-9 AA, Geneva, May 1984.
- [3] J.D. Bjorken, S.K. Mtingwa, "Intrabeam scattering", Particle Accelerators, Vol. 13, p.115, 1983.
- [4] Jie Wei "Evolution of Hadron Beams under Intrabeam Scattering", Proc. of PAC'1993, p.3651.
- [5] G.Parzen, Nucl Instr. Meth. A256, 231 (1987);Proc. 1988 EPAC, Rome, p.281.
- [6] A. Piwinski, Proc CERN Accelerator School, 92-01, p.405; 2 April 1992.
- [7] M.Venturini, "Study of intrabeam scattering in low-energy electron rings", Proceedings of the 2001 PAC, Chicago, pp. 2961 – 2963.
- [8] A.Burov. Private communications.
- [9] W.Press, S.Teukolsky, W.Vetterling, B.Flannery. Numerical Recipes in C. The Art of Scientific Computing (Second Edition). Cambridge University Press (1992)
- [10] G.Parzen, Intrabeam scattering growth rates for a bi-gaussian distribution, BNL, C-A/AP#169, September 2004.

IV. Stochastic cooling

1. Introduction

In order to perform realistic simulation of antiproton beam parameter evolution in experiment at HESR (GSI) in high resolution mode a few new algorithms were introduced into BETACOOOL program [1]. General advantage of this program is a possibility to simulate simultaneously all general effects acting on the beam parameters. In this report general models for stochastic cooling presentation in BETACOOOL program are described.

BETACOOOL program developed by JINR electron cooling group is a kit of algorithms based on common format of input and output files. The program is oriented to simulation of the ion beam dynamics in a storage ring in presence of cooling and heating effects. The version presented in this report includes three basic algorithms: simulation of r.m.s. parameters of the ion distribution function evolution in time, simulation of the distribution function evolution using Monte-Carlo method and tracking algorithm based on molecular dynamics technique. General processes to be investigated with the program are intrabeam scattering (IBS) in the ion beam, electron and stochastic cooling, interaction with internal target. Algorithms for electron cooling and IBS simulation were developed during a few last years in collaboration with BNL and they are described in independent documents. Algorithms for simulation the beam interaction with internal target were developed in collaboration with FZJ [2] and GSI, however to take into account real geometry of the target (namely pellet target) modifications of the algorithms are necessary. More accurate algorithm for the target simulation is described in additional document to this report.

Structure and description of basic algorithms of BETACOOOL program are presented in Introduction. Algorithms for stochastic cooling time calculation are described in the part 2. Part 3 is dedicated to stochastic cooling simulation in the frames of “model particle” algorithm. User manual and software description are given in addendum to this report.

2. Characteristic time calculation

The stochastic cooling for transverse degrees of freedom is simulated under assumption that the quarter wave loop pickup and kicker are located in the ring at positions with zero dispersion and its derivative. The phase advance of the betatron oscillations from pickup to kicker assumed to be $(2k+1)\frac{\pi}{2}$, where k is integer, and the phase errors are minimized. For two transverse degrees of freedom there is no band overlap. Cooling of longitudinal degree of freedom is simulated in accordance with the theory of filter method.

2.1. Transverse degrees of freedom

2.1.1. Cooling rate calculation

The transverse emittance derivative over time in each plane can be written in the following form:

$$\frac{d\varepsilon}{dt} = -\frac{1}{\tau_{cool}}(\varepsilon - \varepsilon_{\infty}), \quad (2.1)$$

where τ_{cool} describes the drift term in the Fokker-Plank equation and the equilibrium emittance ε_∞ corresponds to the diffusion term [3, 4]. The characteristic time of the emittance variation due to action of the stochastic cooling is equal:

$$\frac{1}{\tau} = \frac{1}{\varepsilon} \frac{d\varepsilon}{dt} = - \frac{1}{\tau_{cool}} \frac{\varepsilon - \varepsilon_\infty}{\varepsilon}. \quad (2.2)$$

The transverse cooling time is determined from the parameters of the cooling system as follows:

$$\frac{1}{\tau_{cool}} = \frac{16}{3} \frac{|\eta| \delta W^2}{N f_0} \cdot x J(x). \quad (2.3)$$

Here $\eta = \frac{1}{\gamma^2} - \frac{1}{\gamma_{tr}^2}$ is off-momentum factor of the storage ring, γ is Lorenz factor of the ion, γ_{tr} is critical energy of the ring in the rest energy units. f_0 is the ion revolution frequency. $W = f_{max} - f_{min}$ is the bandwidth of the system with lower frequency f_{min} and upper frequency f_{max} . N is the ion number. Total momentum spread of the beam δ is calculated from r.m.s. value in accordance with the shape of distribution function. For instance, at a parabolic distribution

$$\delta = 4 \frac{\Delta p}{p_{rms}}. \quad (2.4)$$

Formfactor $xJ(x)$ is calculated through a frequency range as follows:

$$xJ(x) = x \left(1 - 2x \ln \left(\frac{x + f_{max}/W}{x + f_{min}/W} \right) + \frac{x^2}{(x + f_{max}/W)(x + f_{min}/W)} \right). \quad (2.5)$$

The x value is proportional to the linear gain of the system from pickup to kicker G_A :

$$x = G_A / R, \quad (2.6)$$

where the coefficient R is determined by parameters of pickup and kiker:

$$R = \frac{16}{3A_1} \frac{|\eta| \delta W}{N} \frac{1}{Z} \frac{h_p h_k}{\sigma_p \sigma_k} \frac{1}{\sqrt{\beta_p \beta_k n_p n_k}} \frac{\beta p c}{(1 + \beta) e^2 f_0^2 l_{loop}}. \quad (2.7)$$

Here $h_{p,k}$ is height of the gap at pickup and kicker, the pickup and kicker sensitivity are given by

$$\sigma_{p,k} = 2 \tanh \left(\frac{\pi w_{p,k}}{2h_{p,k}} \right), \quad (2.8)$$

where $w_{p,k}$ is the electrode width, Z – characteristic impedance, $\beta_{p,k}$ – beta functions in the pickup and kicker position, $n_{p,k}$ is the number of lambda quarter loops in pickup and kicker, l_{loop} is the loop length. β , p and e – are the ion velocity, momentum and charge correspondingly, c is the speed of light. Value A_1 is calculated through the bandwidth as follows

$$A_1 = \frac{1}{W} \int_{f_{\min}}^{f_{\max}} \sin^2 \left(\frac{2\pi f l_{\text{loop}}}{c} \right) df. \quad (2.9)$$

The equilibrium emittance value is determined by the cooling system parameters and the thermal noise power:

$$\varepsilon_{\infty} = \frac{1}{4} \frac{A_3}{A_2} \sqrt{\frac{\beta_k n_k}{\beta_p n_p}} (T_A + T_R) \frac{h_p \sigma_k}{h_k \sigma_p} l_{\text{loop}} \frac{1 + \beta}{\beta p c} G_A, \quad (2.10)$$

wher T_A and T_R are the pickup and preamplifier temperatures correspondingly. The values A_2 and A_3 are the following integrals:

$$A_2 = \frac{1}{W} \int_{f_{\min}}^{f_{\max}} \frac{\sin^2(2\pi f l_{\text{loop}} / c)}{2\pi f l_{\text{loop}} / c} df, \quad (2.11)$$

$$A_3 = \frac{1}{W} \int_{f_{\min}}^{f_{\max}} \left(\frac{\sin(2\pi f l_{\text{loop}} / c)}{2\pi f l_{\text{loop}} / c} \right)^2 df. \quad (2.12)$$

2.1.2. Power consumption

Optimization of the cooling system parameters presumes not only minimization of the equilibrium emittance and cooling time, but also keeping a consumption power in a reasonable range. The consumption power for transverse cooling chain is calculated as a sum of thermal noise power and Schottky power. The thermal noise power in the cooling bandwidth is given by:

$$P_{th} = (T_A + T_R) G_A^2 W, \quad (2.13)$$

and this value has to be corrected to take into account losses in combiner P_{comb} :

$$P_{th,tot} = P_{th} \cdot 10^{P_{\text{comb}}[dB]/10} \quad (2.14)$$

The Schottky power in the cooling band is

$$P_S = N n_p \beta_p Z \left(\frac{\sigma_p}{h_p} \right)^2 e^2 f_0 \varepsilon_{rms} G_A^2 W. \quad (2.15)$$

The total power is calculated as the sum of (2.14) and (2.15) plus losses in an electronic chain. The losses in the electronic chain are input into program as additional parameter P_{loss} and total consumption power is calculated in accordance with:

$$P_{tot} = (P_{th,tot} + P_S) \cdot 10^{P_{\text{loss}}[dB]/10}. \quad (2.16)$$

The loss power includes losses in splitter, reserve noise signal and others losses and by the order of magnitude is about 10 dB.

2.2. Longitudinal degree of freedom

The simulation presumes that the longitudinal cooling is applied using analogous system components as in the case for transverse cooling. Pickup and kicker are then operated in Σ -mode and the signal pass contains a notch filter that provides the necessary information on the energy deviation of a particle for the coherent signal. Simultaneously the filter rejects the noise signals at frequency near the revolution harmonics.

2.2.1. Cooling rate calculation

The ion distribution in the energy space is described by the function $\Psi(E)$, where E is the energy deviation from mean kinetic energy E_0 . The Fokker-Plank equation for the distribution function $\Psi(E,t)$, which describes the particle density in the energy space, has the following form

$$\frac{\partial}{\partial t} \Psi(E,t) = -\frac{\partial}{\partial E} \left[F(E) \Psi(E,t) - D(E,t) \frac{\partial}{\partial E} \Psi(E,t) \right],$$

where E is energy deviation from the mean kinetic energy E_0 .

Drift term in this equation describes the coherent cooling

$$F(E) = \frac{E}{\tau_0},$$

where τ_0 is the “single particle” cooling time. The diffusion term contains two parts

$$D(E,t) = D_{th}(E,t) + D_s(E,t)$$

the beam heating due to thermal noise

$$D_{th}(E,t) = AE^2$$

and beam heating due to the finite Schottky noise density

$$D_s(E,t) = BE^2 \Psi(E,t).$$

To calculate dynamics of the rms beam parameters the Fokker-Plank equation can be reduced to equation for the second moment of the distribution function which is determined by

$$\sigma_E^2 = \frac{1}{N} \int E^2 \Psi(E) dE \quad (2.17)$$

This equation has the following form [5, 4]:

$$\frac{d\sigma_E^2}{dt} = -\frac{2}{\tau_0} \sigma_E^2 + A \sigma_E^2 + \frac{3B}{N} \int E^2 \Psi^2(E,t) dE$$

Rms dynamics algorithm presumes Gaussian distribution in all degrees of freedom. In the energy space it corresponds to the density $\rho(E, t) = \frac{1}{N} \Psi(E, t)$ given by

$$\rho = \frac{1}{\sqrt{2\pi}\sigma_E} \exp\left(-\frac{(E - E_0)^2}{2\sigma_E^2}\right).$$

Thus the integral in the last term is equal to

$$\int E^2 \Psi^2 dE = N^2 \int E^2 \rho^2 dE = \frac{N^2 \sigma_E}{4\sqrt{\pi}},$$

and evolution of the second order momentum of the distribution function is described by the following equation

$$\frac{d\sigma_E^2}{dt} = -\frac{2}{\tau_{cool}} \sigma_E^2 + \frac{3B}{4\sqrt{\pi}} N \sigma_E, \quad (2.18)$$

The values A , B , τ_{cool} and τ_0 are determined from the cooling system parameters as follows:

$$\frac{1}{\tau_{cool}} = \frac{1}{\tau_0} - 3A, \quad (2.19)$$

$$A = A_1 e^2 (T_R + T_A) Z n_k \left(\frac{\kappa}{E_0}\right)^2 G_A^2 \frac{W}{f_0} \left(f_c^2 + \frac{W^2}{12}\right), \quad (2.20)$$

$$B = e^4 n_k n_p Z^2 \frac{|\kappa|}{E_0} G_A^2 f_0 f_c W, \quad (2.21)$$

the “single particle” cooling time τ_0 is given by

$$\frac{1}{\tau_0} = 2A_1 e^2 \sqrt{n_p n_k} Z G_A W f_c \frac{\kappa}{E_0}, \quad (2.22)$$

where $\kappa = \eta \frac{\gamma}{\gamma + 1}$, $f_c = \frac{f_{\min} + f_{\max}}{2}$ is the central frequency of the band. A_1 is determined by the formula (2.9) at the loop length of the longitudinal electrodes.

Characteristic rate for the longitudinal emittance deviation (in Betacool for the longitudinal emittance such a definition $\varepsilon_{long} = \left(\frac{\Delta p}{p}\right)^2$ is used) can be calculated in accordance with

$$\frac{1}{\tau} = \frac{1}{\varepsilon_{long}} \frac{d\varepsilon_{long}}{dt} = \frac{1}{\sigma_E^2} \frac{d\sigma_E^2}{dt} = -\frac{2}{\tau} + \frac{3BN}{4\sqrt{\pi}\sigma_E}. \quad (2.23)$$

Using relation between energy and momentum deviations $\frac{\sigma_E}{E_0} = \frac{1+\gamma}{\gamma} \frac{\Delta p}{p}$ the last equation can be reduced to:

$$\frac{1}{\tau} = -\frac{2}{\tau_{cool}} + \frac{3BN\gamma}{4\sqrt{\pi}\sqrt{\varepsilon_{long}}E_0(1+\gamma)}. \quad (2.24)$$

This formula is used for the longitudinal cooling rate calculation in the present version of the program.

Equilibrium value of the momentum spread corresponds to the cooling rate equality to zero. From the formula (2.24) the value of the equilibrium momentum spread is determined as follows:

$$\frac{\Delta p}{p_{eq}} = \frac{3BN\gamma\tau_{cool}}{8\sqrt{\pi}E_0(1+\gamma)}. \quad (2.25)$$

2.2.2. Power consumption

The filtered thermal noise power in the cooling bandwidth at the kicker input can be estimated from:

$$P_{th} = \frac{1}{3}(T_A + T_R)G_A^2W. \quad (2.25)$$

The filtered Schottky power at the kicker input is

$$P_S = 4A_1Nn_pZe^2f_0G_A^2\eta^2\left(\frac{\Delta p}{p}\right)_{rms}^2W\left(1+\frac{W}{f_0}\right)\left(1+14\frac{W}{f_0}\right). \quad (2.26)$$

The total power consumption is calculated by the same way as for transverse degrees of freedom.

3. Kick of the ion momentum components due to action of stochastic cooling

In the frame of Model Beam algorithm each particle is presented as a 6 co-ordinate vector:

$\vec{X} = \left(x, \frac{p_x}{p}, y, \frac{p_y}{p}, s-s_0, \frac{\Delta p}{p}\right)$, where x and y are the horizontal and vertical co-ordinates, p_x and p_y

are corresponding momentum components, $s-s_0$ is the distance from the bunch center (in the case of coasting beam this variable can have arbitrary value), Δp is the particle momentum deviation from momentum of reference particle p .

Some effects like electron cooling or internal target are located in some fixed points of the ring. Such effects are characterizing by the ring lattice functions in the effect position. Some effects like intrabeam scattering or scattering on residual gas are distributed over the total ring circumference. Average action of such effects can be applied to the beam in “averaged” position in the ring, that has the beta and dispersion functions equal to averaged over the ring ones, the alpha-functions and dispersion derivative are equal to zero. Between the effect position the particle co-ordinates are transformed using linear matrix at random phase advance (the random generation of the phase

advance reflects that the integration step over time is sufficiently longer than revolution period and than betatron oscillation period). Action of each effect is simulated as the particle momentum variation in accordance with Langevin equation:

$$(p_{x,y,s} / p)_{fin} = (p_{x,y,s} / p)_{in} + \Lambda_{x,y,s} \Delta T + \sqrt{D_{x,y,s} \Delta T} \xi_{x,y,s}, \quad (3.1)$$

where p_s is the particle longitudinal momentum deviation, subscript *in* correspond to initial momentum value, subscript *fin* relates to final particle momentum after action of the effect, Λ and D are the drift and diffusion terms for corresponding degree of freedom, ΔT is step of the integration over time, ξ is Gaussian random number at unit dispersion. The regular variation of the particle momentum due to action of drift term can be rewritten as

$$(p_{x,y,s} / p)_{fin} = (p_{x,y,s} / p)_{in} \left(1 + \frac{\Lambda_{x,y,s}}{(p_{x,y,s} / p)_{in}} \Delta T \right). \quad (3.2)$$

Here the value $\frac{\Lambda_{x,y,s}}{(p_{x,y,s} / p)_{in}}$ does not depend on the effect position in the ring, and it can be treated as

a “single-particle” cooling time. At large value of ΔT the absolute value of the term $\frac{\Lambda_{x,y,s}}{(p_{x,y,s} / p)_{in}} \Delta T$

can be larger than unity (in the case of cooling this term has a negative sign). In this case direct application of the formula (3.2) will lead to change a sign of corresponding momentum component and can lead also to increase of its absolute value. This situation corresponds to artificial diffusion heating of the beam on numerical algorithm. To avoid this “numerical” diffusion at

$\left| \frac{\Lambda_{x,y,s}}{(p_{x,y,s} / p)_{in}} \Delta T \right| > 1$ the formula (3.2) is transformed to the following form

$$(p_{x,y,s} / p)_{fin} = (p_{x,y,s} / p)_{in} \times \exp \left\{ \frac{\Lambda_{x,y,s}}{(p_{x,y,s} / p)_{in}} \Delta T \right\}, \quad (3.3)$$

which includes the (3.2) as a limit case at small ΔT .

In the case of random variation of the particle momentum components corresponding to diffusion term in (3.1) the kick has to be calculated taking into account the ring lattice parameters in the effect position. In the simplest case at the constant diffusion the equation for the emittance variation in time can be written as follows:

$$\frac{d\varepsilon_{x,y}}{dt} = \frac{D_{x,y}}{2\varepsilon_{x,y}}, \quad (3.4)$$

that gives

$$\Delta\varepsilon_{x,y} = \frac{D_{x,y}}{2\varepsilon_{x,y}} \Delta T. \quad (3.5)$$

Tacking into account that rms momentum variation relates to the emittance variation as $\langle \theta^2 \rangle = 2 \frac{\Delta \varepsilon_{x,y}}{\beta_{x,y}}$, for the momentum components variation we have:

$$\Delta(p_{x,y} / p) = \sqrt{\frac{D_{x,y}}{\varepsilon_{x,y} \beta_{x,y}}} \Delta T \xi_{x,y}, \quad (3.6)$$

where $\beta_{x,y}$ are the beta functions in the effect position in corresponding planes. For longitudinal degree of freedom emittance is determined as square of the rms momentum spread and at this definition we have:

$$\Delta(\Delta p / p) = \sqrt{k \frac{D_{long}}{2\varepsilon_{long}}} \Delta T \xi, \quad (3.7)$$

where $k = 1$ for coasting beam and $k = 2$ for bunched one.

3.1. Transverse degrees of freedom

For the transverse degree of freedom the drift term in (3.1) is calculated in accordance with the formula (2.3) for the “single particle” cooling time. The regular variation of transverse momentum component are calculated in accordance with (3.2, 3.3):

$$(p_{x,y} / p)_{fin} = \begin{cases} (p_{x,y} / p)_{in} \left(1 - \frac{\Delta T}{\tau_{cool,x,y}} \right), & \text{if } \left| \frac{\Delta T}{\tau_{cool,x,y}} \right| < 1 \\ (p_{x,y} / p)_{in} \exp\left(-\frac{\Delta T}{\tau_{cool,x,y}} \right), & \text{if } \left| \frac{\Delta T}{\tau_{cool,x,y}} \right| > 1 \end{cases} \quad (3.8)$$

Diffusion coefficient for the transverse degrees of freedom can be calculated using formula (2.10) for equilibrium emittance value. The emittance variation in time can be described by the following differential equation:

$$\frac{d\varepsilon_{x,y}}{dt} = -\frac{\varepsilon_{x,y}}{\tau_{cool,x,y}} + \frac{D_{x,y}}{2\varepsilon_{x,y}}. \quad (3.9)$$

From the other hand (2.1) gives

$$\frac{d\varepsilon_{x,y}}{dt} = -\frac{\varepsilon_{x,y}}{\tau_{cool,x,y}} + \frac{\varepsilon_{\infty,x,y}}{\tau_{cool,x,y}},$$

and for the diffusion coefficient we have:

$$D_{x,y} = \frac{2\varepsilon_{x,y}\varepsilon_{\infty,x,y}}{\tau_{cool,x,y}}. \quad (3.10)$$

The diffusion power is proportional to square of the linear gain G_A that can be seen from definitions of the cooling time and equilibrium emittance (2.3, 2.10). This result can be obtained directly from expression for emittance derivative before introduction of ε_∞ as it done for instance in [3].

In accordance with (3.6) for the momentum components variation we have:

$$\Delta(p_{x,y} / p) = \sqrt{\frac{2\varepsilon_{\infty,x,y}}{\tau_{cool,x,y}\beta_{x,y}}} \Delta T \xi_{x,y}. \quad (3.11)$$

In the present version of the program the kick is applied to the ion momentum in “averaged” position of the ring.

3.2. Longitudinal degree of freedom

For longitudinal degree of freedom the “single particle” cooling time τ_0 is given by (2.22), and the regular particle momentum variation is calculated as follows:

$$(\Delta p / p)_{fin} = \begin{cases} (\Delta p / p)_{in} \left(1 - k \frac{\Delta T}{\tau_0}\right), & \text{if } \left|\frac{\Delta T}{\tau_0}\right| < 1 \\ (\Delta p / p)_{in} \exp\left(-k \frac{\Delta T}{\tau_0}\right), & \text{if } \left|\frac{\Delta T}{\tau_0}\right| > 1 \end{cases} \quad (3.12)$$

At arbitrary distribution function the integral $\int E^2 \rho^2 dE$ can be estimated by the value $\frac{N^2 \sigma_E}{6}$, which is averaged for Gaussian and parabolic distributions. In this case the equation (2.18) can be rewritten as

$$\frac{d\sigma_E^2}{dt} = -\frac{2}{\tau_0} \sigma_E^2 + 3A\sigma_E^2 + \frac{B}{2} N\sigma_E$$

or taking into account that $\frac{\sigma_E}{E_0} = \frac{1+\gamma}{\gamma} \frac{\Delta p}{p}$ and $\varepsilon_{long} = \left(\frac{\Delta p}{p}\right)^2$

$$\frac{d\varepsilon_{long}}{dt} = -\frac{2}{\tau_0} \varepsilon_{long} + 3A\varepsilon_{long} + \frac{BN\gamma}{2E_0(\gamma+1)} \sqrt{\varepsilon_{long}}$$

The thermal and Shottky diffusion terms are independent, correspondingly the momentum kick due to diffusion is calculated as:

$$\Delta(\Delta p / p) = \sqrt{\left(\frac{BN\gamma}{2E_0(\gamma+1)}\right)^2 \varepsilon_{long} + (3A\varepsilon_{long})^2 k\Delta T \xi_s}. \quad (3.13)$$

In principle both kicks can be applied independently.

References

- [1] I.N.Meshkov, A.O.Sidorin, A.V.Smirnov, E.M.Syresin, G.V.Trubnikov, P.R.Zenkevich, "Simulation Of Electron Cooling Process In Storage Rings Using Betacool Program", proceedings of Beam Cooling and Related Topics, Bad Honnef, Germany, 2001.
- [2] I.N.Meshkov, R. Maier et al, "Electron cooling application for luminosity preservation in an experiment with internal targets at COSY", Dubna 2001, Jul-4031.
- [3] B.Autin, "Fast betatron cooling in antiproton accumulator", CERN/PS-AA/82-20
- [4] H.Stockhorst, Design deliberations for a stochastic cooling system at HESR, FZJ
- [5] T.Katayama and N.Tokuda, Part. Acc., 1987, Vol. 21

V. Internal Target

1. Introduction

For simulations of the ion distribution function evolution due to action of different heating and cooling affects three basic algorithms are realized in BETACOOOL:

- RMS dynamics simulation,
- Simulation of distribution function evolution using Monte-Carlo method (Model Beam algorithm),
- Multi particle tracking based on Molecular Dynamics technique.

To have a possibility to simulate internal target influence in the frame of all three algorithms this effect is presented in the program at three layers. For multi particle tracking the target is presented as a thin lens associated with some optic element of the storage ring and the target action on the ion is presented in the form of transformation map. On the basis of the map for RMS dynamics simulation a few models for characteristic time of emittance and particle number variation are developed. For investigation of long term processes in the frame of Model Beam algorithm the internal target is presented in the form related to kick of the ion momentum and loss probability calculation.

2. Map of the internal target

Map of an effect is used in turn by turn tracking procedure and has to provide variation of the particle coordinates in 6-dimensional phase space and calculate the particle loss probability. Internal target is treated in BETACOOOL program as a thin lens, therefore the particle co-ordinates are not changed after crossing the target, but all three components of the particle momentum are changed and the particle can be loosed with some probability. Change of the transverse momentum components is related mainly with a multiple Coulomb scattering from nuclei of the target atoms. Change of the longitudinal momentum component takes a place due to ionization energy loss in interaction with electrons of the target atoms.

Detailed simulation of the ion momentum variation can be provided using Monte-Carlo method based on Urban model for the longitudinal degree of freedom and plural scattering model for the transverse ones. In the frame of the Urban model the total energy losses, calculated using Bethe-Bloch formula, are distributed between ionization and excitation events. The number of events has Poissonian distribution around expectation, the energy loss due to ionization are distributed from mean ionization energy to maximum transferable energy determined by kinematics of the process. The plural scattering model is based on generation of scattering angle in accordance with Rutherford cross-section for a screened Coulomb potential.

At large number of events the Coulomb scattering distribution is well presented by the theory of Moliere. It is roughly Gaussian for small deflection angles, but at large angles (larger than a few r.m.s. value) it behaves like Rutherford scattering, having larger tail than a Gaussian distribution. The core of the distribution can be described by rms value of the scattering angle. The ionization energy loss in the simplest case also can be described by two parameters: mean energy loss and standard deviation of the energy loss fluctuations. RMS parameters of the scattering process is a base of Gaussian model of the target simulation. The Gaussian model of the ion interaction with an

internal target permits to provide fast estimations of the heating rates and equilibrium beam parameters in the case of cooling application.

Probability of the particle loss after crossing a target is determined mainly by three processes: single scattering on large angles, charge exchange and nuclear reactions in the target. Cross-section of the single scattering on large angle is calculated in accordance with Rutherford formula. The charge exchange in the target in the present version is taken into account only for fully stripped ions. For such an ion the program calculates cross-section of a capture of an electron in the target. For antiprotons particle losses due to charge exchange are not exist.

2.1. Detailed simulation of the interaction with a target

To simulate the variation of the ion momentum components the program calculates expectations for numbers of elementary events after single crossing the target, i.e. numbers of excitation and ionization of the target toms and number of scattering on the nuclei. Real number of events assumed to be distributed around its expectation in accordance with Poisson low. In each elementary event the momentum variation is calculated as a random number distributed in accordance with corresponding low.

2.1.1. Longitudinal degree of freedom. Urban model

In the frame of Urban model the total energy loss is divided by two parts: excitation of the target atoms and their ionization. It is assumed that the target atoms have only two energy levels with binding energy E_1 and E_2 . The particle – atom interaction will then be an excitation with energy loss E_1 or E_2 , or an ionization with an energy loss distributed according to a function $g(E) \sim \frac{1}{E^2}$:

$$g(E) = \frac{(E_{\max} + I)I}{E_{\max}} \frac{1}{E^2}. \quad (2.1.1)$$

The macroscopic cross-section for excitations ($i = 1, 2$) is

$$\Sigma_i = \frac{\Delta E_{BB}}{\Delta x} (1 - r) \frac{f_i}{E_i} \frac{\ln \frac{E_{\max}}{E_i} - \beta^2}{\ln \frac{E_{\max}}{I} - \beta^2}, \quad (2.1.2)$$

and the macroscopic cross-section for ionization is

$$\Sigma_3 = \frac{\Delta E_{BB}}{\Delta x} r \frac{E_{\max}}{I(E_{\max} + I) \ln \left(\frac{E_{\max} + I}{I} \right)}. \quad (2.1.3)$$

E_{\max} is the maximum transferable energy:

$$E_{\max} = \frac{2m_e c^2 \beta^2 \gamma^2}{1 + 2\gamma \frac{m_e}{M} + \left(\frac{m_e}{M} \right)^2}. \quad (2.1.4)$$

with m_e is the electron mass and M - the projectile mass. I is the mean excitation energy, that can be estimated as $I = 16 \cdot Z^{0.9} \text{ eV}$, E_i – atomic energy levels, f_i – oscillator strength, ΔE_{BB} – mean energy loss after crossing the target calculated in accordance with the Bethe-Bloch equation and Δx is the target thickness. The number of events n_i after single crossing the target is

$$n_i = \Sigma_i \Delta x. \quad (2.1.5)$$

r ($0 \leq r \leq 1$) is the parameter of the model, it determines the relative contribution of ionization and excitation to the energy loss. At high ion energy one can expect that the total energy loss is determined by ionization mainly and $r = 1$.

Parameters f_i , E_i should satisfy the constraints

$$\begin{aligned} f_1 + f_2 &= 1 \\ f_1 \ln E_1 + f_2 \ln E_2 &= \ln I \end{aligned}$$

and they are determined in accordance with the model used in GEANT code:

$$f_2 = \begin{cases} 0, & \text{if } Z \leq 2 \\ 2/Z, & \text{if } Z > 2 \end{cases}, f_1 = 1 - f_2 \quad (2.1.6)$$

$$E_2 = 10 \cdot Z^2 \text{ eV}, E_1 = \left(\frac{I}{E_2^{f_2}} \right)^{1/f_1}. \quad (2.1.7)$$

With these values the atomic level E_2 corresponds approximately the K-shell energy of the atoms and Zf_2 the number of K-shell electrons.

The energy loss due to the excitation is

$$\Delta E_e = n_1 E_1 + n_2 E_2, \quad (2.1.8)$$

where n_1 and n_2 are integer numbers sampled from Poissonian distribution. The energy loss due to ionization is calculated as

$$\Delta E_{ion} = \sum_{i=1}^{n_3} \frac{I}{1 - g \xi_i} \quad (2.1.9)$$

n_3 is integer number sampled from Poissonian distribution, ξ_i are random numbers uniformly distributed from 0 to 1, $g = \frac{E_{\max}}{E_{\max} + I}$.

Summarizing, the algorithm of the ion longitudinal momentum variation is realized in the following consequent steps:

1. At given target thickness Δx the program calculates mean energy loss ΔE_{BB} .
2. The mean energy loss is distributed between excitation and ionization in accordance with r parameter value.

3. In accordance with macroscopic cross-section values the program calculates expectations of the excitation events n_1 and n_2 and ionization events n_3 .
4. Real number of events is generated randomly in accordance with Poisson law.
5. Total energy loss ΔE_{total} is calculated as a sum of excitation (2.1.8) and ionization (2.1.9) losses. The ionization losses are calculated using generator of uniformly distributed random number.
6. Deviation of the longitudinal component of the particle momentum is calculated as:

$$\delta \frac{\Delta p}{p} = \frac{\gamma}{1 + \gamma} \frac{\Delta E_{total}}{AE} \quad (2.1.10)$$

E is the particle kinetic energy per nucleon, A – the particle atomic number.

The expectation of the energy loss ΔE_{BB} is calculated in accordance with the Bethe-Bloch equation:

$$\frac{\Delta E_{BB}}{\rho \Delta x} = -K Z_p^2 \frac{Z_T}{A_T} \frac{1}{\beta^2} \left[\frac{1}{2} \ln \frac{2m_e c^2 \beta^2 \gamma^2 E_{max}}{I^2} - \beta^2 - \frac{\delta}{2} \right] \quad (2.1.11)$$

where ρ is the target density, x is co-ordinate along the ion trajectory, Z_p and Z_T are the charge number of projectile and target atoms, A_T is the target atomic number. K is a constant determining by the following expression:

$$\frac{K}{A} = \frac{4\pi N_A r_e^2 m_e c^2}{A} = 0.307075 \text{ MeV} \cdot \text{g}^{-1} \cdot \text{cm}^2, \quad (2.1.12)$$

r_e is the electron classic radius, N_A is Avogadro number. I is the mean excitation energy, which is equal to 13.6 eV for hydrogen and $(10 \pm 1) \cdot Z$ eV for elements heavier than sulphur.

The density effect correction factor $\delta/2$ in the equation (2.1.11) is much larger for a liquid or solid than for a gas and at very high energies

$$\frac{\delta}{2} \rightarrow \ln \frac{\hbar \omega_p}{I} + \ln \beta \gamma - \frac{1}{2}, \quad (2.1.13)$$

where the plasma energy $\hbar \omega_p$ is determined by electron density in the target:

$$\hbar \omega_p = \sqrt{4\pi n_e r_e^3 m_e c^2 / \alpha} = 28.816 \sqrt{\rho_{[g/cm^3]} \left\langle \frac{Z}{A} \right\rangle} [eV] \quad (2.1.14)$$

Here α is the fine structure constant.

In the program the equation (2.1.11) is simplified in accordance with [1] by introducing of the quantity ξ , which is proportional to the area density ρx of the target (ρ – target density in g/cm^3):

$$\xi = 0.1535 \left[\frac{\text{MeV cm}^2}{\text{g}} \right] \frac{Z_p^2}{\beta^2} \frac{Z_T}{A_T} \rho x. \quad (2.1.15)$$

Neglecting the effect density correction one can express the mean energy loss in the following form:

$$\Delta E_{BB} = 2\xi \left(\ln \frac{E_{\max}}{I} - \beta^2 \right). \quad (2.1.16)$$

2.1.2. Transverse degree of freedom. Plural scattering

More accurate way to calculate the ion momentum deviation is to generate the individual scattering angles by sampling them from the following distribution which is basically the rescaled Rutherford cross-section for a screened Coulomb potential with screening angle χ_α :

$$\frac{dN}{d\theta} = \chi_\alpha^2 \frac{2\theta}{(\theta^2 + \chi_\alpha^2)^2}. \quad (2.1.17)$$

One can generate random number sampled from the distribution shown in eq. 2.1.17 by the following recipe

$$\theta = \chi_\alpha \sqrt{\frac{1}{\xi} - 1}, \quad (2.1.18)$$

where ξ is a random numbers uniformly distributed from 0 to 1. Note that θ is the space scattering angle, to calculate variation of the ion horizontal and vertical momentum components one can assume that orientation of the scattering angle is uniformly distributed in the transverse plane. Finally the ion momentum variation after single scattering event can be generated in accordance with:

$$\Delta x' = \chi_\alpha \left(\sqrt{\frac{1}{\xi_1} - 1} \right) \cos(\pi \xi_2), \quad (2.1.19)$$

$$\Delta y' = \chi_\alpha \left(\sqrt{\frac{1}{\xi_1} - 1} \right) \sin(\pi \xi_2), \quad (2.1.20)$$

where ξ_1 is a random number uniformly distributed from 0 to 1, ξ_2 is a random number uniformly distributed from -1 to 1, $x' = p_x / p$, $y' = p_y / p$ are the relative horizontal and vertical momentum components of the ion.

The number of scatterings Ω_0 within a given target thickness can be calculated from the formulae in the GEANT manual:

$$\Omega_0 = b_c Z_P^2 \frac{t}{\beta^2}, \quad (2.1.21)$$

where t is the target length and b_c is given by the formula

$$b_{c,[cm^{-1}]} = 6702.33 \rho_{[g/cm^3]} Z_s' \exp\left(\frac{Z_E' - Z_X'}{Z_s'}\right), \quad (2.1.22)$$

where ρ is the target density.

For the target material at atomic number A_T

$$\begin{aligned} Z'_s &= \frac{Z_T(Z_T + 1)}{A_T}, \\ Z'_E &= Z'_s \ln Z_T^{-2/3}, \\ Z'_X &= Z'_s \ln \left(1 + 3.33 \frac{\alpha Z_T Z_P}{\beta} \right), \end{aligned} \quad (2.1.23)$$

where α is the fine structure constant.

The screening angle is calculated as

$$\chi_\alpha = \frac{\chi_c}{\sqrt{1.167 \Omega_0}}, \quad (2.1.24)$$

where

$$\chi_c = \chi_{cc} \frac{\sqrt{t}}{A_p m c^2 \gamma \beta}, \quad (2.1.25)$$

$$\chi_{cc, [MeV / \sqrt{cm}]} = 0.39612 \sqrt{Z'_s \rho [g / cm^3]}, \quad (2.1.26)$$

$m c^2 = 931.49432 \text{ MeV}$ is the atomic unit energy.

In the frame of Model beam algorithm at given step of simulation over time the program calculates for each model particle the number of the pellet crossings N_{cross} and generates $N_{cross} \Omega_0$ the scattering events.

2.2. Scattering in accordance with Gaussian law

Assuming Gaussian law of the processes one can calculate particle longitudinal and transverse momentum variations after single crossing the target by random generation of the scattering angle and energy loss:

$$\begin{aligned} x'_f &= x'_0 + \sqrt{\frac{\theta_{str}^2}{2}} \times \xi_1, \\ y'_f &= y'_0 + \sqrt{\frac{\theta_{str}^2}{2}} \times \xi_2, \\ \left(\frac{\Delta p}{p} \right)_f &= \left(\frac{\Delta p}{p} \right)_0 + \left(\frac{\Delta p}{p} \right)_{str} \times \xi_3 - \left(\frac{\Delta p}{p} \right)_{loss}, \end{aligned} \quad (2.2.1)$$

where ξ_1, ξ_2, ξ_3 are independent random values having Gaussian distribution at unit standard deviation. For a thin target the rms scattering parameters $\theta_{str}^2, \left(\frac{\Delta p}{p} \right)_{loss}$ and $\left(\frac{\Delta p}{p} \right)_{str}$ are linearly

depend on the target density and can be calculated with the same analytical formulae in accordance with the local target density in the particle position.

The decrease of the ion relative momentum can be written through the energy losses as

$$\left(\frac{\Delta p}{p}\right)_{loss}^2 = \left(\frac{\gamma}{\gamma+1}\right)^2 \frac{\Delta E_{loss}^2}{E^2}. \quad (2.2.2)$$

The energy loss is determined by (2.1.16). It is the mean value, for finite target thickness there are fluctuations of the energy loss. The ion distribution is skewed toward high values (Landau tail). For a thick layer (when $\Delta E \gg E_{max}$) the distribution is nearly Gaussian. The square of the standard deviation of the ion distribution function in the energy space for a thick target is given by:

$$E_{str}^2 = \xi E_{max} \left(1 - \frac{\beta^2}{2}\right), \quad (2.2.3)$$

Where ξ is given by (2.1.15).

When circulating in a storage ring an ion beam crosses the target at each turn the mean energy loss (2.1.16) leads to deceleration of the beam. For coasting beam without cooling the centre of the ion distribution in momentum space is displaced to smaller values. The fluctuations of the energy loss (2.2.3) lead to increase of the ion beam momentum spread after single crossing the target in accordance with:

$$\left(\frac{\Delta p}{p}\right)_{str}^2 = \left(\frac{\gamma}{\gamma+1}\right)^2 \frac{E_{str}^2}{E^2}. \quad (2.2.4)$$

The r.m.s. scattering angle after crossing the target can be calculated using the formula:

$$\theta_{str}^2 = 2Nx\pi \left(\frac{Z_T Z_P r_p}{A_P \beta^2 \gamma}\right)^2 \left[\ln\left(\frac{\alpha_2^2}{\chi^2}\right) - 1 + \Delta b \right], \quad (2.2.5)$$

Here, Nx is the number of targets atoms per unit area, r_p – classical proton radius. The parametrs α_2 , χ and Δb are given by the equations:

$$\alpha_2 = \frac{\tilde{\lambda}}{(A_T^{1/3} + A_P^{1/3})r_0}, \quad (2.2.6)$$

where $\tilde{\lambda} = \hbar / p$ is De Broglie wavelength, A_T and A_P are the mass numbers of the target and the projectile, $r_0 = 1.3$ fm,

$$\chi^2 = 1.13\alpha_1^2 \left[1 + 3.33 \left(\frac{Z_T Z_P}{137\beta} \right)^2 \right], \quad (2.2.7)$$

where

$$\alpha_1 = \frac{\tilde{\lambda}}{0.885a_0 (Z_T^{2/3} + Z_P^{2/3})^{1/2}}, \quad (2.2.8)$$

$a_0 = 0.529 \cdot 10^{-8}$ cm denotes the Bohr radius,

$$\Delta b = \frac{1}{Z_T} \left\{ \ln \left[\frac{1130\beta^2}{Z_T^{4/3}(1-\beta)^2} \right] - u_{in} - \frac{\beta^2}{2} \right\}, \quad (2.2.9)$$

where u_{in} is a constant determined by the electron configuration of the target atom (from the Thomas-Fermi model one finds $u_{in} = -5.8$, for the H-atom exact calculation yields $u_{in} = -3.6$, for Li- and O-atoms the values of u_{in} are -4.6 and -5.0, respectively).

2.3. Calculation of the particle loss probability

The particle loss probability after crossing the target is determined by the following formula:

$$P_{loss} = \sigma_{total} Nx, \quad (2.3.1)$$

where Nx is the local target density in atoms per unit of square, σ_{total} is the sum of cross-sections of different reactions leading to the particle losses. Among them more important are the single scattering on large angles, capture of an electron in the target (in the general case – charge exchange), nuclear reactions in the target. Correspondingly in the program:

$$\sigma_{total} = \sigma_{ss} + \sigma_{ec} + \sigma_{nr}. \quad (2.3.2)$$

The cross-section for single scattering with an angle larger than the acceptance angle θ is [2]:

$$\sigma_{ss} = 4\pi \left(\frac{Z_T Z_p r_p}{A\gamma\beta^2} \right)^2 \frac{1}{\theta^2}, \quad (2.3.3)$$

where r_p is the proton classic radius. The acceptance angle, under assumption that the horizontal acceptance is substantially larger than the vertical one, is calculated as

$$\theta^2 = \frac{A_z}{\pi\beta_z} \left(1 - \left(\frac{\epsilon_z}{A_z} \right)^2 \right), \quad (2.3.3)$$

where β_z is the beta function in the target position, A_z is the ring acceptance.

For completely stripped ions the cross-section of the electron capture inside the target can be calculated in accordance with the formula [3]:

$$\sigma_{ec} = 1.1 \cdot 10^{-8} [cm^2] \frac{(1 - \exp(-0.037 E_{eff}^{2.2}))(1 - \exp(-2.44 \cdot 10^{-5} E_{eff}^{2.6}))}{E_{eff}^{4.8}}, \quad (2.3.4)$$

where the effective energy in keV is determined as:

$$E_{eff} = \frac{KZ_T^{1.25}}{Z_p^{0.7}}, \quad (2.3.5)$$

K is the ion kinetic energy.

		Detailed model	Gaussian model
Transverse degree of freedom		$\Omega_0/\Delta x$ – number of scattering events per unit of the target length	$\theta_{str}^2/\Delta x$ - rms scattering angle per unit of target length
		$\chi_\alpha^2/\Delta x$ - screening angle per unit of target length	
Longitudinal degree of freedom	of	R – ratio between ionization and excitation events	$\Delta E_{loss}^2/\Delta x$ - mean energy loss per unit of target length
		$n_1/\Delta x$ – number of excitations to the first level per unit of target length	$E_{str}^2/\Delta x$ - rms energy fluctuations per unit of target length
		$n_2/\Delta x$ – number of excitations to the second level per unit of target length	
		$n_3/\Delta x$ – number of excitations to the second level per unit of target length	
Transverse variation	momentum	$\Delta x' = \sum_{i=1}^{\Omega_0} \Delta x'_i$ $\Delta y' = \sum_{i=1}^{\Omega_0} \Delta y'_i$ $\Delta x'_i = \chi_\alpha \left(\sqrt{\frac{1}{\xi_1}} - 1 \right) \cos(\pi \xi_2)$ $\Delta y'_i = \chi_\alpha \left(\sqrt{\frac{1}{\xi_1}} - 1 \right) \sin(\pi \xi_2)$ <p>ξ_1 is a random number uniformly distributed from 0 to 1, ξ_2 is a random number uniformly distributed from -1 to 1</p>	$\Delta x' = \sqrt{\frac{\theta_{str}^2}{2}} \times \xi_1$ $\Delta y' = \sqrt{\frac{\theta_{str}^2}{2}} \times \xi_2$ <p>ξ_1, ξ_2, are Gaussian random numbers</p>
Longitudinal variation	momentum	$\Delta E = n_1 I_1 + n_2 I_2 + \sum_{i=1}^{n_3} \frac{I}{1 - g \xi_i}$ <p>n_1, n_2, n_3 are integer numbers sampled from Poissonian distribution ξ_i are random numbers uniformly distributed from 0 to 1, $g = \frac{E_{max}}{E_{max} + I}$</p>	$\left(\frac{\Delta p}{p} \right)_{loss}^2 = \left(\frac{\gamma}{\gamma + 1} \right)^2 \frac{\Delta E_{loss}^2}{E^2}$ $\left(\frac{\Delta p}{p} \right)_{str}^2 = \left(\frac{\gamma}{\gamma + 1} \right)^2 \frac{E_{str}^2}{E^2}$ $\left(\frac{\Delta p}{p} \right)_+ = \left(\frac{\Delta p}{p} \right)_{str} \times \xi - \left(\frac{\Delta p}{p} \right)_{loss}$ <p>ξ is Gaussian random number</p>

The cross-section of the nuclear reactions is estimated by the value:

$$\sigma_{nr} = \pi \cdot 10^{-26} [cm^2] (A_T^{1/3} + A_p^{1/3})^2 / \beta^2. \quad (2.3.6)$$

In the case of interaction with a pellet target the loss probability is calculated when the particle really crosses the pellet. In opposite case the probability is equal to zero.

3. Variation of the ion momentum in Model Beam algorithm

For simulation of the beam distribution function evolution in time the Model Beam algorithm is used in Betacool. In the frame of this algorithm the ion beam is presented as an array of model or test particles and all the effects changing the distribution function lead to variation of the particle momentum components. Change of the particle momentum after one step of the motion equation integration is calculated in accordance with Langevin equation:

$$\Delta p / p = \Lambda \Delta T + \sqrt{D \Delta T} \xi, \quad (3.1)$$

where Λ is drift term, D is diffusion term, ΔT is step of the integration over time, ξ is Gaussian random number at unit dispersion.

This algorithm can be used for the target simulation when the target is described in the frame of Gaussian model of the scattering process. In this case for transverse degree of freedom only the diffusion term is presented and its value is given by rms scattering angle (2.2.5). For longitudinal degree of freedom the drift term corresponds to the mean energy loss (2.1.16, 2.1.10), the diffusion term corresponds to the energy loss fluctuations and its value is given by (2.2.3, 2.2.4).

For detailed model of the scattering process the program calculates a number of the target crossings during the time ΔT and simulates each crossing independently.

In the frame of Gaussian model for interaction with internal target the diffusion and drift terms are calculated in respect to single crossing the target in accordance with formulae from chapter 2.2. The equation (3.1) can be rewritten in the following form:

$$\begin{aligned} x'_f - x'_0 &= \sqrt{\frac{\theta_{str}^2}{2} N_{cross}} \times \xi_1, \\ y'_f - y'_0 &= \sqrt{\frac{\theta_{str}^2}{2} N_{cross}} \times \xi_2, \\ \left(\frac{\Delta p}{p} \right)_f - \left(\frac{\Delta p}{p} \right)_0 &= \sqrt{\left(\frac{\Delta p}{p} \right)_{str}^2 N_{cross}} \times \xi_3 - \left(\frac{\Delta p}{p} \right)_{loss} N_{cross}, \end{aligned} \quad (3.2)$$

where N_{cross} is the number of the target crossing during interval ΔT , $\xi_{1,2,3}$ – independent Gaussian random numbers. In the general case N_{cross} is a function of the model particle co-ordinates.

For simulation of the particle loss the program generates random number ξ_4 uniformly distributed from 0 to 1. If $\xi_4 > P_{loss} N_{cross}$ the particle is loosed and program changes the number of particles in the total beam and generates a new model particle in the model beam. The loss probability P_{loss} is calculated in accordance with (2.3.1). If $P_{loss} N_{cross} > 1$ the particle is loosed automatically.

When the target at uniform density fully overlaps the beam the crossing number is simply equal to

$$N_{cross} = \frac{\Delta T}{T_{rev}}, \quad (3.3)$$

where T_{rev} is the revolution period.

In the case of pellet or fibre target, when the target length is not a constant inside the beam radius, the number of crossings is calculated for each model particle individually as a function of the particle motion invariants.

3.1. Number of the crossings in the case of pellet target

At integration of the equation of the particle motion with fixed step over time the program calculates number of the pellet crossings N_{cross} and provides the energy loss calculation in the loop from unity up to this number.

For a gas storage cell or for solid target overlapping the total beam the particle crosses the target each time when it crosses the target position in the ring. In the general case at each crossing the target position one needs to check is the particle really crosses the target or not. For this aim the map of the target for the particle momentum variation and loss probability calculation requires the current time of the target position crossing as an additional parameter.

More general case is presented by a pellet target geometry. Now the following model of the pellet target is used in the program (Fig. 2.1):

1. Pellets are approximated by cubes at uniform density, which is equal to the density of the frozen gas. To keep the real density of the pellet the cube dimensions have to be recalculated from the pellet diameter as $x_p = y_p = d^3\sqrt{\pi/6}$, where d is the pellet diameter.
2. All the pellets move in vertical direction with the same velocity v_{pellet} and interval between them is equal to h .
3. The pellets move along the straight line shifted in horizontal direction by the distance of s relatively to the ion beam equilibrium orbit.

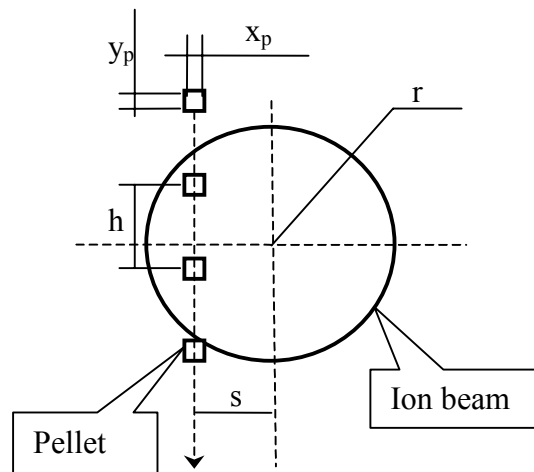


Fig. 3.1. Model of pellet target. x_p - horizontal size, y_p – vertical size, h – interval between pellets, s – horizontal shift, r – beam radius.

The pellet position at given moment of time is calculated under assumption that at zero time its vertical position is in median plane. The particle crosses the pellet when the following conditions are satisfied together:

$$|x_i - s| \leq \frac{x_p}{2} \quad (3.4)$$

$$\left| y_i + v_{\text{pellet}} t \pm h \left[\frac{y_i + v_{\text{pellet}} t}{h} \right] \right| \leq \frac{y_p}{2} \quad (3.5)$$

where x_i and y_i are the horizontal and vertical ion co-ordinates at time t correspondingly, the brackets $[\]$ denote fractional part of the value.

This model can be used for simulation of cluster beam or gas jet target when the jet width is less than the ion beam diameter as well. In these cases the distance between the "pellets" has to be equal to the vertical dimension of the pellet $h = y_p$, and the target density has to be equal to effective cluster beam density or gas jet density with corresponding correction factor depending on geometry.

The number of the pellet crossing by a particle at given invariants of the motion during one step of integration over time ΔT can be calculated at the following additional assumption. Lets suppose, the pellet move across the beam slow enough. Such, that the pellet changes its position in the beam during a few thousands of ion revolutions. In this case one can use simplified description of the particle betatron and synchrotron motion:

$$\begin{cases} x = \sqrt{I_x \beta_x} \cos \varphi_x + D \frac{\Delta p}{p} \\ y = \sqrt{I_y \beta_y} \cos \varphi_y \\ \frac{\Delta p}{p} = \sqrt{I_l} \cos \varphi_l \end{cases} \quad (3.6)$$

where $I_{x,y}$ – Courant-Snyder invariants in horizontal and vertical plane, $\beta_{x,y}$ – corresponding beta functions in the target position. Invariant of the motion in longitudinal plane is equal to square of the amplitude of the particle momentum oscillations, in the case of coasting beam this invariant is equal to square of the particle momentum deviation and the momentum deviation keeps a constant value during revolution in the ring. φ_i are the phases of oscillation and at slow movement of the pellet they are can be treated as an independent random numbers uniformly distributed in the interval from 0 to 2π .

Initially lets discuss situation with coasting ion beam. Lets at moment of t_0 the pellet is located in position where co-ordinates of its centre are x_c and y_c correspondingly. We use the same notation for the pellet parameters as in the Fig. 3.1, and $x_c = s$. The particle horizontal co-ordinate in the target position is inside the target when

$$|x - x_c| \leq \frac{x_p}{2}, \quad (3.7)$$

that is realised when the phases of oscillations lies in the interval

$$\arccos\left(\frac{x_C - \frac{x_p}{2} - D\frac{\Delta p}{p}}{\sqrt{I_x\beta_x}}\right) \geq \varphi_x \geq \arccos\left(\frac{x_C + \frac{x_p}{2} - D\frac{\Delta p}{p}}{\sqrt{I_x\beta_x}}\right). \quad (3.8)$$

If the phase is uniformly distributed from zero to 2π , the probability to have the particle horizontal co-ordinate inside the pellet P_x is equal to

$$P_x = \frac{\varphi_{x,2} - \varphi_{x,1}}{\pi}, \quad (3.9)$$

where $\varphi_{x,1,2} = \arccos\left(\frac{x_C \mp \frac{x_p}{2} - D\frac{\Delta p}{p}}{\sqrt{I_x\beta_x}}\right)$. The probability to have a particle vertical co-ordinate

inside the pellet is

$$P_y = \frac{\varphi_{y,2} - \varphi_{y,1}}{\pi}, \quad (3.10)$$

where $\varphi_{y,1,2} = \arccos\left(\frac{y_C \mp \frac{y_p}{2}}{\sqrt{I_y\beta_y}}\right)$. Because of the pellet movement in vertical direction its co-ordinate is changed with time

$$y_C = y_0 - v_{\text{pellet}} t, \quad (3.11)$$

Assuming, that the vertical size of the ion beam is equal to $2Y$, the probability to cross the target averaged over pellet movement can be estimated by the following expression:

$$P_{\text{cross}} = P_x \frac{v_{\text{pellet}}}{Y} \int_0^{Y/v_{\text{pellet}}} P_y(t) dt. \quad (3.12)$$

Using this value the number of the pellet crossing during period of ΔT can be calculated as follows

$$N_{\text{cross}} = \frac{\Delta T}{T_{\text{rev}}} P_{\text{cross}} \frac{2Y}{h}, \quad (3.13)$$

where multiplier $2Y/h$ gives a number of pellets crossing the beam at the same moment of time. Finally the number of the pellet crossings as a function of the particle Courant-Snyder invariants can be expressed as:

$$N_{\text{cross}} = \frac{\Delta T}{T_{\text{rev}}} \frac{2v_{\text{pellet}}}{\pi^2 h} \left(\arccos\left(\frac{x_C + x_p/2 - D\Delta p/p}{\sqrt{I_x\beta_x}}\right) - \arccos\left(\frac{x_C - x_p/2 - D\Delta p/p}{\sqrt{I_x\beta_x}}\right) \right) \times$$

$$\times \int_0^{T_{\max}} \left(\arccos \left(\frac{v_{\text{pellet}} t + y_p / 2}{\sqrt{I_y \beta_y}} \right) - \arccos \left(\frac{v_{\text{pellet}} t + y_p / 2}{\sqrt{I_y \beta_y}} \right) \right) dt, \quad (3.14)$$

where upper limit of the integration is given by

$$T_{\max} = \frac{\sqrt{I_y \beta_y} - y_p / 2}{v_{\text{pellet}}}. \quad (3.15)$$

And, obviously, the number of crossings is zero if

$$\sqrt{I_x \beta_x} < x_c - x_p / 2 - D\Delta p / p. \quad (3.16)$$

The case of bunched ion beam requires more detailed consideration due to low frequency of synchrotron oscillations in comparison with the frequency of betatron oscillations.

3.2. The pellet target as a fiber at mean density

To calculate expected number of the pellet crossing during given period of time for the ion at given co-ordinates at the target position in the Betacool was used algorithm based on calculation of crossing probability as a function of the ion Courant-Snyder invariants. This algorithm presumes Gaussian distribution of the pellet density in horizontal direction and relatively slow motion of the pellet in vertical direction. The vertical pellet velocity assumed to be so small, that during the time of the pellet motion through the ion beam the ion has a large number of betatron oscillations. This model predicts dependence of the crossing probability on vertical Courant-Snyder invariant of the ion and slight decrease of the effective target density, when the amplitudes of oscillation are comparable with the pellet dimensions. In reality the pellet vertical velocity is about 60 m/s, that corresponds to 60 $\mu\text{m}/\mu\text{s}$ and, for instance, during single antiproton revolution in HESR (2 μs) the pellet displaces by 120 μm and crosses the ion beam during a few revolutions. In this case seems to be more realistic to treat the pellet target at long time scale as uniform medium with averaged parameters.

The model of the pellet target as a medium can be developed on the basic assumptions similar to existing algorithm.

1. All the pellets have the same size, and the pellet shape can be approximated by box at dimensions $l \times x_p \times y_p$ at uniform density, which is equal to the density of the frozen gas (l is the pellet size along the ion trajectory, x_p and y_p are the horizontal and vertical sizes). To keep the real density of the pellet the cube dimensions can be recalculated from the pellet diameter as $l = x_p = y_p = d\sqrt[3]{\pi/6}$, where d is the pellet diameter.
2. All the pellets move in vertical direction with the same velocity v_{pellet} and interval between them is equal to h .
3. Each pellet moves along the straight line shifted in horizontal direction by the distance of s relatively to the ion beam equilibrium orbit.

4. The pellets form a flux at round shape of horizontal cross-section at radius r_f and mean uniform density. In this case, in difference with existing algorithm, the pellet distribution along the horizontal co-ordinate is not Gaussian.

At long period of interaction the pellet target can be treated as a solid target at uniform density determined by the equation:

$$\rho_{eff} = \rho \frac{l x_p y_p}{\pi h r_f^2}, \quad (3.17)$$

where ρ is the real pellet density, $l x_p y_p$ – the volume of the pellet, $h \pi r_f^2$ – the volume where the single pellet is located.

In the frame of discrete model of the target the program calculates number of elementary events after single crossing the pellet. To calculate number of elementary events after long period of time Δt one need to calculate the expectation of the number of the pellet crossings:

$$N_{cross} = P \frac{\Delta t}{T_{rev}}. \quad (3.18)$$

The probability P to cross the pellet during one revolution in the ring for given ion can be expressed as:

$$P = P_y P_x \quad (3.19)$$

where

$$P_y = \begin{cases} \frac{y_p}{h}, & \text{if } y_p < h \\ 1, & \text{if } y_p \geq h \end{cases} \quad (3.20)$$

is the probability to hit the pellet in vertical direction. The probability to cross the pellet in the horizontal direction P_x can be calculated as a ratio between the pellet flux cross-section and cross-section of the line along the ion trajectory at width of x_p (Fig. 3.2).

Length of such a line along ion beam orbit L does not depend on the ion vertical co-ordinate, and depends on horizontal ion co-ordinate x_i as follows:

$$L = 2\sqrt{r_f^2 - (x_i - \Delta_p)^2}, \quad (3.22)$$

when $-r_f < x_i < r_f$, and equal to zero, when the ion co-ordinate is bigger than flux dimensions. Here Δ_p is the horizontal displacement of the pellet flux centre from the ion equilibrium orbit.

$$P_x = \frac{L x_p}{\pi r_f^2}, \quad (3.21)$$

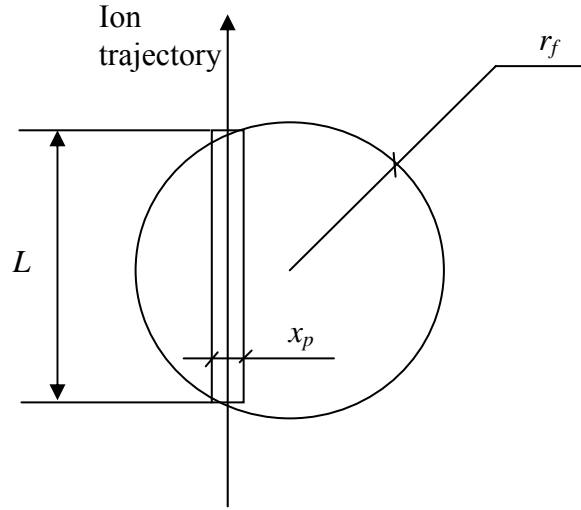


Fig. 3.2. The pellet flux cross-section by the horizontal plane.

During step of ion motion equation integration the ion oscillates in horizontal plane and the target length along the ion trajectory has to be averaged over the betatron oscillations. At given particle co-ordinates in the horizontal phase plane (x_i, x'_i) , its momentum deviation $\Delta p/p$ and lattice parameters in the target position (alpha and beta function - α_x, β_x , horizontal dispersion - D and its derivative D') the particle horizontal co-ordinate in the target position can be expressed by the following formulae:

$$\begin{aligned}
 x_i(\varphi) &= A_x \cos \varphi + D \frac{\Delta p}{p}, \\
 A_x &= \sqrt{I_x \beta_x}, \\
 I_x &= \beta_x x_{\beta}^{\prime 2} + 2\alpha_x x_{\beta} x_{\beta}' + \frac{1 + \alpha_x^2}{\beta_x} x_{\beta}^2, \\
 x_{\beta} &= x_i - D \frac{\Delta p}{p}, \\
 x_{\beta}' &= x'_i - D' \frac{\Delta p}{p}.
 \end{aligned} \tag{3.23}$$

Here φ is the phase of the betatron oscillations. The mean target length $\langle L \rangle$ can be calculated as an integral:

$$\langle L \rangle = \frac{2}{\pi} \int_{\varphi_{\min}}^{\varphi_{\max}} \sqrt{r_f^2 - (x_i(\varphi) - \Delta_p)^2} d\varphi, \tag{3.24}$$

where $\varphi_{\min} = 0$ and $\varphi_{\max} = \pi$, when the ion trajectory lies inside the pellet flux, or are calculated from elementary geometrical reasons:

$$\varphi_{\min} = \arccos \left(\frac{\Delta_p + r_f - D \frac{\Delta p}{p}}{A_x} \right),$$

$$\varphi_{\max} = \arccos \left(\frac{\Delta_p - r_f - D \frac{\Delta p}{p}}{A_x} \right). \quad (3.25)$$

When the number of the pellet crossings during time Δt is known, calculating the number of crossings for all modeling particles one can calculate luminosity in accordance with:

$$L = \frac{N_i}{N_{MP}} \frac{\rho_{\text{pellet}}}{\Delta t} \sum N_{\text{cross}}, \quad (3.26)$$

where N_i and N_{MP} are the total number of ions in the ring and number of modeling particles, ρ_{pellet} is the pellet density in atoms/cm².

The described model of the pellet target was implemented also into RMS dynamics algorithm. For this aim the characteristic heating rates due to interaction with the target are calculated on the basis of the probability to cross the pellet evaluated for the ion at co-ordinates corresponding to the ion beam rms emittances.

4. Different types of target

The characteristic times of the beam parameter variation are used in the frame of RMS dynamics simulation. The physical model used in RMS dynamics simulation is based on the assumption that the ion beam has Gaussian distribution over all degrees of freedom and maximum of the energy spread coincides with the equilibrium energy. The parameters $(\Delta p/p)_{\text{loss}}$, $(\Delta p/p)_{\text{str}}$, θ_{str} are the functions of the target thickness x . Therefore only at uniform target thickness in radial direction inside the beam radius the distribution function will keep a Gaussian shape after crossing the target. This condition is well satisfied for gas storage cell or for solid target overlapping the total beam. However, even in this case the particle mean energy losses can not be treated correctly due to basic assumption of the model.

In the case of target with non-uniform density a self-consistent consideration of the beam parameter evolution in the frame of RMS dynamics algorithm is impossible. However for fast estimations of expected beam parameters one can use simplified model when an “equivalent” target at uniform density presents the real target. The density of this equivalent uniform target – “effective” density - has to be chosen to provide the same variation of the rms parameters of the particle distribution function as the real target. If the effective density is calculated during simulations through the beam rms parameters in the first approximation such a model is self-consistent.

Simplest model of a target presumes that the target at uniform density overlap small part of the beam. In this case the target effective density can be calculated as a product of the real density and probability of the particle crossing the target. The probability of the crossing the target can be calculated analytically through geometry parameters of the target or using Monte Carlo method.

4.1. Gas storage cell and solid targets

For the target at uniform density the parameters $(\Delta p/p)_{loss}$, $(\Delta p/p)_{str}$, θ_{str} does not depends on the ion beam parameters and can be calculated using formulae (2.7 – 2.13). In this case the parameters of the circulating ion beam vary at single pass through the target in accordance with the following expression:

$$\begin{cases} \Delta\epsilon_{h,v} = \frac{\beta_{h,v} \theta_{str}^2}{2} + \left(\frac{(1 + \alpha_{h,v})^2}{\beta_{h,v}} D_{h,v}^2 + 2\alpha_{h,v} D_{h,v} D'_{h,v} + \beta_{h,v} D_{h,v}'^2 \right) \times \left(\frac{\Delta p}{p} \right)_{loss}^2, \\ \Delta\epsilon_{long} = \left(\frac{\Delta p}{p} \right)_{str}^2 \end{cases}, \quad (4.1.1)$$

where $\beta_{h,v}$, $\alpha_{h,v}$ are horizontal and vertical beta and alpha functions, $D_{h,v}$, $D'_{h,v}$ are dispersions and derivatives of the dispersion in the target position. For the transverse rms emittances in the program the usual definition is used.

Then the emittance growth times can be calculated as follows:

$$\frac{1}{\tau_i} = \frac{1}{\epsilon_i} \frac{\Delta\epsilon_i}{T_{rev}}. \quad (4.1.2)$$

In the case of the target with uniform density the ion beam lifetime is calculated through the ion loss probability in accordance with the following formula:

$$\frac{1}{\tau_{life}} = - \frac{P_{loss}}{T_{rev}}. \quad (4.1.3)$$

When the mean energy loss are sufficient in comparison with their fluctuations and does not compensated by additional cooling effect, in the program there is a possibility to include them into an “effective” increase of the momentum spread. In this case the longitudinal emittance variation after crossing the target is calculated as

$$\Delta\epsilon_{long} = \left(\frac{\Delta p}{p} \right)_{str}^2 + \left(\frac{\Delta p}{p} \right)_{loss}^2. \quad (4.1.4)$$

Of course, the treatment of the mean energy loss as an additional stochastic process is incorrect, but permits to estimate necessity of more correct simulations.

4.2. Gas jet, cluster beam and pellet targets

In the case when the target cross-section does not overlap the beam one or the target thickness does not uniform across the beam in the formulae (3.1) one needs to provide averaging over the target geometry. In the previous version of the BETACOOOL program for this aim the probability of the target crossing by an individual particle $P(\epsilon)$ was introduced. At given probability value the emittance growth times are calculated as follows:

$$\frac{1}{\tau_i} = \frac{1}{\varepsilon_i} \frac{\Delta \varepsilon_i}{T_{rev}} P(\vec{\varepsilon}), \quad (4.2.1)$$

and $\Delta \varepsilon_i$ are calculated in accordance with (4.1.1) or (4.1.4) at mean target thickness. The ion beam lifetime is calculated through the ion loss probability by the same way as in formula (4.1.3):

$$\frac{1}{\tau_{life}} = -\frac{P_{loss}}{T_{rev}} P(\vec{\varepsilon}). \quad (4.2.2)$$

In the general case the crossing probability is a function of all three beam rms emittances and it can be calculated in accordance with a model of the target geometry or using Monte Carlo method.

4.2.1. Calculation of the target effective density from geometry parameters

The value $P(\varepsilon)$ can be estimated as a ratio between beam cross section and the target one without any assumption about real geometry of the target position:

$$P(\varepsilon) = \begin{cases} 1 & \text{if } S_b \leq S_t \\ S_t / S_b & \text{if } S_b > S_t \end{cases}, \quad (4.2.3)$$

where S_t is the effective target cross-section, $S_b = \pi r^2$ is the r.m.s. beam cross-section, $r^2 = \sigma_{hor} \sigma_{vert}$ – square of beam radius, σ_{vert} and $\sigma_{hor} = \sqrt{\sigma_{hor,bet}^2 + D^2 \sigma_p^2}$ are the vertical and horizontal r.m.s. beam dimensions correspondingly. The betatron rms beam dimensions are calculated as usual: $\sigma = \sqrt{\varepsilon(1 + \alpha^2)} / \beta$, and σ_p denotes the rms momentum spread. To take into account Gaussian distribution of the particles over transverse co-ordinates the beam cross-section has to be multiplied by factor 2.

In accordance with the pellet model described in the chapter 3 (see Fig. 3.1) the effective cross-section of the pellet target is calculated by averaging the particle vertical position over time:

$$S_t = x_p 2\sqrt{r^2 - s^2} \frac{y_p}{h}. \quad (4.2.4)$$

The factor y_p/h appears after averaging over time assuming that the pellet has a constant vertical velocity. This formula can be used for simulation of cluster beam or gas jet target by the same way as described in the chapter 3.2.

4.2.2. Monte Carlo method of the effective density calculation

More accurate self-consistent calculation of the target effective density is based on Monte Carlo method, which does not need any assumptions on the ion beam geometry. The method is based on the ion beam presentation in the target position in the form of the particle array, which has the same rms parameters as the total ion beam and matched with the ring lattice parameters in the target position. This model beam consists of the particles at the same charge and mass as in the real beam and differs from the real beam only by the particle number.

At the first step of the algorithm the model beam is generated in accordance with given rms parameters and lattice functions at the target position. After that the model beam is propagated through the target particle by particle. The algorithm uses the same model of the pellet target at density averaged over time as in the previous chapter. If the particle horizontal co-ordinate x_i satisfies the condition:

$$|x_i - s| \leq \frac{x_p}{2} \quad (4.2.5)$$

the momentum components of this particle are changed in accordance with

$$\begin{aligned} x'_f &= x'_0 + \sqrt{\frac{\theta_{str}^2}{2}} \times \xi_1, \\ y'_f &= y'_0 + \sqrt{\frac{\theta_{str}^2}{2}} \times \xi_2, \\ \left(\frac{\Delta p}{p}\right)_f &= \left(\frac{\Delta p}{p}\right)_0 + \left(\frac{\Delta p}{p}\right)_{str} \times \xi_3 - \left(\frac{\Delta p}{p}\right)_{loss}, \end{aligned} \quad (4.2.6)$$

where ξ_1, ξ_2, ξ_3 are independent random values having Gaussian distribution at unit standard deviation. Here in difference with the internal target map calculation the rms scattering parameters $\theta_{str}^2, \left(\frac{\Delta p}{p}\right)_{loss}$ and $\left(\frac{\Delta p}{p}\right)_{str}$ are calculated at effective target density, which is related with the real one as

$$\rho_{eff} = \rho \frac{y_p}{h}. \quad (4.2.7)$$

This effective density is used also for calculation of the particle loss probability.

If the particle is outside the target (condition (3.7) is not satisfied) its momentum components are not changed and the loss probability is equal to zero.

After propagation of all the particles through the target final rms parameters of the particle array are calculated. The characteristic times of the emittance variation are calculated than as follows

$$\frac{1}{\tau_i} = \frac{\varepsilon_{i,f} - \varepsilon_{i,0}}{\varepsilon_{i,0} T_{rev}}. \quad (4.2.8)$$

Here index i denotes one of degrees of freedom. The beam lifetime is calculated as

$$\frac{1}{\tau_{life}} = -\frac{\langle P_{loss} \rangle}{T_{rev}}, \quad (4.2.9)$$

where the brackets $\langle \rangle$ denote averaging over the particles.

Accuracy of the characteristic time calculation is determined by the particle number in the model beam. The particle number required to obtain the same accuracy is scaled with the beam and target

parameters as σ_x / x_p . At the pellet diameter of 30 – 60 μm and the beam cross-section of a few millimetres the particle number has to be a few tens of thousands to obtain an accuracy of about a few percents. Accuracy of the calculations does not depend on the pellet velocity value and this algorithm can be applied without additional assumption.

References

- [1] F. Hinterberger, D.Prasuhn, Analysis of internal target effects in light ion storage ring, NIM A 279(1989), 413-422
- [2] N.Madsen, D.Moehl et al, Equilibrium beam in the Antiproton Decelerator (AD), NIM A (2000), 54-59.
- [3] T. Katayama, et. al., Collected Papers of the RIKEN RI Beam Factory, 1988

VI. Colliding Mode

1. Luminosity of colliding beams

1.2. Luminosity calculation in RMS dynamics

There are two options:

- colliding bunch has the same parameters as a calculated one,
- colliding bunch parameters are introduced as input parameters.

In the case, when colliding beams have different parameters the program uses simplest analytical formula:

$$L = N_b \frac{N_1 N_2}{2\pi \sqrt{(\sigma_{x,1}^2 + \sigma_{x,2}^2)(\sigma_{z,1}^2 + \sigma_{z,2}^2)} T_{rev}}, \quad (1.1)$$

N_1 , $\sigma_{x,1}$, $\sigma_{z,1}$ are the particle number, rms horizontal and vertical bunch sizes in the collision point of the beam, which parameters are simulated. Index 2 is related to the colliding bunch. N_b is the bunch number in simulated beam.

If both bunches are the same parameters the formula is simplified:

$$L = N_b \frac{N^2}{4\pi \sigma_x \sigma_z T_{rev}}, \quad (1.2)$$

where N_b is the number of bunches, N – ion number in bunch. This formula corresponds to Gaussian distribution of the ions and does not take into account hour-glass effect.

The life time is calculated in accordance with:

$$\frac{1}{\tau_{life}} = N_{IP} \frac{L \sigma_{reaction}}{N_b N}, \quad (1.3)$$

N_{IP} and $\sigma_{reaction}$ are the number of collision point and cross-section of the ion loss.

1.2. Luminosity calculation in Model Beam

For calculation of luminosity and particle loss in collision point new effect was created. During luminosity calculation in Model Beam algorithm the following procedures were developed:

- procedure presuming different models for luminosity calculation – via local density, coordinate ellipsoid, or profile density,
- calculation of beam-beam parameter in three ways of the beam emittance presentation – RMS, FWHM or emittance occupied by the definite percentage of particles.

The procedures are based on calculation of local ion beam density [particles/cm²] along the ion trajectory.

For axial symmetry beam the luminosity can be calculated using particles co-ordinates or smoothed profiles.

For arbitrary distribution one can use the particle co-ordinates only, in this procedure estimation for hourglass effect is included.

The procedures for luminosity calculation via coordinate ellipsoid, or profile density are based on the same model of the ion bunch. The bunch assumed to has an elliptical cross-section with the sizes $N_\sigma\sigma_x \times N_\sigma\sigma_z$, where $\sigma_{x,z}$ are the horizontal and vertical beam sizes calculated from the model particle array in accordance with the emittance definition, N_σ is the number of rms sizes corresponding to the total beam dimension (this parameter is input in the form **Beam | Distribution** in the tab sheet **Control** at the panel **Coordinate, Profile**). The beam is divided by N_{div} elliptical slices (Fig. 1.1). The parameter N_{div} is input in the form **Effects | Collision point** in the tab sheet **Divisions** – parameter **Particles/Divisions**.

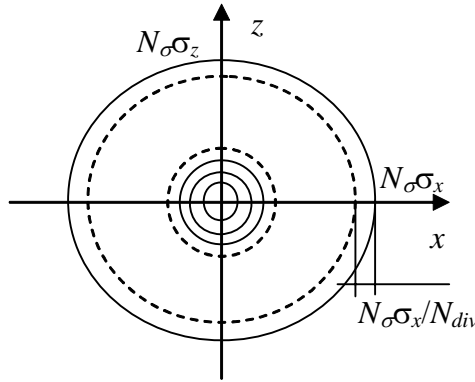


Fig. 1.1. Schematics of luminosity calculation via coordinate ellipsoid or profile density.

The program calculates number of model particles in each slice (two different procedures are used for coordinate ellipsoid and profile density) N_i and calculates an array containing areal density of the model particles in each slice:

$$d_i = \frac{N_i}{\pi h_x h_z (2i + 1)}, \quad (1.4)$$

$i = 0, \dots, N_{div} - 1$, $h_{x,z} = \frac{N_\sigma \sigma_{x,z}}{N_{div}}$. The luminosity is calculated via the slice density as a sum over the model particles:

$$L = N_b \frac{N^2}{N_{model}^2 T_{rev}} \sum_{j=1}^{N_{model}} d_j, \quad (1.5)$$

j is the number of the particle, N_{model} is the number of model particles, d_j is the slice crossing by j -th particle. The particle crosses j -th slice when

$$\left(\frac{x}{jh_x} \right)^2 + \left(\frac{z}{jh_z} \right)^2 < 1, \text{ and} \\ \left(\frac{x}{(j-1)h_x} \right)^2 + \left(\frac{z}{(j-1)h_z} \right)^2 > 1, \quad (1.6)$$

where x, z are the particle coordinates. The algorithm is based on the same assumption as the analytical formula (1) – the bunch dimensions are not changed during collision (it corresponds to the case when the bunch length is sufficiently less than beta-function in the interaction point).

For each model particle the program calculates the loss probability P_{loss} :

$$P_{loss,j} = N_{IP} \frac{N \sigma_{reaction} \Delta t}{N_{model} T_{rev}} d_j, \quad (1.7)$$

where Δt is the step of the algorithm over time.

In the frame of coordinate ellipsoid algorithm the number of particles in i -th slice N_i is calculated in cycle over model particles. For each model particle the program found number of slice for which the conditions (1.6) are satisfied and number of particles in this slice is increased by one.

In the frame of profile density algorithm the averaging over the particle betatron oscillations is used. The particle number in the slice is calculated by the same way as a histogram containing beam profile.

2. Beam-beam effect

Diffusion power due to beam-beam interaction in the collision point is calculated as a function of beam-beam parameter which has a meaning of linear part of betatron tune shift due to beam-beam collision. As a first step in beam-beam effect simulation a few algorithms for beam-beam parameter calculation were developed and tested in the BETACOOOL code. In this part the analytical theory and different numerical algorithms for the beam-beam parameter calculation are described.

2.1. Analytical formulae for beam-beam parameter

We start consideration of beam-beam effects with calculation of an increment of transverse particle momentum after crossing the opposite bunch (see Fig. 2.1). Consider "strong-weak" approximation to beam-beam interaction. In this model it is assumed that particles of a weak-beam (index 2) are influenced by a strong electromagnetic field of the opposite bunch (index 1), while the strong bunch does not feel any field from the weak bunch. Assume that opposite bunch with N_I particles has the Gaussian space charge density distribution with rms bunch size $\sigma_x, \sigma_y, \sigma_z$:

$$\rho(x, y, z, v_I, t) = \frac{q_I N_I}{(2\pi)^{3/2} \sigma_x \sigma_y \sigma_z} \exp\left(-\frac{x^2}{2\sigma_x^2} - \frac{y^2}{2\sigma_y^2} - \frac{(z - v_I t)^2}{2\sigma_z^2}\right). \quad (2.1)$$

Let us come to moving frame of coordinates (noted as prime coordinate system). Longitudinal position in moving frame is

$$z' = \gamma(z - v_I t). \quad (2.2)$$

In the moving frame the space charge density is

$$\rho'(x, y, z') = \frac{q_l N_l}{(2\pi)^{3/2} \sigma_x \sigma_y (\sigma_z \gamma)} \exp\left(-\frac{x^2}{2\sigma_x^2} - \frac{y^2}{2\sigma_y^2} - \frac{z'^2}{2\sigma_z^2 \gamma^2}\right). \quad (2.3)$$

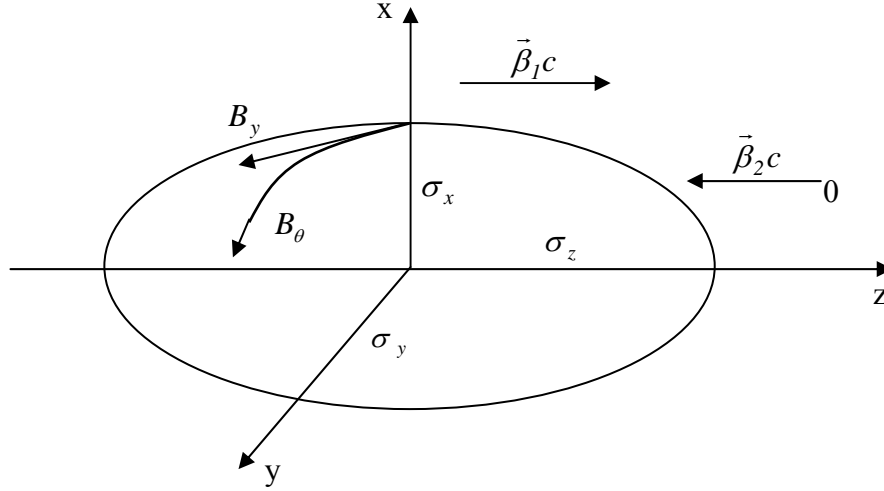


Fig 2.1. Interaction of test particle with strong opposite bunch

Electrostatic potential of the Gaussian bunch is:

$$U'(x, y, z') = \frac{q_l N_l}{4\pi^{3/2} \epsilon_0} \int_0^\infty \frac{\exp\left[-\frac{x^2}{(2\sigma_x^2 + w)} - \frac{y^2}{(2\sigma_y^2 + w)} - \frac{z'^2}{(2\sigma_z^2 \gamma^2 + w)}\right]}{\sqrt{(2\sigma_x^2 + w)} \sqrt{(2\sigma_y^2 + w)} \sqrt{(2\sigma_z^2 \gamma^2 + w)}} dw. \quad (2.4)$$

Transversal components of electrostatic field in the self frame are attained by differentiation of potential (4) $E'_x = -\partial U' / \partial x$, $E'_y = -\partial U' / \partial y$:

$$E_x = -\frac{q_l N_l \gamma}{2\pi^{3/2} \epsilon_0} \int_0^\infty \frac{\exp\left[-\frac{x^2}{(2\sigma_x^2 + w)} - \frac{y^2}{(2\sigma_y^2 + w)} - \frac{\gamma^2 (z - v_l t)^2}{(2\sigma_z^2 \gamma^2 + w)}\right]}{(2\sigma_x^2 + w)^{3/2} \sqrt{(2\sigma_y^2 + w)} \sqrt{(2\sigma_z^2 \gamma^2 + w)}} dw, \quad (2.5)$$

with analogous expression for E_y component. Moving bunch of charged particles creates magnetic field (see Fig. 2.1)

$$B_x = -\beta_1 \frac{E_y}{c}, \quad B_y = -\beta_1 \frac{E_x}{c} \quad (2.6)$$

Equations of transverse test particle motion are

$$\begin{aligned} \frac{dp_x}{dt} &= q_2 [E_x - (-v_2 B_y)] = q_2 E_x (1 + \beta_1 \beta_2), \\ \frac{dp_y}{dt} &= q_2 [E_y - (-v_2 B_x)] = q_2 E_y (1 + \beta_1 \beta_2). \end{aligned} \quad (2.7)$$

To define a change of particle momentum after crossing an opposite bunch, equations (7) have to be integrated along the time of integration. Assume that particle position and Lorentz force are not changed during test particle crosses the opposite bunch (thin lens approximation). Longitudinal equation of motion of test particle $z = -v_2 t$ has to be substituted into expression for field (5). In the adopted approximations the change of transverse particle momentum is

$$\Delta p_x = q_2 (1 + \beta_1 \beta_2) \int_{-\infty}^{\infty} E_x dt = -\frac{q_1 q_2 N_1 (1 + \beta_1 \beta_2)}{2\pi^{3/2} \epsilon_0 (v_2 - v_2)} x \int_0^{\infty} \frac{\exp\left[-\frac{x^2}{(2\sigma_x^2 + w)} - \frac{y^2}{(2\sigma_y^2 + w)}\right]}{(2\sigma_x^2 + w)^{3/2} \sqrt{(2\sigma_y^2 + w)}} dw, \quad (2.8)$$

similar for Δp_y . Consider linear approximation to increment of particle momentum. Integral in Eq. (2.8) can be evaluated analytically:

$$\int_0^{\infty} \frac{\exp\left[-\frac{x^2}{(2\sigma_x^2 + w)} - \frac{y^2}{(2\sigma_y^2 + w)}\right]}{(2\sigma_x^2 + w)^{3/2} \sqrt{(2\sigma_y^2 + w)}} dw \approx \int_0^{\infty} \frac{dw}{(2\sigma_x^2 + w)^{3/2} \sqrt{(2\sigma_y^2 + w)}} = \frac{1}{\sigma_x (\sigma_x + \sigma_y)}. \quad (2.9)$$

Therefore, linear approximation to increment of particle momentum is

$$\Delta p_x = -\frac{q_1 q_2 N_1 (1 + \beta_1 \beta_2)}{2\pi \epsilon_0 (\beta_2 + \beta_1) \sigma_x (\sigma_x + \sigma_y)} x. \quad (2.10)$$

Let us introduce the value of beta-function at the interaction point β_x^* , β_y^* . Then the change of slope of particle trajectory in linear approximation can be written as follow:

$$\Delta \frac{dx}{dz} = \frac{\Delta p_x}{p_z} = 4\pi \frac{\xi_x}{\beta_x^*} x, \quad \Delta \frac{dy}{dz} = \frac{\Delta p_y}{p_z} = 4\pi \frac{\xi_y}{\beta_y^*} y,$$

where ξ_x , ξ_y are beam-beam parameters, which have a meaning of linear part of betatron tune shift due to beam-beam collision:

$$\begin{aligned} \xi_x &= N_1 \frac{\beta_x^*}{4\pi} \frac{q_1 q_2}{4\pi \epsilon_0 m_2 c^2} \frac{(1 + \beta_1 \beta_2)}{\gamma_2 \beta_2 (\beta_1 + \beta_2)} \frac{2}{\sigma_x (\sigma_x + \sigma_y)}, \\ \xi_y &= N_1 \frac{\beta_y^*}{4\pi} \frac{q_1 q_2}{4\pi \epsilon_0 m_2 c^2} \frac{(1 + \beta_1 \beta_2)}{\gamma_2 \beta_2 (\beta_1 + \beta_2)} \frac{2}{\sigma_y (\sigma_x + \sigma_y)}. \end{aligned} \quad (2.11)$$

In the case of arbitrary density distribution in the opposite bunch the beam-beam parameters can be calculated in accordance with the definition:

$$\xi_x = \frac{\beta_x^*}{4\pi p_z} \lim_{x \rightarrow 0} \frac{\Delta p_x}{x}.$$

The momentum variation is calculated with the same formula (8)

$$\Delta p_x = q_2 (1 + \beta_1 \beta_2) \int_{-\infty}^{\infty} E_x dt ,$$

but the electric field component is calculated as a solution of Poisson equation at given distribution shape. For y direction the formulae are similar.

The other way is to use the same formulae (11) but to calculate the beam size as dimensions of the region containing given percent of particles or as a Full Width on Half Maximum (FWHM) of the beam distribution in co-ordinate space. In this case the formulae (11) have to contain additional normalizing factor, which provides coincidence of the different formulae in the case of Gaussian distribution.

For a bunch of a round shape of cross-section ($\sigma_x = \sigma_y = \sigma$) the term $\frac{N}{\pi\sigma^2}$ can be interpreted as a particle local density in the centre of the bunch integrated along z co-ordinate. Such approach permits to calculate the beam-beam parameter without solution of Poisson equation. At the current stage of the software development the algorithm for beam-beam parameter calculation on the basis of different emittance definition and local density evaluation are realized.

2.2. Numerical algorithms for beam-beam parameter calculation

For gold-gold collisions at RHIC the beam-beam parameter is calculated for a collision of two identical bunches. In the frame of Rms dynamics algorithm the analytical formulae (2.11) for beam-beam parameters can be rewritten in the following form:

$$\xi_x = \frac{Z^2 e^2}{A m c^2} \frac{N \beta_x^*}{4 \pi \sigma_x (\sigma_x + \sigma_y)} \frac{(1 + \beta^2)}{\gamma \beta}, \quad (2.12)$$

$$\xi_y = \frac{Z^2 e^2}{A m c^2} \frac{N \beta_y^*}{4 \pi \sigma_y (\sigma_x + \sigma_y)} \frac{(1 + \beta^2)}{\gamma \beta}. \quad (2.13)$$

here $mc^2 = 932$ MeV is nucleon rest energy, A , Z are the ion atomic and charge numbers, N is the ion number, β , γ are relativistic parameters which are equal for both bunches. The rms beam dimensions - $\sigma_{x,y}$ - are calculated from the beam rms emittance under assumption that the dispersion and alpha functions in the collision point are equal to zero:

$$\sigma_{x,y} = \sqrt{\varepsilon_{x,y} \beta_{x,y}^*}. \quad (14)$$

In the frame of Model Beam algorithm the beam dimensions can be calculated in accordance with different emittance definitions or the formulae (2.12, 2.13) can be rewritten using local particle density in the central part of the bunch.

When the emittance is calculated from the model particle array as statistic rms values the beam-beam parameter is calculated using the same formulae (2.14, 2.12, 2.13).

At the beam dimensions definition via FWHM of the model particle distribution the beam-beam parameter in each plane is calculated using the particle number inside the FWHM. For this in the formulae (12, 13) instead of the ion number N one uses the value

$$N_{x,y} = \frac{N_{FWHM,x,y} N}{N_{MB}}, \quad (2.15)$$

where N_{FWHM} is the model particle number inside the area corresponded to FWHM beam dimension in the corresponding plane, N_{MB} is the total particle number in the model beam.

When the emittance is defined as a square of ellipse containing given percent of the ions, the beam rms dimensions for the formulae (2.12, 2.13) is calculated with the normalization factor

$$\sigma = \frac{\sqrt{\varepsilon_\eta \beta^*}}{2 \ln \left(\frac{1}{1-100\eta} \right)}. \quad (2.16)$$

where η is the percent of particles using for emittance definition. At Gaussian distribution the normalization (2.16) provides independence of the beam-beam parameter on the emittance definition.

The beam-beam parameter can be calculated also via local density of the model particles in accordance with the formula:

$$\xi_{x,y} = \rho \frac{Z^2 e^2}{A m c^2} \frac{N \beta_{x,y}^*}{4 N_{MB}} \frac{(1 + \beta^2)}{\gamma \beta}, \quad (2.17)$$

where ρ is the model particle local density in cm^{-2} . The local density is calculated along the trajectory of the ion, located at the equilibrium orbit in the center of the bunch. Algorithm of the local density calculation is the following:

- for each model particle its distance from the equilibrium orbit in radial direction is calculated in accordance with

$$r_i = \sqrt{x_i^2 - y_i^2}, \quad (2.18)$$

- from the obtained array one chooses N_{count} ions having minimum distance from the equilibrium orbit, N_{count} is input parameter for the algorithm (Fig. 2.3),

- mean square distance of the ion from axis is calculated

$$\langle r^2 \rangle = \frac{\sum_{i=1}^{N_{count}} r_{i,min}^2}{N_{count}} \quad (2.19)$$

- finally, the local density is calculated as

$$\rho = \frac{1}{2} \frac{N_{count}}{\pi \langle r^2 \rangle}. \quad (2.20)$$

The multiplier $\frac{1}{2}$ provides equivalence of the formula (17) to formulae (12, 13) in the case of Gaussian distribution. The described algorithm is similar to algorithm for luminosity calculation via local ion density.

2.3. Results of benchmarking

The beam-beam parameter is calculated during dynamics simulation in the case when the effect "Collision Point" is active. Correspondingly all input parameters in the BOLIDE interface are located in the form "Effects | Collision Point" in additional tab sheet (Fig. 2.2). For calculation via local density the particle number N_{count} is the same as for luminosity calculation via local density (Fig. 2.3).

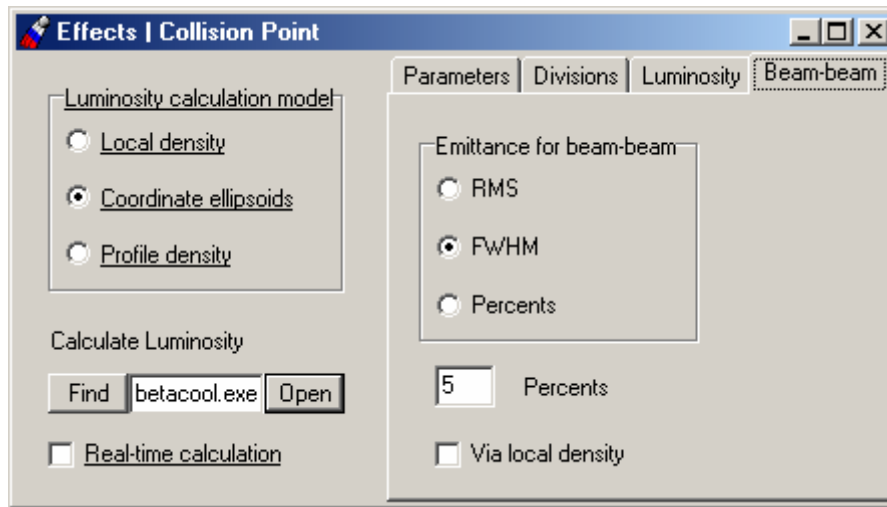


Fig. 2.2. Tab sheet for choice of the model for beam-beam parameter calculation in the frame of Model Beam algorithm. The beam-beam parameter is calculated via local density when the check-box "Via local density" is checked, in the opposite case the calculations are provided in accordance with chosen emittance definition.

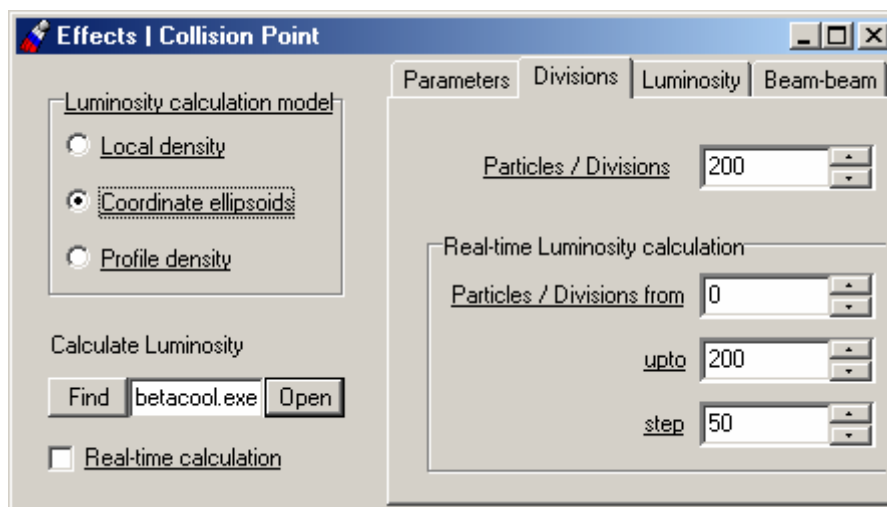


Fig. 2.3. The number of ions for beam-beam parameter calculation via local density N_{count} is input in the counter "Particles/Divisions".

Example of the beam-beam parameter calculations using different algorithms are listed in the Table 1. The beam parameters at the calculations were: horizontal and vertical emittances are $2.5 \cdot 10^{-8}$

$\pi \cdot \text{m-rad}$, momentum spread 0.001 and the ion number is 10^9 . Number of the model particles is 2000. Maximum fluctuation of the result takes a place for calculations via local density due to pure statistics: rms spread of the beam-beam parameter value from realization to realization is about 6%, that is approximately equal to $\frac{1}{\sqrt{N_{count}}}$. In the other cases the spread of results is determined by the model particle number and it is about 1 – 2 %.

Table 2.1. Example of beam-beam parameter calculation for Gaussian bunch.

	ξ_x	ξ_y
RMS Dynamics algorithm	0.001441	0.001441
Model Beam algorithm		
Rms emittance	0.001439	0.001441
FWHM emittance	0.001499	0.001542
30% emittance	0.001393	0.001426
40% emittance	0.001441	0.001373
50% emittance	0.00139	0.001453
60% emittance	0.001385	0.001425
Via local density, $N_{count} = 200$ (different realizations of the model particle array)	0.001497 0.001456 0.001332 0.001459 0.001438 0.001384 0.001424 0.001339 0.001547 0.001276 0.001314 0.001394	

VII. Barrier RF Bucket simulation

The barrier-bucket system application is one of the effective ways to achieve a high luminosity in experiment with internal target simultaneously with small phase space volume of the beam. One of the general effects leading to dilution of the beam quality at interaction with a target is mean energy loss of the particles. This effect sufficiently limits an available target thickness if a maximum cooling power is fixed. If the mean energy losses are compensated, at the same cooling power one can sufficiently increase the target thickness and, correspondingly, the luminosity.

The mean energy loss can be compensated by usual RF system at relatively small voltage amplitude; however this leads to sufficient increase of IBS growth rates. Even at long length of the bunch the particle density in its central part increases significantly in comparison with a coasting beam.

At a barrier-bucket application the particle density inside the bucket is almost uniform. Therefore the IBS growth rates increase by a factor equal to ratio of the ring circumference to the bucket length only. However in difference with a coasting beam the barrier-bucket system compensates the mean energy loss in the target and leads also to increase of an electron cooling efficiency. The last fact is connected with peculiarity of the particle synchrotron motion at barrier-bucket application: when the particle is reflected by the barrier its momentum deviation crosses zero and this corresponds to significant increase of the friction force acting on the particle inside the electron beam.

1. Synchrotron motion in a square wave barrier bucket

The RF voltage time dependence and phase trajectories of ions are sketched in the Fig.1. When the ion passes through the cavity gap at voltage $\pm V_0$ it gains (losses) an equal amount of energy ZeV_0 , i.e.

$$\frac{d(\Delta E)}{dt} = \pm \frac{ZeV_0}{T_0}, \quad (1)$$

where ΔE is the energy deviation from synchronous one, T_0 – revolution period. The ion trajectory in the longitudinal phase space $(t-t_0, \Delta E)$ inside the bucket can be written in the following form:

$$(\Delta E)^2 = \begin{cases} A_E^2 & \text{if } |t-t_0| \leq T_2/2 \\ A_E^2 - \left(|t-t_0| - \frac{T_2}{2} \right) \frac{2\beta^2 E_0 ZeV_0}{T_0 |\eta|} & \text{if } T_2/2 \leq |t-t_0| \leq (T_2/2) + T_1 \end{cases} \quad (2)$$

where A_E is the maximum energy deviation from synchronous energy E_0 , βc is the ion velocity, η is the ring off-momentum factor. The phase space trajectory is composed of a straight line in the RF gap region and a parabola in the square RF wave region.

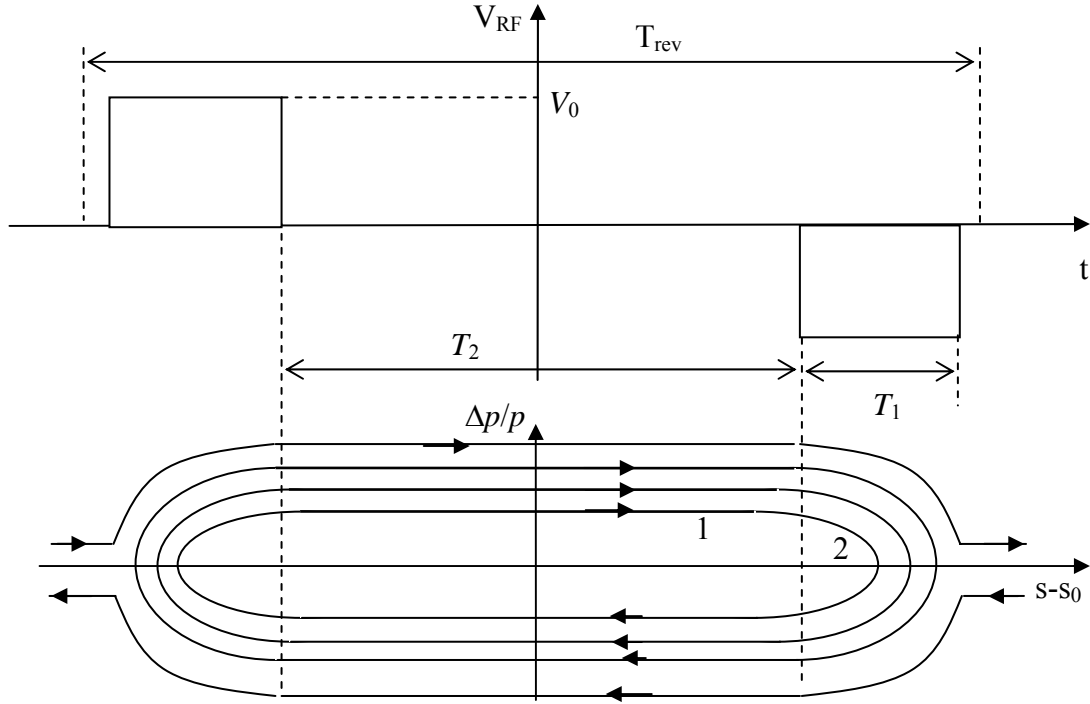


Fig.1. RF voltage and particle trajectories in the longitudinal phase space at square wave barrier-bucket. V_0 is the voltage height, T_1 is the pulse width, T_2 is the gap duration.

The maximum energy deviation or the barrier height that a barrier RF wave can provide is

$$\Delta E_b = \left(\frac{ZeV_0T_1}{T_0} \frac{2\beta^2 E_0}{|\eta|} \right)^{1/2}. \quad (3)$$

The period of synchrotron oscillations is

$$T_s = 2 \frac{T_2}{|\eta|} \left(\frac{\beta^2 E_0}{|A_E|} \right) + 4 \frac{|A_E|}{ZeV_0} T_0. \quad (4)$$

The relation between rms energy spread σ_E and maximum energy deviation of “rms ion” can be found from the following equation:

$$\frac{1}{T_s} \int_0^{T_s} (\Delta E)^2 dt = \sigma_E^2. \quad (5)$$

When the maximum energy deviation of the “rms” particle is known one can estimate the bucket length as

$$S_b = \left(\frac{T_2}{T_0} + \frac{A_{E,rms}^2}{\beta^2 E_0 ZeV_0} \right) C, \quad (6)$$

where C is the ring circumference.

To implement the Barrier Bucket simulation into BETACOOOL code the equation of the synchrotron motion has to be rewritten in the phase space ($s-s_0$, $\delta = \frac{\Delta p}{p}$). The equation is

$$\begin{cases} \frac{d(s-s_0)}{dt} = |\eta| \beta c \delta_A \\ \frac{d\delta}{dt} = 0 \end{cases} \quad (7)$$

at the part of the trajectory 1 (Fig. 1), and

$$\begin{cases} \frac{d(s-s_0)}{dt} = |\eta| \beta c \delta \\ \frac{d\delta}{dt} = -\frac{ZeV_0}{Cp_0} \end{cases} \quad (8)$$

at the part 2. Here δ_A is the amplitude of the momentum deviation, C is the ring circumference, p_0 – synchronous momentum.

The time of flight of the first part of the trajectory can be found from the first equation of (7) using the condition $(s-s_0)(t_1) = \frac{\beta c T_2}{2}$:

$$t_1 = \frac{T_2}{2|\eta|\delta_A}. \quad (9)$$

Solution of the second equation of the system (8)

$$\delta = \delta_A - \frac{ZeV_0}{Cp_0} t \quad (10)$$

permits to calculate time of flight the trajectory part 2 from the condition $\delta(t_2) = 0$

$$t_2 = \frac{Cp_0\delta_A}{ZeV_0}. \quad (11)$$

The period of synchrotron oscillations in this notation is

$$T_s = 4(t_1 + t_2) = \frac{2T_2}{|\eta|\delta_A} + \frac{4Cp_0\delta_A}{ZeV_0}, \quad (12)$$

which coincides with (4). From the equations (9), (11) the σ_δ^2 can be expressed as

$$\sigma_\delta^2 = \frac{t_1\delta_A^2 + \int_0^{t_2} \delta^2 d\tau}{t_1 + t_2}.$$

where δ is given by (10). That leads to

$$\frac{(2/3)|\eta|Cp_0\delta_A^4 + ZeV_0T_2\delta_A^2}{2|\eta|Cp_0\delta_A^2 + ZeV_0T_2} = \sigma_\delta^2.$$

Introducing

$$\xi^2 = \frac{ZeV_0T_2}{2|\eta|Cp_0} \quad (13)$$

one can obtain

$$\delta_A^2 = \frac{\sqrt{9(\xi^2 - \sigma_\delta^2)^2 + 12\xi^2\sigma_\delta^2} - 3(\xi^2 - \sigma_\delta^2)}{2}. \quad (14)$$

If this value is larger than the barrier height the particle oscillates outside the bucket and formula (14) is not correct. The maximum momentum deviation $\delta_{A,\max}$ corresponding to the barrier height can be calculated using solution of the motion equation in the 2 part of the trajectory:

$$s - s_0 = |\eta|\beta c \delta_A t - \frac{|\eta|\beta c ZeV_0}{2Cp_0} t^2. \quad (15)$$

The maximum momentum deviation satisfies to the equation $(s - s_0)(t_2) = \beta c T_1$, that gives

$$\delta_{A,\max}^2 = \frac{2T_1}{T_0} \frac{ZeV_0}{\beta c p_0 |\eta|}, \quad (16)$$

which coincides with (3) after required substitutions. The distance which particles crosses inside the RF wave is

$$(s - s_0)_{in} = |\eta|\beta c \delta_A t_2 - \frac{|\eta|\beta c ZeV_0}{2Cp_0} t_2^2 = \frac{|\eta|\beta c Cp_0 \delta_A^2}{2ZeV_0},$$

and total trajectory length is

$$S_b = T_2 \beta c + \frac{|\eta|\beta c Cp_0 \delta_A^2}{ZeV_0}. \quad (17)$$

For a particle outside the bucket ($\delta_A > \delta_{A,\max}$) the time of flight through the decelerating RF pulse can be found from quadratic equation (15) with $(s - s_0)(t) = \beta c T_1$:

$$t_d = t_2 \left(1 - \sqrt{1 - \frac{\delta_{A,\max}^2}{\delta_A^2}} \right), \quad (18)$$

where t_2 is determined by (11). The momentum deviation after crossing the decelerating wave is equal to

$$\delta_M = \delta_A \sqrt{1 - \frac{\delta_{A,\max}^2}{\delta_A^2}}. \quad (19)$$

When this particle crosses the accelerating wave the solution of the motion equation is

$$s - s_0 = |\eta| \beta c \delta_M t + \frac{|\eta| \beta c Z e V_0}{2 C p_0} t^2,$$

and the time of flight is

$$t_{acc} = t_2 \frac{\delta_M}{\delta_A} \left(\sqrt{1 + \frac{\delta_{A,\max}^2}{\delta_M^2}} - 1 \right) = t_d. \quad (20)$$

Momentum deviation after crossing the second wave is

$$\delta = \delta_M \sqrt{1 + \frac{\delta_{A,\max}^2}{\delta_M^2}} = \delta_A. \quad (21)$$

The time of flight through the second gap between RF waves is

$$t_g = \frac{T_0 - T_2 - 2T_1}{|\eta| \delta_M}$$

and the period of synchrotron oscillations is

$$T_{s,out} = 2t_1 + t_d + t_g + t_{acc} = \frac{T_2}{|\eta| \delta_A} + \frac{2Cp_0 \delta_A}{ZeV_0} \left(1 - \sqrt{1 - \frac{\delta_{A,\max}^2}{\delta_A^2}} \right) + \frac{T_0 - T_2 - 2T_1}{|\eta| \sqrt{\delta_A^2 - \delta_{A,\max}^2}}. \quad (22)$$

For the particle at given longitudinal co-ordinates ($s-s_0$, δ) the amplitude of oscillations can be calculated in accordance with the phase trajectory equation. The result is obvious, when ($s-s_0$) lies in one of the gaps between RF waves. Inside the wave it is equal to

$$\delta_A^2 = \delta^2 + \frac{2ZeV_0}{|\eta| \beta c C p_0} (s - s_0), \quad (23)$$

where ($s-s_0$) is measured from the beginning of the wave. Knowing the amplitude the particle co-ordinates at random phase of the oscillation can be generated by generation of random number uniformly distributed between 0 and T_s (or $T_{s,out}$, when $\delta_A > \delta_{A,\max}$) and calculate momentum deviation and longitudinal co-ordinate in accordance with equation of the phase space trajectory.

2. Modifications of RMS dynamics algorithm

2.1. Internal target and IBS

Simulations of intrabeam scattering and interaction with internal target require only slight modifications. At interaction with a target the mean energy loss has to be excluded and characteristic growth time for momentum spread should be calculated using expression for the energy loss fluctuations. However in presence of dispersion in the target position the emittance deviation has to be calculated taking into account mean energy loss:

$$\begin{cases} \Delta\epsilon_{h,v} = \frac{\beta_{h,v}\theta_{rms}^2}{2} + \left(\frac{1 + \alpha_{h,v}^2}{\beta_{h,v}} D_{h,v}^2 + 2\alpha_{h,v} D_{h,v} D'_{h,v} + \beta_{h,v} D_{h,v}'^2 \right) \times \left(\frac{\Delta p}{p} \right)_{mean}^2 \\ \Delta\epsilon_l = \left(\frac{\Delta p}{p} \right)_{str}^2 \end{cases} \quad (24)$$

Here $\epsilon_{h,v}$ are the transverse rms emittances. Longitudinal emittance of the ion beam is determined in the program as a mean square of the particle momentum deviation:

$$\epsilon_l = \langle \delta^2 \rangle. \quad (25)$$

θ_{rms}^2 , $\left(\frac{\Delta p}{p} \right)_{mean}$ and $\left(\frac{\Delta p}{p} \right)_{str}$ are the rms scattering parameters – scattering angle and momentum deviation due to mean energy loss and energy loss fluctuations. $\beta_{h,v}$, $\alpha_{h,v}$ are horizontal and vertical beta and alpha functions, $D_{h,v}$, $D'_{h,v}$ are dispersions and derivatives of the dispersion in the target position.

To realize this algorithm the procedure
vectorU xTarget::Rates(xTime&time, xBeam&beam, xRing&ring)
was modified.

The IBS process in the first approximation can be simulated using formulae for coasting beam at substitution of the bucket length instead the ring circumference. The bucket length can be calculated in the following steps: for given longitudinal emittance to calculate amplitude of the rms particle oscillations using formula (3.14), for this amplitude to calculate the bucket length in accordance with (3.17).

2.2. Electron cooling time calculation

The characteristic cooling time in the frame of rms dynamics model is determined as a change of the rms particle invariant of the motion after crossing the cooling section. It is calculated in accordance with:

$$\frac{1}{\tau_{cool}} = \frac{1}{I} \frac{\langle \delta I \rangle}{T_{rev}}, \quad (26)$$

where T_{rev} is the particle revolution period in the storage ring, the brackets mean averaging over the phases of betatron and synchrotron oscillations:

$$\langle \delta \vec{I} \rangle = \frac{1}{8\pi^3} \int \int_0^{2\pi} \int \delta \vec{I}(\vec{I}, \varphi_x, \varphi_y, \varphi_s) d\varphi_x d\varphi_y d\varphi_s, \quad (27)$$

where $I_{x,y,l}$ are the corresponding invariants of the particle motion.

The Courant – Snider invariants of the “rms particle” relate to the rms beam emittance as

$$I_{x,y} = 2\varepsilon_{x,y}. \quad (28)$$

In the case of **coasting beam** the cooling time is calculated by averaging over two values of the momentum deviation:

$$\delta = \pm \sqrt{\varepsilon_l}. \quad (29)$$

In the linear approximation, for a **bunched beam** one can express the particle momentum deviation and its longitudinal co-ordinate (distance from the bunch center) as a function of the phase of synchrotron oscillations:

$$\delta = \sqrt{I_l} \cos \varphi_s, \quad s - s_0 = \beta_l \sqrt{I_l} \sin \varphi_s. \quad (30)$$

here the "synchrotron function" is determined as:

$$\beta_l = \frac{R|\eta|}{Q_s}, \quad (31)$$

where R is the mean ring radius, Q_s is the synchrotron tune:

$$Q_s = \frac{1}{\beta} \sqrt{\frac{ZehV|\eta|}{A2\pi m_p c^2 \gamma}}, \quad (32)$$

h is the harmonic number, V is the RF voltage amplitude, β, γ are relativistic parameters, Z and A are the ion charge and atomic numbers, m_p is the proton mass, $\eta = \frac{1}{\gamma^2} - \frac{1}{\gamma_{tr}^2}$.

For the “rms particle” the invariant of the longitudinal motion is calculated as: $I_l = 2\varepsilon_l$.

In the case of **barrier bucket** the maximum momentum deviation of the “rms particle” can be calculated using (14). Averaging of the invariant deviation is simply to perform over $t-t_0$ using the phase space trajectory equation (10), (15). The synchrotron period T_s in this algorithm is divided by a few equidistant intervals. In the time of T_i the particle co-ordinate and momentum deviation are calculated in accordance with the following formulae:

$$\begin{aligned} \text{if } 0 \leq T_i < t_1 \\ s - s_0 &= |\eta| \beta c \delta_A T_i \\ \delta &= \delta_A \end{aligned}$$

$$\begin{aligned}
& \text{if } t_1 \leq T_i < t_1 + 2t_2 \\
& \quad s - s_0 = |\eta| \beta c \delta_A T_i - \frac{|\eta| \beta c Z e V_0}{2 C p_0} (T_i - t_1)^2 \\
& \quad \delta = \delta_A - \frac{Z e V_0}{C p_0} (T_i - t_1) \\
& \text{if } t_1 + 2t_2 \leq T_i < 3t_1 + 2t_2 \\
& \quad s - s_0 = |\eta| \beta c \delta_A (2t_1 + 2t_2 - T_i) \\
& \quad \delta = -\delta_A \\
& \text{if } 3t_1 + 2t_2 \leq T_i < 3t_1 + 4t_2 \\
& \quad s - s_0 = -\beta c \frac{T_2}{2} - |\eta| \beta c \delta_A (T_i - 3t_1 - 2t_2) + \frac{|\eta| \beta c Z e V_0}{2 C p_0} (T_i - 3t_1 - 2t_2)^2 \\
& \quad \delta = \frac{Z e V_0}{C p_0} (T_i - 3t_1 - 2t_2) - \delta_A \\
& \text{if } 3t_1 + 4t_2 \leq T_i < T_s \\
& \quad s - s_0 = |\eta| \beta c \delta_A (T_i - T_s) \\
& \quad \delta = \delta_A
\end{aligned}$$

where t_1 is given by formula (9), t_2 – (11).

After crossing the cooling section one needs to recalculate new ion co-ordinates ($s-s_0, \delta$) into rms momentum deviation. The new amplitude of the particle oscillations δ_A is calculated in accordance with (3.23) and corresponding rms momentum deviation is given by:

$$\langle \delta^2 \rangle = \frac{\delta_A^4 + 3\xi^2 \delta_A^2}{3(\delta_A^2 + \xi^2)}, \quad (3.33)$$

where ξ is given by (3.13).

3. Model beam algorithm

3.1. Generation of the ion initial distribution in the given ring position

Generation of initial ion distribution in the longitudinal phase space, generation of new model particle at losses are based on procedures for generation of individual ion co-ordinates and matching of the ion with the ring lattice in the generation position.

The particle coordinates are generated under assumption of Gaussian shape of the distribution function in all degrees of freedom. Each particle co-ordinate is calculated in accordance with:

$$x_i = \sigma_{x_i} \sqrt{-2 \ln \xi_{1,i}} \sin(2\pi \xi_{2,i}), \quad (34)$$

ξ_1 and ξ_2 are random values uniformly distributed in the interval from 0 to 1 generated with the standard random generator.

In the transverse planes one needs to match the particle coordinates with the lattice parameters of the ring. This procedure is realized by the following steps.

1. The particle “betatron” co-ordinates are distributed initially around a canonical ellipse at half-axis equal to the standard deviations for transverse co-ordinates and their derivatives (Fig.2):

$$\sigma_x = \sqrt{\varepsilon_x \beta_x}, \quad \sigma_{x'} = \sqrt{\varepsilon_x \gamma_x}.$$

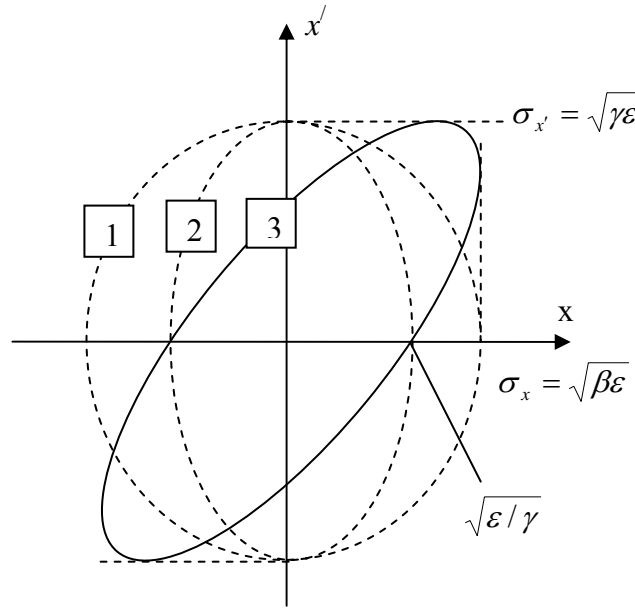


Fig.2. Matching of the ion coordinate with the ring lattice in the transverse phase space.

2. Matching with the lattice parameters the derivatives of the particle transverse co-ordinates are not changed. The transverse “betatron” co-ordinates are changed:

$$x_\beta = \frac{x_{in}}{\sqrt{1 + \alpha_x^2}} - \frac{\alpha_x}{\gamma_x} x', \quad (35)$$

these transformations are shown schematically in the Fig. 2.

3. The matching with the dispersion and its derivative:

$$x = x_\beta + D_x \delta, \quad x' = x'_\beta + D'_x \delta. \quad (36)$$

For a **coasting beam** the particle momentum deviation is distributed in accordance with Gaussian law at standard deviation of $\sigma_\delta = \sqrt{\varepsilon_l}$. The longitudinal co-ordinate is generated in accordance with:

$$s - s_0 = l_c \sqrt{3} \xi, \quad (37)$$

where l_c is the cell dimension for tracking algorithm, ξ is a random number uniformly distributed from -1 to 1. This algorithm is required for Molecular Dynamics simulations. In the Model Beam algorithm the longitudinal co-ordinate is not used. The cell length in the MD algorithm is usually sufficiently shorter than an optic element length and one can assume, that the lattice functions at the cell length are constants.

For a **bunched beam** in the longitudinal phase space the standard deviations of co-ordinate and momentum are calculated in accordance with the formulae:

$$\sigma_\delta = \sqrt{\varepsilon_l}, \quad \sigma_s = \beta_l \sigma_\delta. \quad (38)$$

Generation of the ion co-ordinates in the case of **Barrier Bucket** can be realized in the following steps.

1. Initially the momentum deviation is generated in accordance with Gaussian law at standard deviation equal to $\sqrt{\varepsilon_l}$.
2. For the given momentum deviation the maximum momentum deviation is calculated in accordance with the formula (14).
3. The phase of the synchrotron oscillation is generated to be uniformly distributed from 0 and 2π . At given maximum deviation and phase the values of the momentum deviation and longitudinal co-ordinate are calculated using equation of the phase space trajectory.

If the absolute value of the particle momentum deviation is larger than the barrier height the particle circulates in the ring outside the bucket.

3.2. The betatron and synchrotron motion simulation

The Model Beam algorithm realizes Monte-Carlo simulation method of solution of Langevin equation based on an assumption, that the integration step over time is sufficiently longer than the decoherence period (a few thousands of revolutions). In this case the phase advance of betatron and synchrotron oscillations on the integration step is an arbitrary number. In the transverse phase space the betatron motion is simulated using linear transformation matrixes from one effect position to another. The vector of “betatron” coordinates $\begin{pmatrix} x_\beta \\ x'_\beta \end{pmatrix}$ ($x_\beta = x - D\delta$, $x'_\beta = x' - D'\delta$) is multiplied by the matrix with coefficients

$$R_{11} = \sqrt{\frac{\beta_2^x}{\beta_1^x}} (\cos \mu_x + \alpha_1^x \sin \mu_x), \quad R_{12} = \sqrt{\beta_2^x \beta_1^x} \sin \mu_x,$$

$$R_{21} = -\frac{(\alpha_2^x - \alpha_1^x) \cos \mu_x + (1 + \alpha_2^x \alpha_1^x) \sin \mu_x}{\sqrt{\beta_2^x \beta_1^x}}, \quad R_{22} = \sqrt{\frac{\beta_1^x}{\beta_2^x}} (\cos \mu_x - \alpha_2^x \sin \mu_x),$$

where β_1 , α_1 are the lattice functions in the first effect position, β_2 , α_2 – in the second effect position, μ_x is a random number uniformly distributed from 0 and 2π . The same is for the vertical plane.

The synchrotron oscillations are simulated for a bunched beam only. The synchrotron motion is assumed to be linear (as well as the betatron one). The vector of longitudinal ion co-ordinates $\begin{pmatrix} s - s_0 \\ \delta \end{pmatrix}$ is multiplied by the matrix

$$\begin{pmatrix} \cos \mu & \beta_l \sin \mu \\ -\frac{\sin \mu}{\beta_l} & \cos \mu \end{pmatrix}, \quad (39)$$

where μ is a random number uniformly distributed from 0 and 2π . The particle oscillations are provided between actions of effects, which change the particle momentum components in accordance with friction and diffusion components. The particle losses from the bunch are taking into account by introducing of two input parameters: the separatrix length L_{sep} and height A_l (longitudinal acceptance). The ion is lost when $|s - s_0| > L_{sep} / 2$ or $|\delta| > A_l$. In this case instead the lost model particle the program generates new one using one of algorithm simulating the particle loss.

In the case of a **Barrier Bucket** the simulation of the synchrotron motion can be based on the phase space trajectory equation. At variation of the ion co-ordinates due to its synchrotron motion one needs to calculate amplitude of the particle momentum deviation (from its actual momentum and longitudinal co-ordinate, formula (14)). Thereafter the phase of synchrotron oscillations is generated uniformly between 0 and 2π and new co-ordinate and momentum has to be calculated as a function of the phase.

The bucket height can be less than the longitudinal acceptance, in this case the synchrotron motion has to be simulated for the ions outside the bucket.

4. Numerical model of barrier bucket

The analytical model has the static potentials of the barrier bucket with rectangular shape which is resolved analytically in the longitudinal phase space. The using of the analytical model is very difficult for the moving bucket with the arbitrary shape.

A numerical model of the RF bucket is implemented in the BETACOOOL code when the motion of one particle through each barrier is calculated independently. After crossing of the barrier the particle can increase energy, decrease energy or can be reflected from barrier (Fig.3).

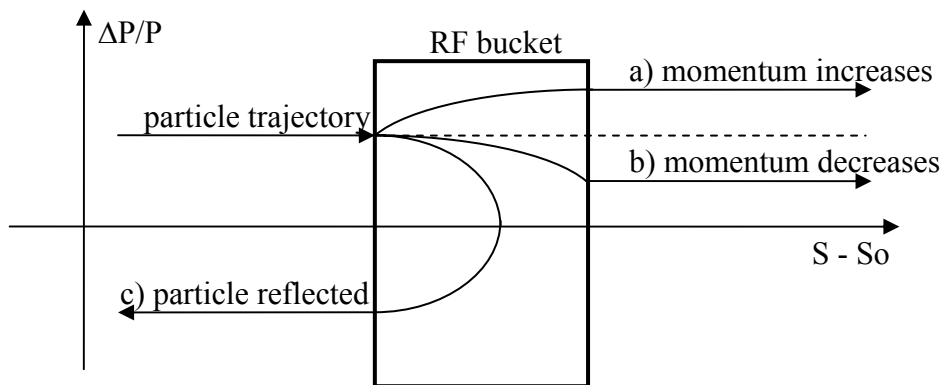


Fig.3. Particle trajectories trough barrier in longitudinal phase space.

For the description of the individual synchrotron motion of each particle one can use the series of the barriers (Fig.4) and the numerical integration over longitudinal phase space. If the integration step of the Model Beam algorithm is larger than the synchrotron period, we can assume that for the static barriers the synchrotron period is random.

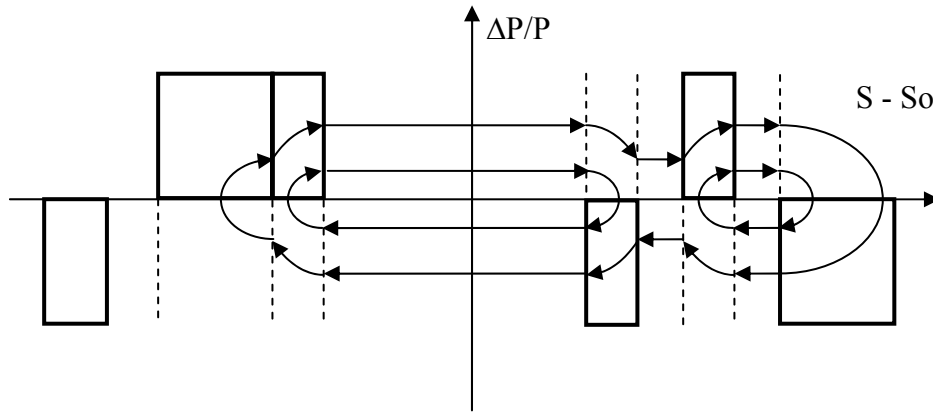


Fig.4. Particle trajectories in series of barrier buckets.

An approximation of the arbitrary shape of the barrier bucket can be done with the numerical integration over series of the rectangular barriers (Fig.5).

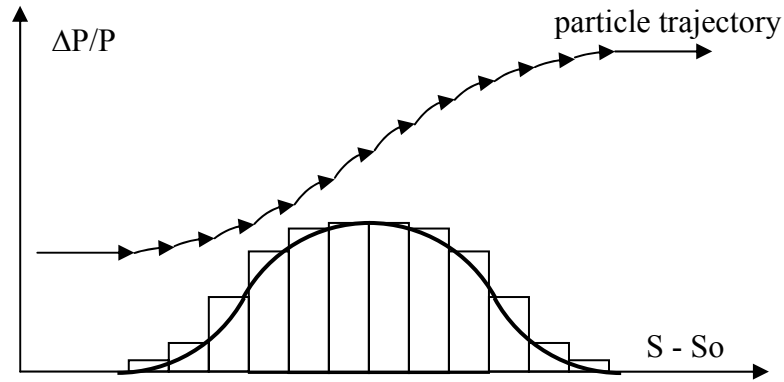


Fig.5. Approximation of sin shape with series of rectangular barriers.

The Model Beam algorithm realizes a Monte-Carlo method for a solution of a Langevin equation based on an assumption, that the integration step over time is sufficiently longer than a decoherence period (a few millions of revolutions). In this case the phase advance of the betatron and synchrotron oscillations during the integration step is an arbitrary number. In the transverse phase space the betatron motion is simulated using linear transformation maps.

In the case of a barrier bucket application the period of synchrotron oscillation is determined by the particle momentum deviation. At a low momentum spread it can be of the order of a few seconds. Correspondingly, the decoherence time can be compared or even longer than the step of the integration over time. To take into account this peculiarity of the synchrotron motion two algorithms were developed: at random and at regular phase advances during the integration step.

At the random phase advance the amplitude of the particle momentum deviation is calculated from its actual momentum and longitudinal co-ordinate. Thereafter the phase of synchrotron oscillations is generated uniformly between 0 and 2π and the new co-ordinate and the momentum are calculated as functions of the phase.

At the regular phase advance the phase of the synchrotron oscillations of the particle is calculated from its co-ordinate and momentum deviation. The phase advance for each particle is calculated from the period of its synchrotron oscillations as $\Delta\varphi = 2\pi \cdot \Delta t / T_s$, where Δt is the integration step. New particle co-ordinates are obtained from the phase trajectory equation.